

RACE-OC Project: Rotation and variability in young stellar associations within 100 pc

★ ★★

S. Messina¹, S. Desidera², M. Turatto¹, A. C. Lanzafame^{1,3}, and E. F. Guinan⁴

¹ INAF-Catania Astrophysical Observatory, via S.Sofia, 78 I-95127 Catania, Italy
e-mail: sergio.messina@oact.inaf.it; massimo.turatto@oact.inaf.it

² INAF-Padova Astronomical Observatory, Vicolo dell'Osservatorio 5, I - 35122 Padova, Italy
e-mail: silvano.desidera@oapd.inaf.it

³ University of Catania, Dept. of Physics and Astronomy, via S.Sofia, 78 I-95127 Catania, Italy
e-mail: Alessandro.Lanzafame@oact.inaf.it

⁴ Dept. of Astronomy and Astrophysics, Villanova University, Villanova, 19085, PA, USA
e-mail: edward.guinan@villanova.edu

ABSTRACT

Context. Angular momentum and its interplay with magnetic fields represent a promising tool to probe the stellar internal structure and evolution of low-mass stars

Aims. Our goal is to determine the rotational and magnetic-related activity properties of stars at different stages of evolution. For this reason, we have focussed our attention primarily on members of clusters and young stellar associations of known ages. In this study, our targets are 6 young loose stellar associations within 100 pc and ages in the range 8-70 Myr: TW Hydrae (~ 8 Myr), β Pictoris (~ 10 Myr), Tucana/Horologium, Columba, Carina (~ 30 Myr), and AB Doradus (~ 70 Myr). Additional data on α Persei and the Pleiades from the literature is also considered.

Methods. Rotational periods of stars showing rotational modulation due to photospheric magnetic activity (i.e. starspots) have been determined applying the Lomb-Scargle periodogram technique to photometric time-series obtained by the All Sky Automated Survey (ASAS). The magnetic activity level has been derived from the amplitude of the V lightcurves. The statistical significance of the rotational evolution at different ages has been inferred applying a two-sided Kolmogorov-Smirnov test to subsequent age-bins.

Results. We detected the rotational modulation and measured the rotation periods of 93 stars for the first time, and confirmed the periods of 41 stars already known from the literature. For further 10 stars we revised the period determinations by other authors. The sample was augmented with periods of 21 additional stars retrieved from the literature. In this way, for the first time we were able to determine largest set of rotation periods at ages of ~ 8 , ~ 10 and ~ 30 Myr, as well as increase by 150% the number of known periodic members of AB Dor.

Conclusions. The analysis of the rotation periods in young stellar associations, supplemented by Orion Nebula Cluster (ONC) and NGC 2264 data from the literature, has allowed us to find that in the 0.6 - 1.2 M_{\odot} range the most significant variations of the rotation period distribution are the spin-up between 9 and 30 Myr and the spin-down between 70 and 110 Myr. Variations between 30 and 70 Myr are rather doubtful, despite the median period indicates a significant spin-up. The photospheric activity level is found to be correlated to rotation at ages greater than ~ 70 Myr and to show some additional age dependence beside that related to rotation and mass.

Key words. Stars: activity - Stars: late-type - Stars: rotation - Stars: starspots - Stars: open clusters and associations: individual: TW Hydrae, beta Pictoris, Tucana/Horologium, Columba, Carina, AB Doradus

1. Introduction

Rotation is one of the basic stellar properties which undergoes dramatic changes along the whole stellar life. Such changes depend both on the evolution of the internal structure - e.g., stellar radius contraction during pre main sequence (PMS) and its expansion during post main sequence

(Post MS) - and on the presence and evolution of intense magnetic fields (Kawaler 1988; MacGregor & Brenner 1991; Krishnamurthi et al. 1997). Indeed, stellar magnetic fields play a fundamental role in the rotational history of late-type stars. During the PMS T-Tauri phase, they are responsible for the star-disk coupling which maintains the star's rotation rate slow, in spite of the gravitational contraction (see, e.g., Scholz et al. 2007). During the MS and Post MS, they are responsible for the angular momentum loss through magnetized stellar winds, as well for the redistribution of angular momentum through coupling processes between internal radiative zone and external convection zone (e.g., Barnes 2003). Thus, evolution of angular

Send offprint requests to: Sergio Messina

* The online Tables A.1-A.6 and on-line Figs. ??-?? are available in electronic form at the CDS via anonymous ftp to [cdsarc.u-strasbg.fr](ftp://cdsarc.u-strasbg.fr) (130.79.128.5) or via <http://cdsweb.u-strasbg.fr/cgi-bin/qcat?J/A+A/>

** Based on the All Sky Automated Survey photometric data

momentum and magnetic activity offer complementary diagnostics to study the mechanisms by which rotation and magnetic fields influence each other.

Our knowledge on the rotation properties at different stellar ages is increasing thanks to a number of valuable projects either of decennial long-term monitoring of very young open clusters (see, e.g., Herbst & Mundt 2005; Herbst et al. 2007) or of seasonal monitoring of intermediate-age open clusters (e.g., MONITOR, Hodgkin et al. 2006; EXPLORE/OC Extrasolar Planet Occultation Research, von Braun et al. 2005). Differently than field stars, stars in open clusters form samples that are complete in mass and homogeneous in environmental conditions, initial chemical composition, age and interstellar reddening. Such stellar samples allow us to accurately investigate the dependence on age and metallicity of different stellar properties and of their mutual relationship.

However, much still needs to be done since the number of studied open clusters, as well as the number of periodic variables discovered in most clusters, have not been large enough to fully constrain the various models proposed to describe the mechanisms that drive the angular momentum evolution. Specifically, the sequence of ages at which the angular momentum evolution has been studied has still significant gaps and the sample of available periodic cluster members for a number of clusters is not as complete as necessary. Furthermore, at most ages we have only one representative cluster, a situation which does not allow us to investigate, e.g., the dependence on metallicity or on initial environment conditions.

RACE-OC, which stands for Rotation and ACTivity Evolution in Open Clusters, is a long-term project aimed at studying the evolution of the rotational properties and the magnetic activity of late-type members of stellar open clusters (Messina 2007; Messina et al. 2008). The RACE-OC targets are in stellar associations and open clusters with ages in the range from about 1 to about 600 Myr, for which no rotation and activity investigations have been carried out so far. Top priority is given to the open clusters that fill the gaps of the relationship among age, activity and rotation. Nonetheless, we have also included clusters already extensively studied such as the very young Orion Nebula Cluster (Parihar et al. 2009). The motivation behind this is to enrich further the sample of periodic rotational variables and to explore the long-term magnetic activity, e.g., to search for activity cycles and surface differential rotation (SDR), by making repeated observations of same clusters over several years.

In the present study we considered stellar associations with distances less than 100 pc and ages younger than about 100 Myr. In fact, while very few open clusters are within 100 pc, recent investigations successfully identified a number of loose associations of nearby young stars (Zuckermann & Song 2004; Torres et al. 2008). Like open clusters, the physical association among the members allows a much robust age determination than for isolated field stars. Furthermore, the brightness and the proximity to the Sun make it possible to carry out several complementary observations of individual objects that allow to put the rotational properties of these stars in a broader astrophysical context. These observations include, e.g., high-resolution spectroscopy, trigonometric parallaxes, census of visual and spectroscopic binaries, IR excess, searches for planets.

A knowledge of the rotational properties of very young stars, as a function of age and spectral type (=mass), is important for a number of issues: a) some high-precision radial velocity studies of these targets are on-going (Setiawan et al. 2008; Günther & Esposito 2007b), in spite of the challenge represented by the activity-induced radial velocity jitter. As this is due to the occurrence of active regions on stellar surface, an independent determination of rotational period is useful to disentangle radial velocity variations due to rotational modulation from those due to Keplerian motion (e.g., Lanza 2010a); b) an accurate knowledge of the rotational properties of parent stars can illuminate how the star's angular momentum and planet formation influence each other. The planet formation may alter significantly the rotational history of the parent stars and, conversely, 'anomalous' rotation may reveal evidence of planet formation processes (Pont 2009; Lanza 2010b); c) the knowledge of rotation periods of young stars allows us to investigate the effect of rotation on the Lithium depletion (da Silva et al. 2009) and to establish a connection between rotation and Lithium on a basis firmer than using the projected rotational velocity to estimate rotation; d) finally, a comparison between the rotational properties of single stars and stars in binary systems can give some insight on the effect of binarity in the early stages of the rotational evolution.

The nearby loose young stellar associations we selected are: TW Hydrae, β Pictoris, Tucana/Horologium, Columba, Carina and AB Doradus. All but the latter have an age in the range between ~ 8 and ~ 30 Myr, which is quite unexplored by earlier rotational studies. In fact, to date no rotation period distribution was known in the age range from ~ 4 Myr (NGC 2264; Lamm et al. 2004) to ~ 40 Myr (IC 4665; Scholz et al. 2009).

This is an important age range in the rotational history of low-mass stars, when circumstellar disks dissipate and stars are free to spin their rotation up while they contract toward the zero age main sequence (ZAMS). This is also the age range of planet formation. Observations and theoretical studies of our planetary system (see Zuckerman & Song 2004 and references therein) indicate that giant planets form in less than 10 Myr and Earth-like planets in less than 30 Myr. Thus, the study of these stars allows to shed light on formation and early evolution of planetary systems. Indeed, nearby young stars are the prime targets for searches for planets with the direct imaging technique, as planets are brighter at young ages (Burrows et al. 1997). Several surveys already observed with the best state-of-art adaptive optics or space instruments a number of members of young associations (e.g., Chauvin et al. 2009; Nielsen & Close 2009). Efforts in this direction have recently lead to the first planet discoveries (e.g., Marois et al. 2008) and there are exciting perspectives for the use of future more sensitive instruments that will be available within a few years (e.g., Beuzit et al. 2008).

In Sect. 2 we present the young loose associations considered in the present study. In Sect. 3 we describe the photometric data on which this study is based. In Sect. 4 we present the rotation period search. The results on the rotation period distributions and a discussion in the context of angular momentum evolution are given in Sect. 5 and 6. Sect. 7 contains our conclusions.

Association	abbrev.	Age (Myr)	Distance (pc)	known members	late-type members	periodic members	ASAS period	literature period	new period (+revised)
TW Hydrae	TWA	8	48	36	29	23	12	11	4 (+0)
β Pictoris	β Pic	10	31	51	32	27	25	2	10 (+1)
Tucana/Horologium	Tuc/Hor	30	48	54	35	29	27	2	19 (+5)
Columba	Col	30	82	35	23	19	19	0	15 (+2)
Carina	Car	30	85	23	21	19	19	0	16 (+1)
AB Doradus	AB Dor	70 ^a	34	91	64	48	42	6	29 (+1)

^a Value taken from the literature but different from our estimate.

Table 1 Name, abbreviation, age, and mean distance of the nearby associations under study (Torres et al. 2008), together with the number of known members; late-type (later than F) members selected for period search; total number of periodic members; periodic members discovered from ASAS photometry; periodic members with period adopted from the literature; new periods determined from this study (and periods revised by us with respect to earlier literature values).

2. The sample

The sample of our investigation is taken from the recent compilations by Zuckerman & Song (2004) and Torres et al. (2008), that includes an updated analysis of the membership of nearby associations younger than 100 Myr.

We selected the following associations that have a mean distance smaller than 100 pc: TW Hydrae, β Pictoris, Tucana/Horologium, Columba, Carina¹, and AB Doradus. These associations are reported with ages in the range from ~ 8 to ~ 70 Myr.

The Torres et al. (2008) list of members is significantly more extended than the previous ones, thanks to the availability of the SACY (Search for Associations Containing Young stars) database of observation of young stars (Torres et al. 2006). Only a very small number of objects have discrepant membership with respect to the previous investigations (Zuckermann & Song 2004).

Our initial target list included nearly 300 stars. As the SACY sample was originally selected from bright ROSAT sources, a large majority of the targets is represented by late-type stars and is then suitable for the photometric search of rotational modulations. We excluded only a fraction ($\sim 30\%$) of stars with spectral types earlier than F9, since they are not expected to show any rotationally-induced variability due to their shallow convective zones. We note that a few members, although with unknown spectral type, were included in the search sample since their B–V colors were consistent with a late spectral type. We further excluded stars fainter than $V \sim 13$, as photometric errors of ASAS data, on which our study is based, become too large to allow a meaningful analysis. After applying these selection criteria, we are left with 204 stars. The list of our target associations, together with age, mean distance, and number of known late-type members is reported in Table 1.

The stars in young stellar associations have been studied extensively in the past years especially in the context of the study of the formation of planetary systems. As a result, a significant fraction of the targets has accurate spectroscopic characterisation. The search for planetary companions using direct imaging or radial velocities has also lead to a quite complete census of the binarity and to investigations on the presence of circumstellar gaseous or dusty disks. We exploited such resources in order to better understand

¹ This association should not be confused with the closer but older Carina-Near Moving Group identified by Zuckerman et al. (2006)

trends and correlations between the rotational periods and other properties.

Most of the spectroscopic observations (spectral types, projected rotational velocity $v \sin i$) are from SACY database (Torres et al. 2006). Information on binarity of the targets was taken from Torres et al. (2006, 2008), and Bonavita et al. (2010, in preparation). Additional bibliography for individual targets is given in Appendix A.

3. Data

3.1. The ASAS photometry

The All Sky Automated Survey (ASAS) is the major source of photometric observations on which the present analysis is based. The ASAS project started in 1997 with the goal to photometrically monitor millions of stars brighter than 14 magnitude in the V band and distributed all over the sky at declinations $\delta < +28^\circ$, to investigate any kind of photometric variability (Pojmanski 1997; 2002).

Presently, ASAS is carried out by two observing stations. One is at Las Campanas Observatory, Chile (since 1997). It consists of two wide-field telescopes, equipped with F200/2.8 Minolta telephoto lenses and 2K \times 2K AP-10 CCD Apogee cameras, covering 8.8 \times 8.8 deg of the sky through the V and I filters. The other station (the Northern Station) is at Haleakala, Hawaii, Maui (since 2006), and is equipped with two wide-field Nikon F200/2.0 APO-G-10 telephoto lenses observing simultaneously in the standard V and I filters. Data acquisition and processing is fully automated. The data reduction pipeline used to process ASAS data is described in detail by Pojmanski (1997). The linear scale at focal plane is 16 arcsec/pixel. The FWHM of stellar images is 1.3-1.8 pixels. Aperture photometry is used to extract stellar magnitudes through 5 apertures (ranging from 1 to 3 pixels in radius, which corresponds to 16 to 48 arcsec). Smaller apertures give better accuracy for brighter stars, whereas larger apertures for the fainter stars. In the following analysis, we selected the magnitudes time series of each target by selecting the aperture giving the best photometric precision. Due to the low spatial resolution, a check of the presence of any star close to the target star is crucial, especially for fainter stars for which larger apertures (up to a 48 arcsec radius) are used to extract the stellar magnitudes. All cases when nearby stars are not spatially resolved are discussed in Appendix A. The astrometric calibration is currently based on the ACT catalog (Astrographic Catalog 2000 + Tycho, Urban et al. 1998) and achieves an accuracy around 3 arcsec. Calibration to the standard system

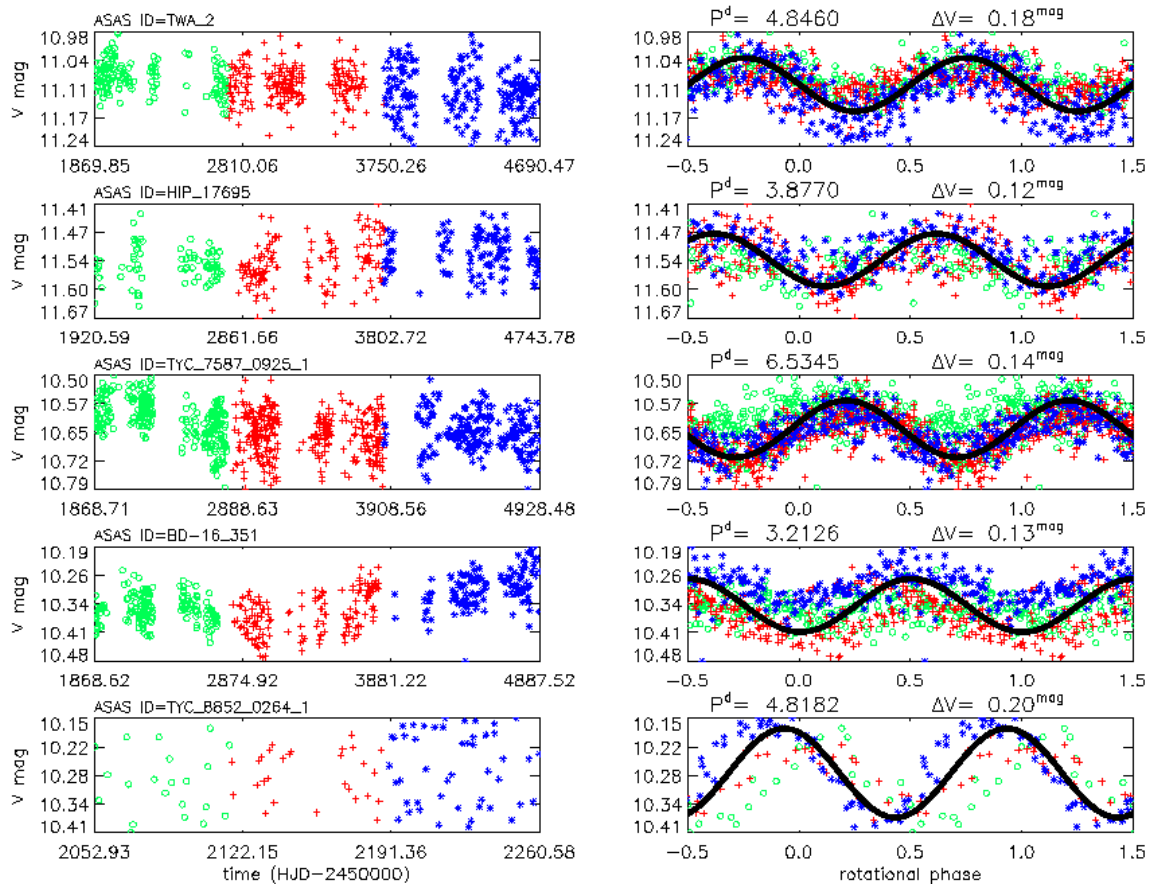


Fig. 1 Representative example of light curves in our sample. V-band data time series in the left panels and phased light curve in the right panels together with the sinusoidal fit with the rotation period (thick solid line). Different symbols and colors help identify measurements collected in different time intervals.

is based on the Tycho photometry (Perryman et al. 1997) and is accurate at about 0.05-mag level. Default exposure time is 2 minutes in the I and 3 minutes in the V filter. The systems routinely secure from 160 to 200 frames per night in V and from 230 to 300 frames per night in I. At this rate, the telescopes can carry out photometry of the available sky in two filters in about 2 days.

3.2. Data from the literature

A few stars of our sample are not in the ASAS database, being located at declination $\delta > +28^\circ$. We checked the bibliographical sources of all targets using ADS (Astrophysical Data System) to see whether previous determinations of rotation period existed. A number of stars had the rotation period already determined within the ASAS survey and, therefore, they were found listed in the ASAS Catalogue of Variable Stars (ACVS). Nonetheless, we made our period search also for these stars and, in a number of cases (10), we came to a different determination of the rotation period. Such cases are individually discussed.

In Tables A.1-A.6² we list the following information taken from the literature and used to discuss the results of our period search: target name; coordinates; V magnitude; B–V and V–I colors; M_V absolute magnitude; distance; projected equatorial velocity; computed stellar mass and radius; spectral type; and notes on membership.

4. Photometry rotation period search

We have used the **Lomb-Scargle periodogram** method to search for significant periodicities related to the stellar rotation in the data time series. In the following subsections we briefly describe our procedure to determine the rotation period of our targets.

4.1. Time series sectioning

Since our analysis is focussed on solar and late-type stars, we expect to detect the stellar rotation period by analysing the flux modulation induced by surface inhomogeneities

² Available in the online material

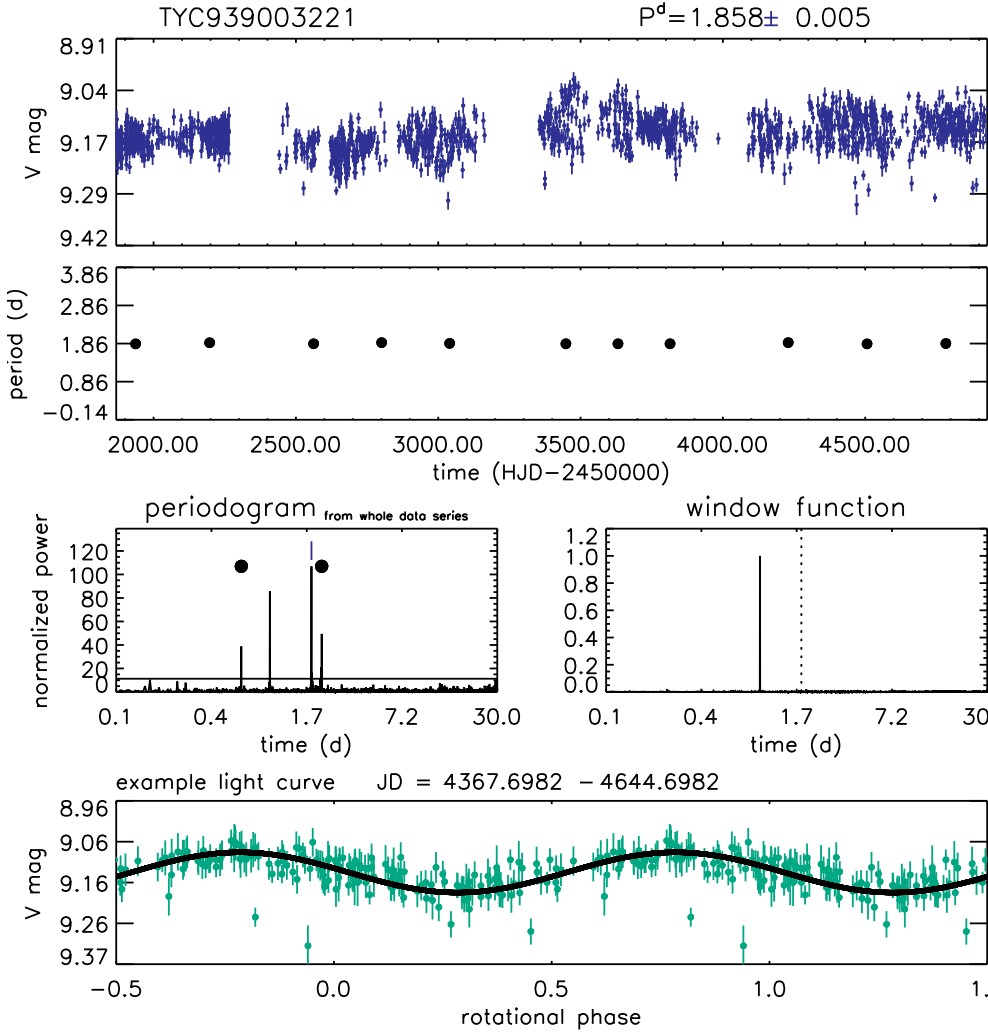


Fig. 2 *Top panel*: stellar V-magnitudes vs. time of TYC 9390 03221. *Second panel from top*: rotation periods vs. time detected with a confidence level over 99%. *Third panels (left)*: periodogram with evidence of 4 peaks with confidence level larger than 99%. Large bullets represents the peaks related to beat periods. *Third panels (right)*: window function with evidence of a peak at about 1 day owing to the data sampling. The vertical dotted line indicates that the $P=1.8581$ d period is not affected by the window function peak. *Bottom panel*: example light curve with data collected from MJD4367 to MJD4644 and phased with the $P=1.8581$ d rotation period. The solid line is a sinusoidal fit.

unevenly distributed along the stellar longitude. Such surface inhomogeneities can be either cool or hot spots arising from magnetic activity, which is particularly efficient in stars with fast rotation ($P < 10$ -20 days) and deep outer convection zone (spectral types from G to M). Indeed, the observed variability is dominated by phenomena that are manifested on different time scales (see, e.g., Messina et al. 2004). The shortest time scale, of the order of seconds to minutes, is related to micro-flaring activity. Its stochastic nature increases the level of intrinsic noise in the observed flux time series. The variability on time scales from several hours to days is mostly related to the star’s rotation. The variability on longer time scales, from months to years, is related to the growth and decay of active regions (ARGD) as well as to the presence of starspot cycles. These may be similar to the ~ 11 yr sunspot cycle.

Long-term monitoring of field stars (see, e.g., Messina & Guinan 2003) shows that, because of ARGD and sur-

face differential rotation, lightcurves’ amplitude and shape change with typical timescales of about 2-3 months, or even less for the fastest rotators ($P \sim 1$ day). Such changes, if not taken into account, can introduce aliases and lead to incorrect results. Therefore, a reasonable approach to the period search is to divide the complete data time series of each target (which is typically of about 8 yr in our case) into consecutive intervals not exceeding 2 months and to carry out the period search in each interval separately. Following such an approach, we obtained on average 10-15 intervals per target suitable for the period search.

Notwithstanding the 2-3 months timescale of lightcurve variation, Fourier analysis of long timespan series with sufficiently dense measurements can lead to a period determination with much higher confidence level and precision than the analysis of sectioned timeseries (e.g., Parihar et al. 2009). Here we anticipate that, without sectioning the data, we successfully detected the significant rotation peri-

ods in about 85% of our periodic targets.

In Fig. 1 we plot some representative example light curves together with the sinusoidal fit with the rotation period. There are stars such as TWA 2 and HIP 17695 whose amplitudes and phase of minima remain constant in time. Other stars, such as TYC 7587 0925 1 and BD -16 351, show constant phases of minima but variable amplitudes. In these cases a Fourier analysis of the complete time series without sectioning resulted in very precise rotation period determinations. On the other hand, stars like TYC 8852 0264 1 have lightcurve phases of minima that change in less than two months. In such cases an accurate period determination requires timeseries sectioning.

4.2. Lomb-Scargle periodogram

The **Lomb-Scargle** technique (Press et al. 1992; Scargle 1982; Horne & Baliunas 1986) was developed to search for significant periodicities in unevenly sampled data. The algorithm calculates the normalized power $P_N(\omega)$ for a given angular frequency $\omega = 2\pi\nu$. The highest peaks in the calculated power spectrum (periodogram) correspond to the candidate periodicities in the analyzed time series data. In order to determine the significance level of any candidate periodic signal, the height of the corresponding power peak is related with a false alarm probability (FAP), that is the probability that a peak of given height is due to simply statistical variations, i.e. to Gaussian noise. This method assumes that each observed data point is independent from the others. However, this is not strictly true for our time series data consisting of data that are generally collected with a time sampling much shorter than both the periodic or the irregular intrinsic variability timescales we are looking for ($P^d = 0.1-30$). This correlation can have a significant impact on the period determination as it has been highlighted by, e.g., Herbst & Wittenmyer (1996), Stassun et al. (1999), Rebull (2001), Lamm et al. (2004). We decided to determine the FAP in slightly different way than Scargle (1982) and Horne & Baliunas (1986), as discussed in the next sub-section, to overcome this problem.

4.3. False alarm probability

Following the approach outlined by Herbst et al. (2002), Monte Carlo simulations are used to determine the relationship between the normalized power and the FAP. Specifically, after dividing the data time series of each target into a number of intervals, the data of each interval were randomized by scrambling the day numbers of the Julian Day (JD) while keeping photometric magnitudes and the decimal part of the JD unchanged. This method preserves the same time sampling as in the original data set within the same night. Then, we applied a periodogram analysis to about 1000 "randomized" data time series for each time interval and retained the highest power peak of each computed periodogram. The FAP related to a given power P_N is taken as the fraction of randomised light curves that have the highest power peak exceeding P_N which, in turn, is the probability that a peak of this height is simply due to statistical variations, i.e. white noise. As the rotation period, we selected that corresponding to the highest power peak detected in the periodogram and with confidence level larger than 99% (FAP < 0.01), as computed from the men-

tioned simulations. The same procedure was repeated for each time interval and for all targets.

4.4. Alias detection

To identify the true periodicities in the periodogram, it is crucial to take into account that a few peaks, even with large power and high confidence levels, can be aliases arising from both the data sampling and the length of the time interval during which the observations are collected. In this respect, an inspection of the spectral window function helps to identify which peaks in the periodogram may be alias.

In Fig. 2 we plot, as an example, the ASAS photometric data time series of one of our targets (TYC 9390 0322 1). V-band magnitudes together with their uncertainties are plotted vs. the Heliocentric Julian Day (HJD) on the top panel. The periodogram in the middle left panel shows the presence of 4 peaks with a large power exceeding the 99% confidence level (solid horizontal line), but only one is related to the stellar rotation. If we look at the window function in the middle right panel, we find a major peak at about 1d which arises from the observation timing of about 1 day imposed by the rotation of the Earth and the fixed longitude of the observation site. This inspection allows us to identify the 1-d peak in the periodogram (marked by a vertical dotted line) as an alias. This peak is generally present in the periodogram of all the targets, being the observation timing similar for all the ASAS targets. The highest peak at $P=1.858$ days is actually that one related to the stellar rotation period, whereas the remaining two peaks (marked by bullets) arise from the convolution between the power spectrum and the window function. These alias periods are beat periods (B) between the star's rotation period (P) and the data sampling and they obey to the relation

$$\frac{1}{B} = \frac{1}{P} \pm n \quad (n = 1, 2, 3, \dots) \quad (1)$$

A method to check whether secondary peaks are beat periods is to perform a prewhitening of the data time series by fitting and removing a sinusoid with the star's rotation period from the data. After removing the primary frequency from the data time series and recomputing the periodogram, all the other peaks disappear, confirming that they are beat frequencies.

4.5. Uncertainty in the rotation periods

We followed the method used by Lamm et al. (2004) to compute the errors associated with the period determinations. The uncertainty in the period can be written as

$$\Delta P = \frac{\delta\nu P^2}{2} \quad (2)$$

where $\delta\nu$ is the finite frequency resolution of the power spectrum and is equal to the full width at half maximum of the main peak of the window function $w(\nu)$. If the time sampling is not too non-uniform, which is the case related to our observations, then $\delta\nu \simeq 1/T$, where T is the total time span of the observations. From Eq. (2) it is clear that the uncertainty in the determined period not only depends on the frequency resolution (total time span) but it is also proportional to the square of the period. We also computed the error of the period determinations following the prescription suggested by Horne & Baliunas (1986) which is

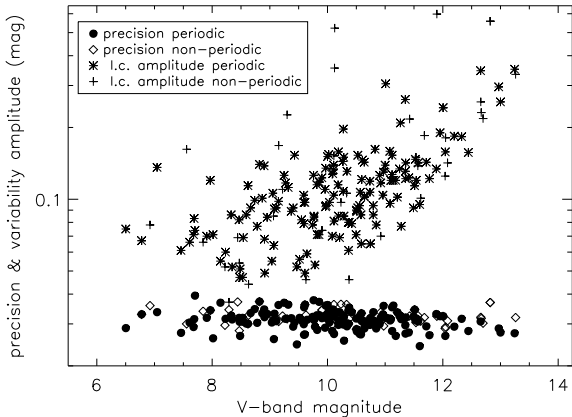


Fig. 3 Photometric precision and peak-to-peak variability amplitude vs. V-band magnitude of target stars.

based on the formulation given by Kovacs (1981). The period uncertainty computed according to Eq. (2) was found to be a factor 5-10 larger than the uncertainty computed by the Horne & Baliunas (1986) technique. In this paper we conservatively report the errors computed using Eq. (2) and, therefore, the precision in the periods could be better than that quoted in this paper.

4.6. Data precision

The precision of the ASAS photometry of the target stars under analysis is in the range 0.02-0.03 mag, as shown in Fig. 3. We remind, as discussed in Sect. 3.1, that we are using for each star the best aperture to extract the magnitude time series, which changes from star to star according to its magnitude. Therefore, we are comparing precision as determined from different apertures in Fig. 3. This is the reason for which we do not observe the typical trend of decreasing accuracy toward fainter stars in the magnitude range under analysis. Each star's precision is computed by averaging the uncertainty associated to the data points of the complete time series. We plot also the amplitudes of the light curves of our targets. We see that all stars for which we could determine the rotation period have a light curve amplitude at least a factor 2.5 larger than the corresponding photometric accuracy. This circumstance permits the period search to detect high power peaks in the periodogram with large confidence level and, consequently, to determine reliable rotation periods. We found that the best photometric accuracy for our targets was achieved by extracting the magnitude with apertures from 15 to 30 arcsec. Using the ADS and SIMBAD databases, we have checked whether our target stars had nearby stars within the aperture radius whose flux contribution may affect our analysis. Such cases are mentioned in Appendix A, dedicated to the discussion of individual cases.

5. Results

We determined the rotation period of 144 out of the selected 204 stars. We determined the rotation periods for the first time for 93 of them. We confirmed the period determined by other authors for 41 stars and revised the periods for 10

stars. Rotation periods of further 21 stars were retrieved from the literature. We found non periodic variability in 33 stars. The remaining 6 stars in the sample have neither ASAS data nor periods reported in the literature. A summary for each association is reported in Table 1.

A comparison of our results with previous rotation period determinations was possible for 51 stars (Fig. 4). We confirm the results reported in the literature in 41 cases. Our periods differ in 10 cases from the periods reported either in the ACVS (in 9 cases) or in the literature (only the case of HIP 9892; Koen & Eyer 2002). A close inspection of our periodograms showed that in all 9 cases of disagreement with respect to ACVS no power peak at all exists at the period value reported in the ACVS (see on-line Figs ??-??). Moreover, when we compute the rotation phases using the ACVS period, in all, but the case of HIP 12545, we obtain unconvincing light curves, that is with a high phase dispersion and without any evident modulation. On the contrary, our rotation periods were detected with a confidence level greater than 99% both in at least 8-10 time intervals in which we divided the complete time-series (i.e. in over 60% of the time intervals) and in the periodogram computed without data sectioning. The same holds for HIP 9892 whose periodogram does not show any peak at the period reported by Koen & Eyer (2002). We note that in 6 cases (TYC 8852 0264 1, TYC 8497 0995 1, TYC 7026 0325 1, TYC 7584 1630 1, TYC 8160 0958 1, and HIP 9892) the period is twice our value, which may be caused by the presence of two major spot groups located at opposite stellar hemispheres. However, the light curves in this circumstance should be double-peaked when they are phased with the long period, and this is not observed. In other 2 cases (TYC 7617 0549 1 and TYC 5907 1244 1), the ACVS period is consistent with a beat period, according to Eq.(1). Finally, it is not possible to reconcile the discrepant results with neither beat periods nor with spot groups at opposite hemispheres in just 2 cases (HIP 12545 and HIP 76768).

Note that our rotation period determinations include 10 stars in the TWA and 5 in the Tuc/Hor associations (flagged with an a apex in Tables 3 and 5) that were eliminated by Torres et al. (2008) from the high-probability member list, and two other stars, HIP 84586 and V4046 Sgr, that are tidally locked binaries. These stars are expected to have a different rotational history than single stars, because of enhanced rotation rates from tidal synchronization.. All these 17 stars will not be considered in the following analysis on the rotation period distribution.

The results of our period search are summarised in Tables 3-8. To prevent overestimating the maximum V-band light-curve amplitude (ΔV_{\max}) we took the difference between the median values of the upper and lower 15% data points of the timeseries section with the largest amplitude (see, e.g., Herbst et al. 2002). In the following analysis we will not use the brightest observed magnitude V_{\min} , rather the V magnitudes (corrected for duplicity in the case of binary systems) taken from Torres et al. (2008), and reported in the online Tables A.1-A.6. The rotation periods, together with uncertainty and normalized power, determined in the individual timeseries sections, are listed in the online Table A.7.

The light curves of all stars for which the ASAS photometry allowed us to determine the rotation period are plotted in the on-line Figs ??-??.

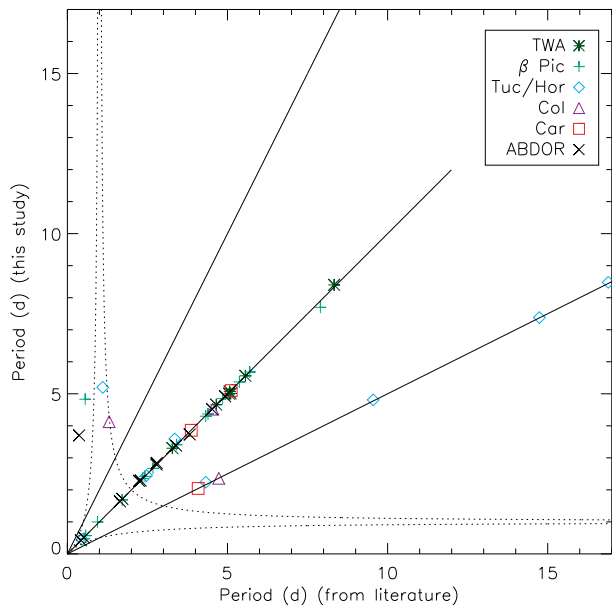


Fig. 4 Our rotation periods as a function of the periods derived from either ACVS or the literature. Straight solid lines represent the loci where our periods are equal to, or they are a factor 0.5 and 2 larger than the literature values. The curved lines represent the loci of beat periods, according to Eq. (1).

In Appendix A we report some detail on the nature (binarity and spectral classification) of individual targets and on the rotation periods when these were found in disagreement with previous determinations.

5.1. $V \sin i$ vs. equatorial velocity

About 75% of the periodic variables in our sample have known projected equatorial velocities ($v \sin i$). We also derived stellar radii by comparing the position of each target in the colour-magnitude diagram with the Baraffe et al. (1998) evolutionary tracks (see Sect. 6.1). When rotation period, $v \sin i$, and stellar radius are known, it is possible to compare equatorial velocity $v_{eq} = 2\pi R/P$ and $v \sin i$ to check the consistency between the two and derive the stellar inclination.

In Fig. 5 we compare $v \sin i$ and v_{eq} , marking the loci of $v \sin i = v_{eq}$, corresponding to equator-on orientation, and $v \sin i = \pi/4 v_{eq}$, corresponding to a randomly orientated rotation axis distribution. The major uncertainty of the equatorial velocity derives from the radius estimate. The reported $v \sin i$ uncertainties are 10% on average. Only 7 stars (flagged with an apex *c* in Tables 3-8 and plotted with circled symbols in Fig. 5) have inconsistent $v \sin i/v_{eq}$ (i.e., much larger than unity). Four out of seven stars (TYC 9344 0293 1, TYC 9529 0340 1, TYC 7100 2112 1, and TYC 8586 2431 1) have only one measurement of $v \sin i$, whereas they have well established rotation periods. It is important to carry out additional spectroscopic measurements to check the correctness of the $v \sin i$ value of these stars. Three other stars (TYC 8852 0264 1, TYC 7059 1111 1, and TYC 7598 1488 1) have each 2-3

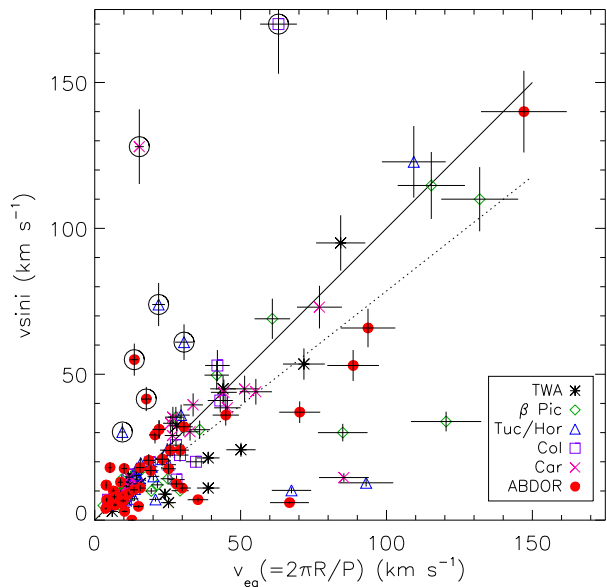


Fig. 5 $v \sin i$ from the literature vs. equatorial velocity $v_{eq} = 2\pi R/P$. The solid line marks $v \sin i = v_{eq}$, whereas the dotted line $v \sin i = (\pi/4)v_{eq}$.

independent $v \sin i$ measurements, which give similar values within the errors. These also have well established rotation periods which are confirmed by literature values. The discrepancy in the case of TYC 7598 1488 1 may arise from an incorrect value of parallax. In fact, Cutispoto (1998b) reports a photometric parallax larger than the one reported by Torres et al. (2008) which produces a larger stellar radius and would partly solve the disagreement of v_{eq} with $v \sin i$. Whereas in the other two cases the discrepancy requires further investigation to be addressed.

We have checked that the results of the following analysis on the rotation period distribution do not change if the seven stars with inconsistent $v \sin i/v_{eq}$ are either considered or not. One of these stars is anyway excluded from the following analysis because it is a rejected member of β Pictoris. The average $v \sin i$ for each association are reported in Table 2. This is obviously based on the periodic variable sample excluding members with inconsistent $v \sin i/v_{eq}$. In Table 2, r represents the correlation coefficient from the linear Pearson statistics, whereas the labels a and b give the significance level of the correlation coefficient. The significance level represents the probability of observing a value of the correlation coefficient larger than r for a random sample having the same number of observations and degrees of freedom.

Taken at face values, mean inclinations are not consistent with the value expected for completely randomly orientated rotational axis distribution. However, an investigation on preferential orientations of rotational axis in young associations must take into account several observational biases and is outside the scope of this paper.

Table 3 TW Hydrae Association. Summary of period searches: Star’s name; ASAS number; rotation period and its uncertainty; fraction of timeseries sections in which the rotation period is detected with confidence level higher than 99%; maximum light curve amplitude (ΔV_{\max}); photometric accuracy (σ_{acc}); brightest V magnitude (V_{\min}); B–V color; spectral type and note on binarity; note on period, and variable star designation if it exists. Targets are listed according to increasing TWA number (and increasing ASAS number for the other associations).

name	ID _{ASAS}	P (d)	ΔP (d)	timeseries sections	ΔV_{\max} (mag)	σ_{acc} (mag)	V_{\min} (mag)	B–V (mag)	Sp.T.	mult.	note	variable’s name
TW Hya	110152-3442.3	2.80	0.04	...	0.25	0.031	11.00	0.97	K6Ve	S	P _{lit}	
TWA 2	110914-3001.7	4.86	0.02	13/16	0.18	0.031	11.10	1.48	M2Ve	V	new	
TWA 3A	111028-3731.9	12.10	1.47	M4Ve	V	...	
TWA 3B	no-ASAS	13.07	1.52	M4Ve	V	...	
TWA 4A	112205-2446.7	2.52	0.20	...	0.09	...	8.94	1.17	K5V	Q	P _{lit}	TV Crt
TWA 4B	112205-2446.7	14.8	0.3	9/14	0.09	0.032	8.92	1.17	K5V	Q	new	
TWA 5	113155-3436.5	0.776	0.001	2/15	0.22	0.031	11.56	1.47	M2Ve	T	P=P _{ACVS}	
TWA 6 ^a	101829-3150.0	0.54	0.49	...	10.88	1.31	M0Ve	S	P _{lit}	
TWA 7	104230-3340.3	5.00 ^b	0.03	1/15	0.11	0.030	11.73	1.46	M2Ve	S	P=P _{lit}	
TWA 8A	113241-2651.9	4.66	0.06	4/14	0.27	0.029	12.14	1.46	M3Ve	V	P=P _{lit}	
TWA 8B	no-ASAS	0.78	0.08	...	15.20	1.10	M5	V	P _{lit}	
TWA 9A	114824-3728.8	5.01	0.01	13/14	0.18	0.027	11.22	1.26	K5V	V	P≠P _{ACVS} ; P=P _{lit}	
TWA 9B	no-ASAS	3.980	0.08	...	14.00	1.43	M1V	V	P _{lit}	
TWA 10	123504-4136.6	8.4	0.1	2/14	0.33	0.027	13.04	1.43	M2Ve	S	P=P _{lit}	
TWA 12 ^a	112105-2446.7	3.30	0.01	7/14	0.45	0.030	12.70	1.53	M1Ve	S	P=P _{ACVS} =P _{lit}	
TWA 13A	112117-3446.8	5.56	0.03	8/15	0.20	0.031	11.09	1.42	M1Ve	V	=1/2 P _{ACVS} ; P=P _{lit}	
TWA 13B	112117-3446.8	5.35	0.03	4/12	0.27	0.031	11.96	1.47	M5	V	P=P _{lit}	
TWA 14 ^a	111326-4523.7	0.63	0.11	...	12.52	1.30 ¹	M0	S	P _{lit}	
TWA 15A ^a	123421-4815.2	0.65	0.13	1.45 ¹	M2	V	P _{lit}	
TWA 15B ^a	123420-4815.3	0.72	0.05	1.45 ¹	M2	V	P _{lit}	
TWA 16 ^a	123456-4538.1	12.69	...	M1.5	B	...	
TWA 17 ^a	132045-4611.6	0.69	0.12	1.20 ¹	K5	S	P _{lit}	
TWA 18 ^a	132137-4421.9	1.11	0.08	0.030	13.12	1.30 ¹	M0.5	S	P _{lit}	
TWA 19AB ^a	114721-4953.1	K7	V	...	
TWA 20	123138-4559.0	13.42	1.10	M2	S	...	
TWA 21 ^a	101315-5230.9	4.43	0.02	7/15	0.13	0.037	9.82	1.00	K3Ve	V	new	
TWA 23 ^e	120727-3247.0	12.81	1.35 ¹	M1	S	...	
TWA 24 ^a	120942-5854.8	0.680 ^b	0.004	6/12	0.08	0.030	10.28	0.94	K1Ve	S	new	
TWA 25	121531-3948.7	5.07	0.02	12/14	0.23	0.032	11.37	1.41	M1Ve	S	P=P _{ACVS}	

V=visual companion; S=single star; B=binary system; T= triple system; Q=quadruple system; P_{lit}: period as given in the literature; P_{ACVS}: period in ACVS; ^a rejected member and excluded from rotation period distribution; ^b period undetected in the periodogram of the complete time series; ^c not included in the member list because of incomplete kinematic information; ¹ inferred from spectral type.

Table 4 As in Table 3 for the β Pictoris association.

name	ID _{ASAS}	P (d)	ΔP (d)	timeseries sections	ΔV_{\max} (mag)	σ_{acc} (mag)	V_{\min} (mag)	B–V (mag)	Sp.T.	mult.	note	variable’s name
TYC 1186 706 1	002335+2014.5	7.7 ^b	0.3	1/6	0.09	0.028	10.80	1.4	K7.5V	S	P=P _{lit}	
HIP 12545	024126+0559.3	1.25	0.01	4/7	0.15	0.031	10.32	1.21	K6Ve	SB1	P=2P _{ACVS}	
GJ 3305	043737-0229.5	6.10	0.03 ¹	...	10.59	1.45	M0.5	T	P _{lit}	
HIP 23200	045935+0147.0	4.37	0.03	9/14	0.15	0.032	10.18	1.39	M0.5Ve	S	P=P _{ACVS} =P _{lit}	V1005 Ori
HIP 23309	050047–5715.4	8.60	0.07	12/15	0.12	0.031	10.02	1.40	M0Ve	S	new	
HIP 23418	050159+0959.0	6.42	0.04	1/10	0.12	0.034	11.57	1.54	M3V	SB2+V	new	
BD-21 1074	050650-2135.1	13.3 ^b	0.2	4/14	0.07	0.034	9.94	1.52	M2	T	new	
HIP 29964	061828–7202.7	2.67	0.01	12/15	0.12	0.032	9.78	1.13	K4Ve	S	P=P _{ACVS}	AO Men
TWA 22	101727-5354.4	M5	S	...	
HIP 76629	153857–5742.5	4.3	0.2	7/15	0.12	0.034	7.97	0.81	K0V	SB+V	P=P _{lit}	V343 Nor
HIP 84586 ^e	171726–6657.1	1.688	0.003	8/13	0.07	0.034	6.77	0.76	G5IV	SB2+V	P=P _{lit}	V824 Ara
TYC 8728 2262 1	172955–5415.8	1.819	0.007	8/16	0.11	0.036	9.61	0.85	K1V	S	new	
TYC 8742 2065 1	174834–5306.7	2.61	0.02	8/16	0.09	0.033	8.95	0.83	K0IV	SB2+V	new	
HIP 88399	180303-5138.9	12.50	...	M2+F6V	B	...	
V4046 Sgr ^e	181411–3247.5	2.42	0.18	10/14	0.09	0.033	10.57	0.90	K5	SB2+V	P=P _{lit}	V4046 Sgr
UCAC2 18035440	181422-3246.2	12.78	1.36	M1Ve	SB?	...	
HIP 89829	181952–2916.5	0.57	0.003	8/14	0.19	0.037	8.80	0.69	G1V	S	P=P _{ACVS}	
TYC 9077 2489 1	184537–6451.8	0.345	0.04	7/12	0.16	0.033	9.3	1.19	K5Ve	SB2+V	new	
TYC 9073 0762 1	184653–6210.6	5.37	0.04	10/15	0.33	0.032	12.08	1.46	M1Ve	S	P=P _{ACVS}	
TYC 7408 0054 1	185044–3147.8	1.089	0.002	10/15	0.19	0.033	11.26	1.35	K8Ve	S	new	
HIP 92680	185306–5010.8	0.997	0.001	10/13	0.09	0.032	8.37	0.77	K8Ve	S	P=P _{lit}	PZ Tel
TYC 6872 1011 1	185804–2953.1	0.504	0.004	3/15	0.12	0.032	11.64	1.30	M0Ve	S	new	
TYC 6878 0195 1	191145–2604.2	5.65	0.05	7/12	0.09	0.032	10.33	1.1	K4Ve	V	new	
HIP 102141AB	204151–3226.1	10.40	1.54	M4+M4.5	B	...	AT Mic
HIP 102409	204510–3120.4	4.85	0.02	6/11	0.10	0.030	8.68	1.49	M1Ve	S	P=P _{lit}	AU Mic
TYC 6349 0200 1	205603–1710.9	3.41	0.05	7/10	0.11	0.028	10.55	1.22	K6Ve+M2	V	P=P _{ACVS}	AZ Cap
TYC 2211 1309 1	220042+2715.2	0.476	0.001	1/1	0.08	0.034	11.39	1.40	M0.0V	S	P=P _{lit}	
TYC 9340 0437 1	224249–7142.3	4.48	0.03	6/12	0.16	0.030	10.65	1.35	K7Ve+K5V:e	B	new	
HIP 112312	224458–3315.1	2.355	0.005	2/11	0.19	0.026	12.12	1.48	M4IVe	V	P=P _{ACVS}	WW PsA
TYC 5832 0666 1	233231–1215.9	5.68	0.05	5/12	0.16	0.028	10.69	1.43	M0Ve	S	P=P _{ACVS}	
HIP 11437	no-ASAS	13.6928	0.03	...	10.62	1.21	K8	V	P _{lit}	AG Tri
HIP 10679	no-ASAS	7.75	0.62	G2V+F5V	B	...	

V=visual companion; S=single star; B=binary system; T= triple system; P_{lit}: period as given in the literature; P_{ACVS} period in ACVS; ¹ derived from B-band light curve; ^b period undetected in the periodogram of the complete timeseries; ^e tidally-locked binary system, excluded from rotation period distribution.

Table 5 As in Table 3 for the **Tucana/Horologium Association**.

name	ID _{ASAS}	P (d)	ΔP (d)	timeseries sections	ΔV_{\max} (mag)	σ_{acc} (mag)	V_{\min} (mag)	B-V (mag)	Sp.T.	mult.	note	variable's name
HIP 490	000553-4145.2	7.53	0.59	G0V	S	...	
HIP 1113	001353-7441.3	3.72	0.01	13/17	0.09	0.034	8.79	0.74	G8V	S	new	
HIP 1910	002409-6211.1	1.750	0.003	11/20	0.13	0.031	11.42	1.40	M0Ve	V	new	
HIP 1993	002515-6130.8	4.35	0.02	11/19	0.15	0.031	11.43	1.35	M0Ve	S	new	CT Tuc
HIP 2729	003451-6155.0	0.37	0.002	...	0.10	0.035	9.64	1.05	K4Ve	S	P _{lit}	
TYC 9351 1110 1	004220-7747.7	2.57	0.01	8/14	0.12	0.033	10.24	1.06	K3Ve	S	new	
HIP 3556 ^a	004528-5137.5	11.91	1.48	M3	
TYC 8852 0264 1 ^a	011315-6411.6	4.81 ^c	0.02	8/11	0.20	0.029	10.37	0.87	K1V	S	P=1/2P _{ACVS}	
HIP 6485	012321-5728.9	3.59	0.01	5/13	0.08	0.030	8.57	0.68	G7V	S	=P _{lit}	
HIP 6856	012809-5238.3	9.07	0.91	K1V	S	...	CC Phe
HIP 9141	015749-2154.1	3.02	0.01	3/12	0.08	0.026	8.05	0.65	G4V	V	new	DK Cet
HIP 9892	020718-5311.9	2.24 ^b	0.03	7/13	0.06	0.030	8.63	0.65	G7V	SB1	P =1/2P _{lit}	
TYC 8489 1155 1	020732-5940.3	10.68	1.16	K5Ve	V	...	
RBS 332 ^a	023652-5203.1	1.538	0.001	6/15	0.24	0.032	12.05	1.48	M2Ve	...	new	
TYC 8497 0995 1	024233-5739.6	7.38	0.05	10/16	0.14	0.031	11.07	1.23	K5Ve	S	P=1/2P _{ACVS}	
TYC 8491 0656 1	024147-5259.9	1.275 ^b	0.005	5/13	0.09	0.030	10.22	1.26	K6Ve	V	new	
AF Hor	024147-5259.5	12.21	1.49	M2V	V	...	AF Hor
TYC 7026 0325 1	031909-3507.0	8.48	0.10	10/17	0.15	0.028	11.20	1.30	K7Ve	S	P≠P _{ACVS}	
TYC 8060 1673 1	033049-4555.9	3.74	0.04	7/15	0.09	0.027	9.63	0.95	K3V	S	new	
TYC 7574 0803 1	033156-4359.2	2.94	0.01	12/16	0.15	0.031	10.98	1.30	K6Ve	S	new	
HIP 16853	033653-4957.5	7.63	0.59	G2V	SB	...	
HIP 21632	043844-2702.0	4.25	0.02	...	0.08	0.031	8.51	0.61	G3V	S	P _{lit}	
TYC 8083 0455 1	044801-5041.4	8.46	0.05	4/15	0.12	0.030	11.53	1.35	K7Ve	S	new	
TYC 5907 1244 1	045249-1955.0	5.20	0.04	12/13	0.11	0.031	9.96	0.87	...	SB2	P≠P _{ACVS}	
TYC 5908 230 1	045932-1917.7	4.06	0.02	11/17	0.15	0.030	10.68	1.20	new	
BD-09 1108	051537-0930.8	2.72	0.01	5/12	0.11	0.032	9.87	0.67	G5	S	new	
TYC 7048 1453 1	051829-3001.5	1.70	0.02	2/15	0.09	0.024	11.65	1.27	K4Ve	S	new	
TYC 7600 0516 1 ^a	053705-3932.4	2.45	0.01	7/15	0.10	0.031	9.59	0.80	K1V(e)	S	P=P _{lit}	AT Col
TYC 7065 0879 1 ^a	054234-3415.7	3.89 ^b	0.02	7/15	0.09	0.027	10.64	0.82	K0V	V	new	
HIP 105388	212050-5302.0	3.36	0.01	7/15	0.10	0.033	8.71	0.72	G7V	S	new	
HIP 105404 ^a	212100-5228.7	0.435334 ^{b,d}	0.000002	3/15	0.10	0.033	8.97	0.88	G9V	EB	P=P _{ACVS}	BS Ind
HIP 107345	214430-6058.6	4.50	0.02	5/13	0.10	0.030	11.64	1.41	M0Ve	S	new	
TYC 9344 0293 1	232611-7323.8	1.32 ^c	0.02	8/12	0.13	0.033	11.95	1.39	...	SB	new	
TYC 9529 0340 1	232749-8613.3	2.31 ^c	0.01	11/13	0.11	0.036	9.37	0.69	new	
HIP 116748AB	233939-6911.8	2.85	0.02	5/12	0.06	0.031	8.26	0.70	G6V+K3Ve	B	new	DS Tuc

V=visual companion; S=single star; B=binary system; P_{lit}: period as given in the literature; P_{ACVS} period in ACVS;

^a rejected member and excluded from rotation period distribution; ^b period undetected in the periodogram of the complete timeseries;

^c $v \sin i$ inconsistent with $v_{\text{eq}}=2\pi R/P$; ^d tidally-locked binary system.

Table 6 As in Table 3 for the **Columba Association**.

name	ID _{ASAS}	P (d)	ΔP (d)	timeseries sections	ΔV_{\max} (mag)	σ_{acc} (mag)	V_{\min} (mag)	B-V (mag)	Sp.T.	mult.	note on period	variable's name
TYC 8047 0232 1	015215-5219.6	2.40	0.01	5/14	0.11	0.028	10.88	0.95	K2V(e)	BD	new	
BD-16 351	020136-1610.0	3.21	0.01	9/13	0.13	0.029	10.40	1.10 ¹	K5	S	new	
TYC 7558 0655 1	023032-4342.4	8.80	0.23	4/14	0.08	0.025	10.33	1.07	K5V(e)	S	new	
HIP 16413	033121-3031.0	2.25	0.01	4/14	0.07	0.028	9.86	0.64	G7IV	B	new	
TYC 5582 1169 1	040217-1521.5	3.78	0.04	7/15	0.07	0.028	10.12	1.01	K3/4	S	new	
HIP 19775	041423-3819.0	2.345	0.008	3/12	0.07	0.025	9.10	0.58	G3V	S	new	
TYC 6457 2731 1	042110-2432.3	9.42	0.62	G2V	S	...	
TYC 7584 1630 1	042149-4317.5	2.360	0.008	8/15	0.10	0.029	10.23	0.69	G7V	S	P=1/2P _{ACVS}	
TYC 7044 0535 1	043451-3547.3	10.91	0.84	K1Ve	S	...	
TYC 8077 0657 1	045153-4647.2	2.834	0.001	13/20	0.11	0.031	9.81	0.69	G5V	B	new	
TYC 8080 1206 1	045305-4844.6	4.52	0.03	9/18	0.15	0.029	10.79	0.87	K2V(e)	S	P=P _{ACVS}	
TYC 8086 0954 1	052855-4535.0	4.50 ^b	0.05	4/15	0.11	0.030	11.45	0.86	K1V(e)	S	new	
HIP 25709	052924-3430.9	5.96	0.05	2/15	0.04	0.030	8.50	0.65	G3V	SB2	new	
TYC 7597 0833 1	054516-3836.8	10.95	0.70	G9V	S	...	
TYC 6502 1188 1	055021-2915.3	1.37 ^b	0.04	3/15	0.09	0.026	11.24	0.66	K0V(e)	S	new	
TYC 8520 0032 1	055101-5238.2	1.203 ^b	0.005	8/14	0.10	0.031	10.60	0.75	G9IV	S	new	
TYC 7617 0549 1	062607-4102.9	4.13	0.02	10/15	0.12	0.030	10.08	0.80	K0V	S	P≠P _{ACVS}	
TYC 8107 1591 1	062806-4826.9	1.293 ^b	0.002	8/15	0.11	0.032	11.01	0.65	G9V	S	new	
TYC 7100 2112 1	065247-3636.3	0.83 ^{b,c}	0.002	11/15	0.12	0.035	11.18	0.62	K2V(e)	S	new	
TYC 8118 0871 1	065623-4646.9	4.38	0.05	12/17	0.14	0.028	10.01	0.78	K0V(e)	S	new	
TYC 7629 2824 1	070152-3922.1	1.335	0.002	9/12	0.14	0.032	11.32	0.63	G9V(e)	S	new	
AG Lep	no-ASAS	1.895	0.05	...	9.62	0.60	G5V	S	P _{lit}	AG Lep
TYC 5346-132-1	no-ASAS	9.81	0.74	G7	

S=single star; B=binary system; BD= brown dwarf companion; ¹: inferred from spectral type;

^b period undetected in the periodogram of the complete timeseries;

^c: $v \sin i$ inconsistent with $v_{\text{eq}}=2\pi R/P$; P_{lit}: period as given in the literature; P_{ACVS} period in ACVS.

6. Rotation period evolution

6.1. Color-Magnitude diagrams

We use the M_V vs. $V-I$ CMD and a set of low-mass PMS evolutionary tracks to derive masses and radii and check the evolutionary stages of our targets (see Fig. 6). Evolutionary tracks (mass range from 0.2 to $1.0M_{\odot}$ at steps

of 0.1) are taken from Baraffe et al. (1998) (initial metallicity $[M/H]=0.0$, initial helium mass fraction $Y=0.275$, initial mixing length parameter $H_P=1.0$).

The $V-I$ colors of a few stars, with the exception of the β Pictoris members, have never been measured. To overcome this limitation and position all the stars in the same CMD, we derived empirical relations between $V-I$

Table 7 As in Table 3 for the **Carina Association**.

name	ID _{ASAS}	P (d)	ΔP (d)	timeseries sections	ΔV_{\max} (mag)	σ_{acc} (mag)	V_{\min} (mag)	B–V (mag)	Sp.T.	mult.	note on period	variable's name
TYC 9390 0322 1	055329-8156.9	1.858	0.005	11/12	0.14	0.036	9.20	0.79	K0V	V	new	
HIP 30034	061913-5803.3	3.85	0.01	6/10	0.10	0.031	9.33	0.86	K1V(e)	BD	new	AB Pic
HIP 32235	064346-7158.6	3.83	0.01	9/12	0.09	0.031	9.11	0.70	G6V	S	new	
HIP 33737	070030-7941.8	5.10	0.03	11/12	0.14	0.034	10.16	0.91	K2V	S	P=P _{ACVS}	
TYC 8559 1016 1	072124-5720.6	4.61	0.03	7/12	0.13	0.030	10.80	0.64	K0V	V	new	
TYC 8929 0927 1	082406-6334.1	0.79	0.02	9/12	0.09	0.037	9.89	0.63	G5V	S	new	
TYC 8930 0601 1	084200-6218.4	1.224	0.004	10/14	0.16	0.035	11.04	0.80	K0V	S	new	
TYC 8569 1761 1	084553-5327.5	1.28	0.003	10/16	0.07	0.033	10.46	0.63	G2V	S	new	
TYC 9395 2139 1	085005-7554.6	1.1435	0.005	11/14	0.10	0.032	10.62	0.76	G9V	SB2?	new	
TYC 8569 3597 1	085156-5355.9	1.942	0.005	10/14	0.09	0.033	10.84	0.69	G9V	SB2	new	
TYC 8582 3040 1	085746-5408.6	1.94	0.005	8/14	0.16	0.030	11.71	0.88	K2IV(e)	S	new	
TYC 8160 0958 1	085752-4941.8	2.043	0.001	8/15	0.15	0.027	10.55	0.73	G9V	S	P=1/2P _{ACVS}	
TYC 8586 2431 1	085929-5446.8	3.64 ^c	0.01	9/14	0.11	0.033	10.16	0.66	G5IV	S	new	
TYC 8586 0518 1	090003-5538.4	0.916	0.36	8/12	0.11	0.031	10.84	0.68	G5V	S	new	
TYC 8587 1126 1	090929-5538.4	0.77 ^b	0.003	2/12	0.05	0.033	10.24	0.73	G8V	S	new	
TYC 8587 2290 1	091317-5529.1	1.50	0.01	4/12	0.05	0.035	10.41	0.66	G5V(e)	S	new	
HIP 46063	092335-6111.6	3.86	0.02	14/14	0.15	0.031	10.27	0.86	K1V(e)	S	P=P _{ACVS}	V479 Car
TYC 8584 2682 1	093226-5237.7	10.86	0.76	G8V(e)	S	...	
TYC 8946 1225 1	094309-6313.1	1.70 ^b	0.01	2/11	0.07	0.034	10.40	0.68	G6V	S	new	
HD 107722	122329-7740.9	8.31	0.45	G6V	S	...	
TYC 8634 1393 1	114552-5520.8	5.35 ^b	0.04	3/12	0.05	0.030	10.24	1.01	K5Ve	S	new	

V=visual companion; BD= brown dwarf companion; S=single star; B=binary system; P_{lit}: period as given in the literature; P_{ACVS} period in ACVS; ^b period undetected in the periodogram of the complete timeseries; ^c: $v \sin i$ inconsistent with $v_{\text{eq}}=2\pi R/P$.

Table 2 Summary of results of the comparison between $v \sin i$ and equatorial velocity.

Association	# stars	$\langle \sin i \rangle \pm \sigma$	r	significance level
TWA	13	0.72±0.35	0.85	a
β Pic	27	0.91±0.34	0.84	a
Tuc/Hor	23	1.02±0.56	0.83	a
Col	12	0.94±0.31	0.86	a
Car	15	0.95±0.25	0.64	b
ABDOR	44	1.02±0.71	0.77	a
all	134	0.95±0.50	0.78	a

a: confidence level > 99.999%; b: confidence level = 99.995%.

and B–V using all the stars belonging to the same association and having both colors measured. In Fig. 7 we give an example of the polynomial fit used to obtain V–I colors from B–V in the case of Tucana/Horologium. In Table 9 we list the polynomial coefficients we determined for each association. The average error on the derived V–I colors is about 0.05 mag.

Fig. 6 also includes those targets of the TW Hya and Tuc/Hor associations that were rejected by Torres et al. (2008) from the high-probability member list. Although considered in our period search, their rotation periods are not included in the following rotation period distribution analysis.

There are four stars which significantly deviate from the sequence traced by the other members. In Tucana/Horologium it is the case of TYC 5908-230-1 whose spectral type is unknown and whose V–I color is derived from B–V. In Columba it is the case of BD–16351 whose V–I color is derived from B–V. In AB Dor this is the case of HIP 17695 and TYC 70840794 1. Their rotational properties, however, do not deviate from the average of their respective associations.

To better visualize the evolutionary and the rotational stage of our targets, we considered three additional well studied open clusters of known age: α Persei (70 Myr), Pleiades (110 Myr) and NGC2516 (150 Myr). The more evolved clusters (with respect to our targets) allow us to identify in the CMD the position of the ZAMS in the mass

Table 9 Polynomial fit coefficients to derive V–I from B–V color, for stars with no V–I observations.

	a	b	c	d	e
TW Hya					
B–V > 0.5	3.163	-5.014	3.028
Tucana/Horologium					
B–V > 0.5	+0.821	-3.550	+9.978	-9.190	+3.047
Columba					
B–V > 0.5	-0.417	2.142	-0.578
Carina					
B–V > 0.5	0.296	0.545	0.260
AB Dor					
B–V < 1.6	+10.19	-44.25	+72.94	-50.35	+12.66
B–V > 1.6	+0.648	-0.494	+0.960

range of our association members. The early-type (more massive) members of all three clusters have already reached the ZAMS, whereas the late-type (low mass) members are still approaching it. The list of confirmed members of the α Persei and Pleiades open clusters is compiled from the WEBDA database. The $(V-I)_c$ colors and Johnson V magnitudes are from Stauffer et al. (1985, 1989) for α Persei, and from Stauffer (1982a, 1982b, 1984) and Prosser et al. (1991) for the Pleiades. The rotation periods are taken from the compilation by Messina et al. (2003, and references therein). The V–I colors, originally given in the Kron system, have been transformed into the Cousins system by using the Bessel (1979) color-color relations. Color excess $E(B-V) = 0.10$ and distance modulus $(m-M) = 6.60$ for the α Persei and $E(B-V) = 0.04$ and $(m-M) = 5.60$ for the Pleiades (O’Dell et al. 1994) have been used to position the cluster members in the CMD. Photometry, rotation periods, color excess and distance modulus of NGC 2516 members are all taken from Irwin et al. (2009).

6.2. Rotation period distribution

A major goal of this paper is to look for statistically relevant differences in the rotation rate of stars in young stellar associations that can be ascribed to angular momentum evolution.

Table 8 As in Table 3 for the **AB Doradus Moving Group**.

name	ID _{ASAS}	P (d)	ΔP (d)	timeseries sections	ΔV_{\max} (mag)	σ_{acc} (mag)	V_{\min} (mag)	B-V (mag)	Sp.T.	mult.	note on period	variable's name
HIP 5191	010626-1417.8	7.13	0.05	2/8	0.05	0.025	9.49	0.91	K1V	V	new	
HIP 6276	012032-1128.1	8.43	0.79	G9V	S	...	
TYC 8042 1050 1	021055-4604.0	1.116 ^b	0.001	7/12	0.15	0.029	11.48	0.91	K3IVe	V	new	
HIP 10272	021216+2357.5	6.13	0.03	2/4	0.07	0.038	7.94	1.13	K1	B	new	
HIP 13027	024727+1922.3	6.90	0.68	G0+G5	B	...	
HIP 14684	030942-0934.8	5.46	0.08	2/10	0.07	0.026	8.51	0.81	G0	S	new	IS Eri
HIP 14809	031114+2225.0	8.51	0.71	G5	V	...	
HIP 17695	034723-0158.3	3.87	0.01	4/7	0.15	0.031	11.60	1.51	M3	S	new	
TYC 5899-0026 1	045224-1649.4	M3	S	...	
HIP 22738AB	045331-5551.5	1.496	0.01	3/10	0.06	0.031	10.78	1.56	M3Ve	V	new	
TYC 7587 0925 1	050230-3959.2	6.53	0.06	11/12	0.12	0.030	10.71	0.88	K4V	S	new	
HD 32981	050628-1549.5	0.985 ^b	0.01	4/14	0.09	0.030	9.16	0.58	F8V	S	new	
HIP 25283	052430-3858.2	9.34	0.08	7/12	0.07	0.028	9.06	1.25	K6V	S	new	
HIP 25647	052845-6526.9	0.5140	0.0003	2/10	0.13	0.033	6.74	0.83	K0V	Q	P=P _{lit}	AB Dor
TYC 7059 1111 1	052857-3328.3	2.29 ^c	0.01	8/14	0.11	0.027	10.61	1.06	K3Ve	S	P=P _{lit}	UX Col
TYC 7064 0839 1	053504-3417.9	7.82	0.18	1/14	0.15	0.026	11.83	1.08	K4Ve	S	new	
HIP 26373	053657-4757.9	4.52	0.02	6/14	0.09	0.031	7.73	0.85	K0+K6V	V	P=P _{lit}	UY Pic
HIP 26401A	053713-4242.9	9.55	0.67	G7V+K1V	B	...	WX Col
CP-19878	053923-1933.5	1.49	0.01	6/13	0.12	0.028	10.57	0.91 ¹	K1V	S	new	
TYC 7605 1429 1	054114-4118.0	2.75 ^b	0.02	3/14	0.15	0.030	12.29	0.87	K4IVe	S	new	
TYC 6494 1228 1	054413-2606.3	1.83	0.01	2/14	0.12	0.029	10.96	0.86	K2Ve	SB?	new	
HIP 27727	055216-2839.4	2.84	0.01	9/14	0.08	0.033	9.12	0.63	G3V	SB?	P=P _{lit}	TZ Col
TYC 7598 1488 1	055751-3804.1	3.73 ^c	0.04	6/11	0.09	0.029	9.64	0.69	G6V(e)	S	P=P _{lit}	TY Col
TYC 7079 0068 1	060834-3402.9	3.38	0.01	9/12	0.14	0.031	10.36	0.79	G9Ve	S	P=P _{ACVS}	
TYC 7084 0794 1	060919-3549.5	1.717	0.004	6/12	0.11	0.031	11.13	1.69	M1Ve	S	P=P _{ACVS}	
HIP 30314	062231-6013.1	6.54	0.61	G1V	V	...	
HIP 31711	063800-6132.0	2.60	0.05	...	6.25	0.62	G2V	SB+V	P _{lit}	AK Pic
HIP 31878	063950-6128.7	9.06	0.08	4/10	0.07	0.032	9.78	1.26	K7V(e)	S	new	
TYC 7627 2190 1	064119-3820.6	2.67 ^b	0.02	3/10	0.11	0.027	11.47	1.19	K2Ve	...	new	
UCAC2 06727592	064753-5713.5	6.05	0.05	5/11	0.11	0.032	11.54	0.90 ¹	K4V	S	new	
TYC 8558 1148 1	071051-5736.8	2.94	0.01	4/11	0.07	0.031	10.53	0.68	G2V	S	new	
TYC 1355-214-1	072344+2025.0	2.79	0.02	6/8	0.16	0.036	10.08	1.15	K3	S	P=P _{lit}	
HIP 36108	072618-4940.8	3.89	0.04	1/11	0.05	0.029	9.81	0.43	G7V	B	new	
HIP 36349	072851-3014.8	1.642	0.006	15/15	0.15	0.032	10.01	1.44	M1Ve	B	P=P _{lit}	V372 Pup
TYC 9493 0838 1	073100-8419.5	4.94	0.03	6/11	0.09	0.035	10.04	0.83	G9V	S	new	
HIP 51317	102856+0050.5	9.65	1.51	
HIP 76768	154028-1841.8	3.70	0.02	4/10	0.09	0.029	10.44	1.24	K3/4V	B	P≠P _{ACVS}	
HIP 81084	163342-0933.2	7.45	0.11	2/10	0.07	0.030	11.30	1.44	M0.5	S	new	
HIP 82688	165408-0420.4	7.82	0.59	G0	
TYC 7379 0279 1	172856-3244.0	10.40	0.93	
BD-13 4687	173746-1314.8	0.447	0.002	11/11	0.19	0.033	10.10	0.93	K3/4IV	S	new	
HIP 93375	190106-2842.8	8.55	0.56	G1V	V	...	
HIP 94235	191058-6016.3	2.24	0.01	2/10	0.04	0.031	8.37	0.59	G1V	V	new	
TYC0486-4943	193304+0345.7	1.35 ^b	0.02	5/10	0.10	0.035	11.20	0.95	K3V	S	new	
HD 189285	195924-0432.1	4.85	0.03	2/12	0.06	0.031	9.54	0.71	G5	S	new	
TYC 5164-567-1	200449-0239.3	4.68	0.06	5/7	0.10	0.032	10.17	1.00	new	
HD 199058	205421+0902.4	8.81	0.63	G5	
TYC1090-0543	205428+0906.1	2.28	0.007	2/9	0.14	0.029	11.79	1.07	P=P _{lit}	
TYC 6351 0286 1	211305-1729.2	4.92	0.07	6/10	0.12	0.029	10.69	1.21	K6Ve	S	P=P _{ACVS}	
HIP 106231	213102+2320.1	0.42312 ^b	0.007	4/6	0.10	0.036	9.19	1.05	K8	S	P=P _{ACVS} =P _{lit}	LO Peg
HIP 107684	214849-3929.1	4.14	0.02	5/10	0.06	0.031	9.67	0.69	G7V	S	new	
HIP 113579	230019-2609.2	2.169 ^b	0.007	1/10	0.06	0.027	7.49	0.65	G5V	B	new	
HIP 113597	230028-2618.7	9.63	1.34	K7V	S	...	
HIP 114530	231154-4508.0	5.17	0.02	4/10	0.07	0.030	8.82	0.80 ¹	G8V	B	new	
HIP 116910	234154-3558.7	2.294	0.007	6/10	0.11	0.029	9.45	0.71	G8V	S	new	
HIP 118008	235611-3903.1	8.22	0.97	K3V	S	...	
PW And	no-ASAS	1.762	0.13	...	8.86	0.92	K2V	S	P _{lit}	PW And
HIP 63742	no-ASAS	6.5400	0.06	...	7.73	0.85	G5V	B	P _{lit}	PX Vir
HIP 86346	no-ASAS	1.842	0.02	...	10.29	1.23	M0	T	P _{lit}	
HIP 114066	no-ASAS	4.502	0.03	...	10.87	1.44	M0	S	P _{lit}	
HIP 16563	no-ASAS	1.430	0.006	8.15	0.80	G5+M0	B	P _{lit}	V577 Per
HIP 12635	no-ASAS	10.21	0.88	...	B	...	
HIP 12638	no-ASAS	8.70	0.71	G5	B	...	
HIP 110526AB	no-ASAS	10.70	1.57	M0	B	...	

V=visual companion; S=single star; B=binary system; QUAD=quadruple system; ¹: inferred from spectral type;

^c: $v \sin i$ inconsistent with $v_{\text{eq}}=2\pi R/P$; P_{lit}: period as given in the literature; P_{ACVS} period in ACVS;

^b: period undetected in the periodogram of the complete timeseries.

The main influence of stellar mass on the angular momentum evolution is to determine the timescale of contraction towards the ZAMS and, below approximately 1.2 M_{\odot} , the amount of angular momentum stored in the radiative core (see, e.g., Allain 1998; Bouvier 2008; Keppens et al. 1995). In order to limit the range of possible variations, a binning in mass of our sample is therefore desirable. The paucity of stars available and the uncertainties in mass, however, allow only a rather broad mass binning. In the

following analysis we shall consider stars in the range 0.8-1.2 M_{\odot} and compare the results with a larger sample in the range 0.6-1.2 M_{\odot} . In the former case, we limit the angular momentum evolution timescales range still maintaining a sufficient number of stars for the statistical analysis; in the latter we increase the number of stars at the expenses of mixing quite different evolution timescales.

Colour or spectral type can be used as indicators of mass. The relationship color or spectral type vs. mass

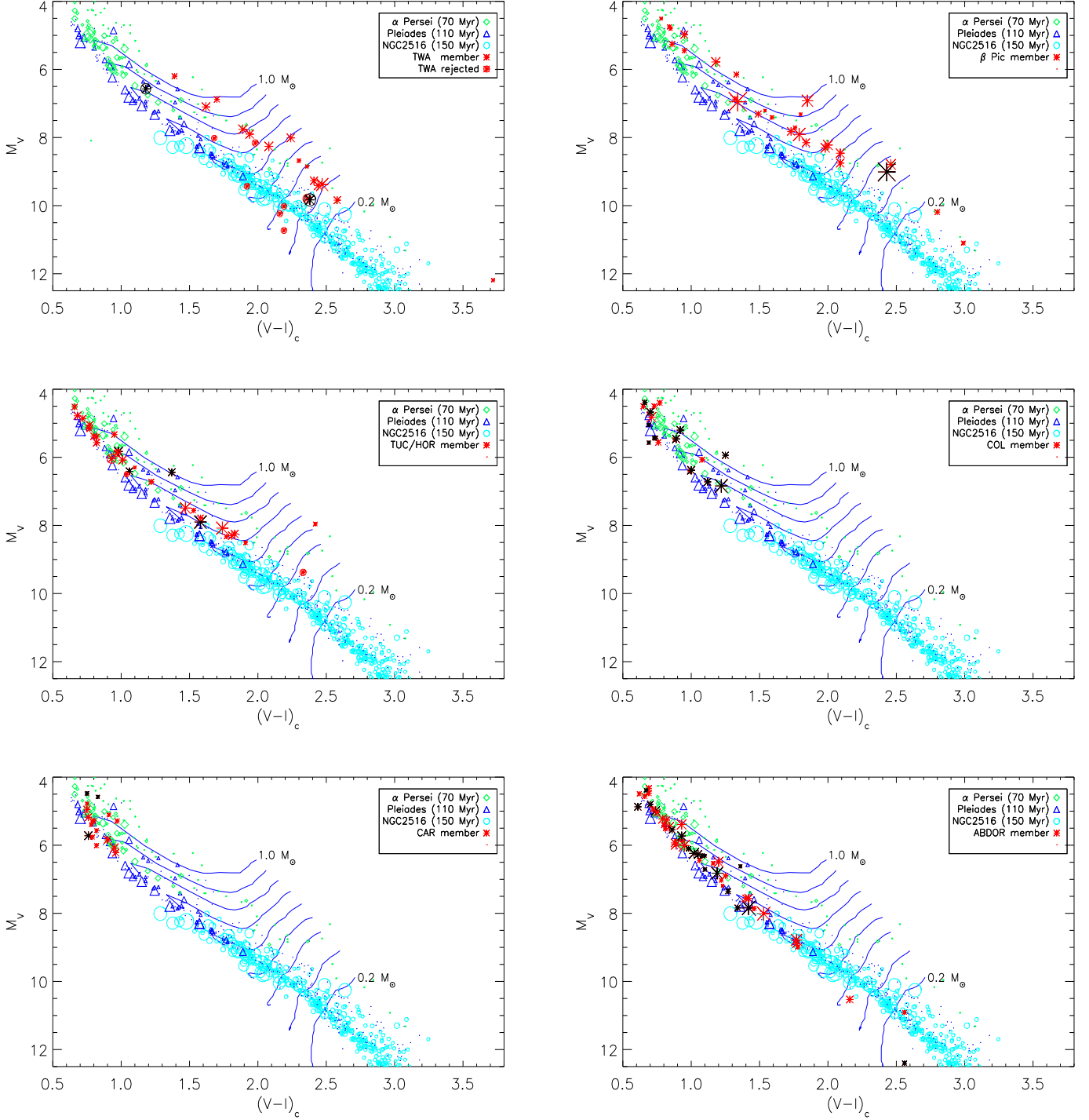


Fig. 6 Color-Magnitude diagrams of the six associations under analysis with overplotted PMS tracks (solid lines) from Baraffe (1998). Different symbols indicate stars belonging to different association/clusters; the symbol size is proportional to the rotation period. Dots represent cluster stars with unknown rotation period. Black symbols represent stars whose $V-I$ color is derived from $B-V$.

changes, however, with the age of the stellar system, particularly in the PMS phase, and the MS relationship cannot be applied to PMS stars. Without age discrimination, PMS stars of similar colors or spectral types can belong to quite different mass ranges, especially between ≈ 0.7 and $1 M_{\odot}$ where the evolutionary tracks turn abruptly towards higher temperatures before settling to the ZAMS (see Fig. 6). In

order to take the PMS evolution into account, we derived stellar masses and radii by comparing the position in the CMD with the Baraffe (1998) isochrones. The uncertainties on the estimated mass and radius mostly derive from the uncertainty on: a) $V-I$ color (especially for the lowest stellar masses); b) V magnitude (subject to variations up to a few tenths of magnitude due to the magnetic activity); c)

parallax; d) metallicity. We estimated the cumulative uncertainty to be approximately $0.1 M_{\odot}$ in mass and $0.05 R_{\odot}$ in radius, which is acceptable for the purposes of our analysis. The derived masses and radii are listed in the online Tables A.1-A.6. The mass histogram of the complete sample of periodic variables is reported in Fig. 8. About 91% of our targets have masses between 0.6 and $1.2 M_{\odot}$; 60% have masses between 0.8 and $1.2 M_{\odot}$.

The uncertainties in age and the paucity of stars in each association impose also a rather broad binning in age. In order to maintain statistical significance, almost coeval associations are put in the same age bin. In this way we consider TW Hya and β Pictoris, which have estimated ages of ~ 8 and ~ 10 Myr, in the same age bin; Tucana/Horologium, Carina and Columba members will be considered coeval stars with an estimated age of ~ 30 Myr. The age of AB Dor is estimated to be approximately 70 Myr by Torres et al. (2008), and therefore coeval to the α Persei cluster. We found, however, that the period distribution vs. $V-I$ is more similar to the Pleiades than α Persei (see Fig. 9 and discussion below), and therefore we assign AB Dor to the 110 Myr age bin together with the Pleiades.

In Fig. 9 we compare the distribution of rotation periods of AB Dor with that of α Persei (top panel) and the Pleiades (bottom panel). Adopting the Barnes (2003) classification scheme, we can easily identify three different groups of stars in Fig. 9. The rotation upper boundary forms a sequence, populated by stars which are subject to the long timescale spin-down controlled by the stellar wind magnetic breaking. The dashed line represents the expected theoretical period distribution according to Eq. (1) and (2) of Barnes (2003). This group of stars shows an almost one-to-one correspondence between rotation period and color, which is definitively reached by the age of 500-600 Myr as shown by members of the Hyades (Radick et al. 1987) and Coma Berenices (Collier Cameron et al. 2009) open clusters. Very fast rotators ($P \lesssim 1$ d) form a different sequence; the dotted line in Fig. 9 represents their expected theoretical period distribution computed using Eq. (15) of Barnes (2003). A third intermediate group is populated, according to the Barnes (2003) scheme, by stars which are moving from the very fast rotators to the slow rotators sequence. The identification of such sequences is rather difficult in the period vs. $V-I$ distribution of the younger association shown in Fig. 10, TW Hya and β Pictoris (top panel) and for Tucana/Horologium, Carina and Columba (bottom panel). In this case, stars are still contracting towards the ZAMS and are either still magnetically locked to their circumstellar disk or they just left this phase.

From the comparison of the rotational period vs. $V-I$ distribution AB Dor with those of α Persei and the Pleiades shown in Fig. 9 we notice that the population of very fast rotators in α Persei in the color range $0.5 < V-I < 1.0$ is missing among both AB Dor and Pleiades members. This population is expected to have migrated from the very fast rotators to the slow rotators sequence in the age range from 70 to 110 Myr. The AB Dor mean and median rotation periods are also much closer to those of the Pleiades than α Persei. A two-sided two-dimensional Kolmogorov-Smirnov test confirms that the AB Dor rotation period distribution is more similar to the Pleiades than α Persei, the KS probability that the periods are drawn from the same distribution being much lower for AB Dor / α Persei (0.5%) than for AB Dor / Pleiades (43%). Furthermore, looking at the AB Dor

CMD (Fig. 6), we see that the α Persei members are generally redder, which is consistent with a younger age than AB Dor. This is consistent also with the works of Luhman et al. (2005) and Ortega et al. (2007) which suggest a common origin of AB Dor and the Pleiades.

Among slow rotators, we note two outliers: the α Persei member AP 121 and the Pleiades member HII 2341, whose rotation period is well above the upper boundary. We suggest that the rotation period of this two targets, taken from the literature, is incorrect and we do not include them in the final sample to derive rotation period histograms and distributions.

To put our analysis in context with earlier stellar angular momentum evolution, we considered also rotational periods for members of the Orion Nebula Cluster (ONC, ~ 1 Myr) and NGC 2264 (~ 4 Myr). Rotation periods of ONC members were taken from Herbst et al. (2002), of NGC 2264 members from Rebull et al. (2002) and Lamm et al. (2004). Age-binned rotation period histograms of the full dataset are shown in Fig. 11.

Fig. 12 shows the rotation period evolution from ONC to AB Dor (plus Pleiades) for stars with mass between 0.6 and $1.2 M_{\odot}$ (left panel) and for the restricted sample with mass between 0.8 and $1.2 M_{\odot}$ (right panel). Both mean and median period decrease slowly but systematically with age from ONC to α Persei, apart the mean period from ONC to NGC 2264 in the 0.6 - $1.2 M_{\odot}$ sample which is essentially constant. Given the paucity of the data and because distributions are not Gaussian, we investigated the significance of such variations by performing a two sided KS test at consecutive samples in age. We expect that, if the variation of the mean and median are significant, the KS probability that the period realisations in two consecutive time bins are drawn from the same distribution will be low. To avoid ambiguities that arise from the color evolution at early stage, we apply only the one-dimensional two-sided KS test to the restricted mass range 0.8 - $1.2 M_{\odot}$ and compare the results with those obtained in the extended 0.6 - $1.2 M_{\odot}$ range.

In Table 10 we list, for each age bin and for both the (0.6 - $1.2 M_{\odot}$) and (0.8 - $1.2 M_{\odot}$) ranges, the mean and median rotation period, the number of stars used in the test and the two-sided KS probability that the realisations at consecutive sample ages are drawn from the same distribution.

Considering the 0.8 - $1.2 M_{\odot}$ range first, we see that the moderate rotation spin-up from ~ 1 to ~ 9 Myr is also associated with a KS probability of 70% for the 1 vs. 4 Myr and 63% for the 4 vs. 9 Myr age bins. The KS probability decreases to 17% for the 9 vs. 30 Myr age bins and rises up again to 45% for the 30 vs. 70 Myr age bins. The KS probability then decreases for the 70 vs. 110 Myr age bins, when we also see an unambiguous rotation spin-down. The most significant variations are then the spin-up between 9 and 30 Myr and the spin-down between 70 and 110 Myr. Between 1 and 9 Myr the moderate spin-up is poorly supported by the KS test. The KS test on the spin-up between 30 and 70 Myr does not allow us to draw definitive conclusions. For the 0.8 - $1.2 M_{\odot}$ range the analysis is therefore consistent with a considerable disk-locking before 9 Myr, followed by a moderate but unambiguous spin-up from 9 to 30 Myr, consistent with stellar contraction towards the ZAMS. Variations between 30 and 70 Myr are rather doubtful, despite the median indicates a significant spin-up. In fact the mean rotation period does not indicate any spin-up at all

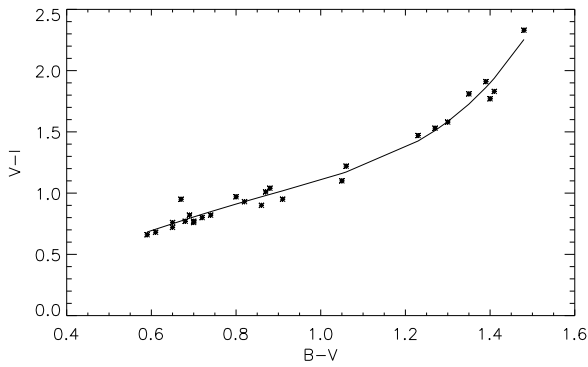


Fig. 7 Empirical relation to derive $V-I$ from $B-V$ colors for the Tucana/Horologium members lacking $V-I$ measurements.

and the KS-probability does not support a strong difference in the period distribution at these two age bins. This situation may be due to the heterogeneity of the sample: all stars with masses above $1 M_{\odot}$ are expected to complete their contraction toward the ZAMS at ages earlier than about 30 Myr, but stars with lower mass will end the contraction towards the ZAMS later (around 50 Myr for a star of $0.8 M_{\odot}$). The unambiguous spin-down from 70 to 110 Myr is consistent with the fact that, starting from the 70 Myr age bin, all stars in the $0.8 - 1.2 M_{\odot}$ mass range have entered the MS phase and therefore the angular momentum evolution is dominated by wind-braking.

The same considerations can be applied to the extended ($0.6 - 1.2 M_{\odot}$) range, despite all KS-probabilities are lower than in the ($0.8 - 1.2 M_{\odot}$) range. At ages earlier than 9 Myr, evidences for a moderate spin-up are rather poor, the two-sided test giving a probability around 60% that the distributions in the 1 and 4 Myr and in the 4 and 9 age bins are the same. The spin-up from 9 to 30 Myr remains unambiguous, with a probability of only 9% that the period distributions in these two age bins are the same. The moderate spin-up from 30 to 70 Myr is somewhat more significant, which is likely due to a higher number of stars ending their contraction towards the ZAMS at ages later than 30 Myr (85 Myr for a star of $0.6 M_{\odot}$). The spin-down between 70 and 110 Myr remains also unambiguous, the KS-probability for these two bins being only 11%.

The most recent work on rotation and activity in PMS stars was carried out by Scholz et al. (2007) and based on data of four associations in the age range from ~ 4 to ~ 30 Myr (η Chamaleontis, TW Hya, β Pictoris and Tucana/Horologium). It is based on $v \sin i$ measurements and the stellar mass is inferred from the spectral type, differently than our comparison with evolutionary tracks. Their study shows a monotonic increase of $v \sin i$ (decrease of rotation period) until an age of about 30 Myr, which is the oldest age considered in their analysis.

Despite some difference with respect to the Scholz et al. (2007) analysis, we substantially confirm their results, however on a firmer basis thanks to the use of rotation periods instead of $v \sin i$ values and of a more numerous sample of associations and members.

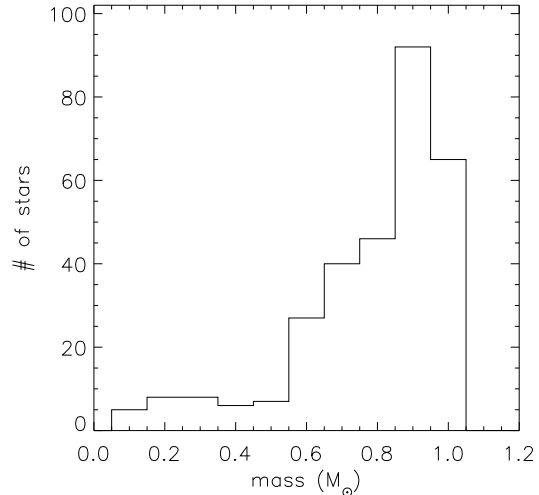


Fig. 8 Histogram of masses for the complete sample of periodic stars inferred from comparison with Baraffe et al. (1998) evolutionary tracks.

6.3. Rotation-photospheric activity connection

The periodic light modulations shown by our stars arise from the presence of temperature inhomogeneities (i.e. starspots) on the stellar photosphere. Possibly, similar to the Sun, such inhomogeneities originate from photospheric magnetic fields whose total filling factor and distribution depend on the properties of the dynamo mechanism operating in the stellar interior. The amplitude of the light curve provides a lower limit on the amount of magnetic fields asymmetrically distributed along the stellar longitude, which is in turn proportional to the total magnetic field filling factor. As shown by Messina et al. (2001, 2003), the upper bound of the light curve amplitude distribution is observed to decrease with increasing rotation period, when the dynamo becomes less efficient. In Fig. 13 we plot the maximum V-band peak-to-peak light curve amplitude vs. rotation period of stars in the associations under analysis. Such values represent the largest amplitude ever measured in all time sections in which the complete data time series of each target was divided, as explained in Sect. 4.1. Bullets represent stars with masses $M > 0.6 M_{\odot}$, whereas open triangles stars with masses $M < 0.6 M_{\odot}$. Circled symbols are those stars whose measured $v \sin i$ values are inconsistent with the equatorial velocity $v_{\text{eq}} = 2\pi R/P$. In four out of six associations, the upper bounds of the light curve amplitude distributions do not show any evident correlation with the rotation period. The only two exceptions are β Pic and AB Dor associations, whose upper lightcurve amplitude bound decreases with increasing rotation period. To improve our statistics, we combined data from coeval clusters as well data from α Persei and Pleiades clusters, as earlier done for the rotation period distributions. In Fig. 14 we note that the maximum light curve amplitude upper bound (solid line) begins to clearly correlate with the rotation periods starting from an age of ~ 70 Myr. Therefore, the photospheric activity behaviour of our young members of loose associations older than 70 Myr seem to be similar to those observed in older stars where an α - Ω dynamo

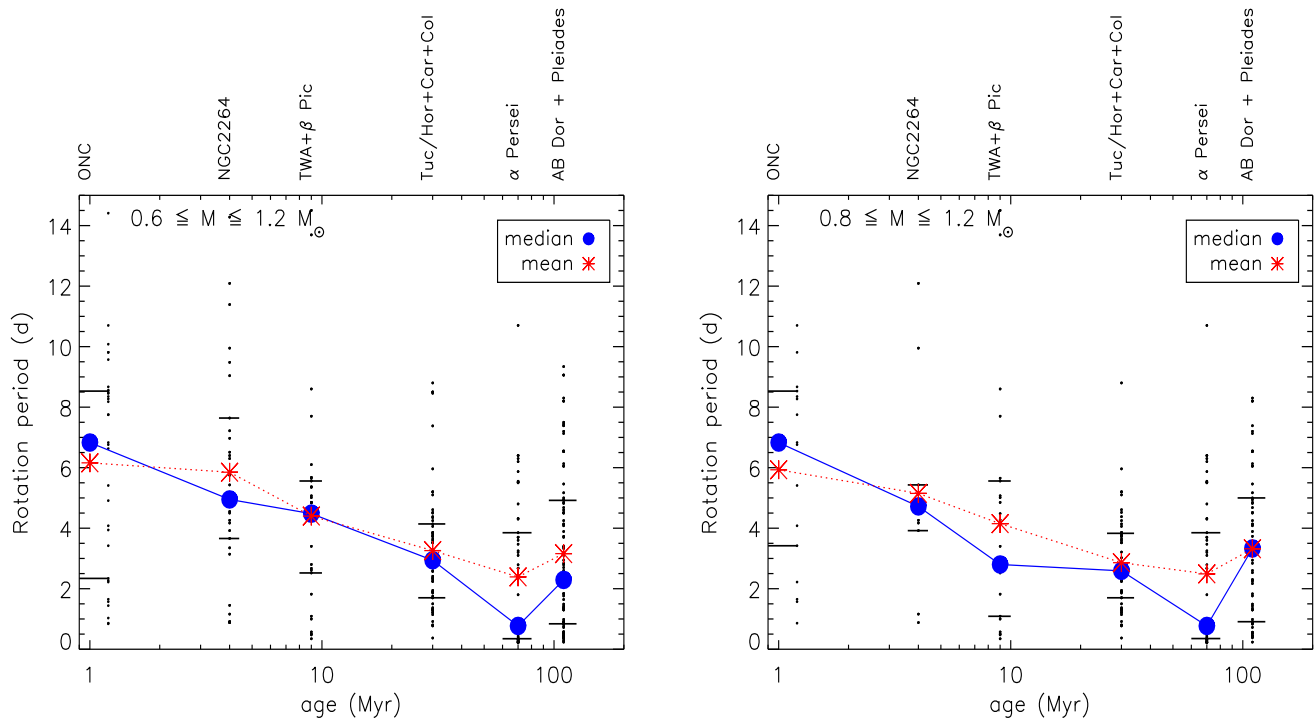


Fig. 12 Rotation period evolution vs. time in the 0.6-1.2 (left panel) and in the 0.8-1.2 (right panel) solar mass ranges. Small dots represent the individual rotation period measurements. Bullets connected by solid lines are the median periods, whereas asterisks connected by dotted lines are mean periods. Short horizontal lines represent the 25th and 75th percentiles of rotation period.

operates. Unfortunately, we have no data of very low mass (VLM) stars in our associations to study differences in magnetic activity with respect to higher-mass stars. Low-mass dM stars have a deep convection zone and stars with masses $< 0.3 M_{\odot}$ (i.e. later than dM3/4) are expected to be fully convective and may generate magnetic fields via a turbulent α^2 dynamo.

We note evidence of a dependence of the light curve amplitude also on age. Considering stars of similar mass and rotation period, the light amplitudes are observed to be largest in the youngest associations TW Hya and β Pic, where the variability is dominated by hot/cool spots and disk-accretion phenomena. Then, the amplitudes are observed to decrease until an age of ~ 30 Myr, where we expect that the variability arises chiefly from cool spots. Then, the light curve amplitudes are observed to increase again reaching a maximum level at ~ 110 Myr, which remains constant until an age of ~ 230 Myr, as shown by a similar study among the members of the intermediate age open cluster M11 (Messina et al. 2009). After this age, stars appear to show periodic light modulations of smaller amplitudes (see, e.g., Messina et al. 2009; Hartman et al. 2009; Radick et al. 1987). In other words, stars with similar rotation, mass and internal structure but with different ages, produce on average different light curves amplitude and, consequently, either different amount of magnetic fields or different surface distribution of magnetic fields. To understand which unknown, yet age-dependent, parameters play a role in the activity level is a challenge.

7. Conclusions

We have analysed the rotational properties of late-type members of six young associations within 100 pc and with age in the range 8-110 Myr. Our period search was based on photometric time series taken from the ASAS catalog. Our analysis has allowed us to obtain the following results:

- We newly discovered the rotation period of 93 stars, confirmed the period already known from the literature of 41 stars, revised the period of 10 stars, and finally we retrieved from the literature the period of 21 additional stars. After excluding all the stars rejected by Torres et al. (2008) from the high-probability member list, our final sample consists of 150 periodic confirmed members.
- We determined for the first time the rotation periods of a number of confirmed members in β Pictoris (10 stars), Tucana/Horologium (17 stars), Columba (15 stars), and Carina (16 stars), as well we increased the number of known periodic members of AB Doradus (+150%) and TWA (+15%).
- A two-dimensional two-sided Kolmogorov-Smirnov test applied to period-color distributions allowed us to confirm that the AB Dor association is older than 70 Myr (as reported by Torres et al. 2008) and likely coeval of the Pleiades cluster, i.e. 110 Myr old.
- Comparing the $v \sin i$ values from the literature with the calculated equatorial velocity $v_{\text{eq}} = 2\pi R/P$, where P and R are rotation period and stellar radius, we found that the average inclination of the stellar rotation axis in each association is generally higher than expected from a random distribution of stellar axes.

Table 10 List of target associations/clusters, age, number of stars used to make the statistics, median and mean rotation period, and significance level that consecutive period distributions are drawn from the same distribution.

Target	age (Myr)	0.6-1.2 M_{\odot}				0.8-1.2 M_{\odot}				
		# stars	P_{median} (d)	P_{mean} (d)	KS	# stars	P_{median} (d)	P_{mean} (d)	KS	
ONC	1	33	6.83	6.17	0.57	16	6.83	5.93	0.70	1 vs. 4 Myr
NGC 2264	4	26	5.43	6.19	0.59	10	4.72	5.15	0.63	4 vs. 9 Myr
TW Hya + β Pic	9	30	4.83	4.52	0.09	23	3.40	4.31	0.17	9 vs. 30 Myr
Tuc/Hor + Car + Col	30	62	2.85	3.22	0.36	53	2.60	2.87	0.45	30 vs. 70 Myr
α Persei	70	54	0.77	2.39	0.11	48	0.77	2.49	0.26	70 vs. 110 Myr
AB Dor + Pleiades	110	89	2.29	3.16	...	48	3.33	3.32

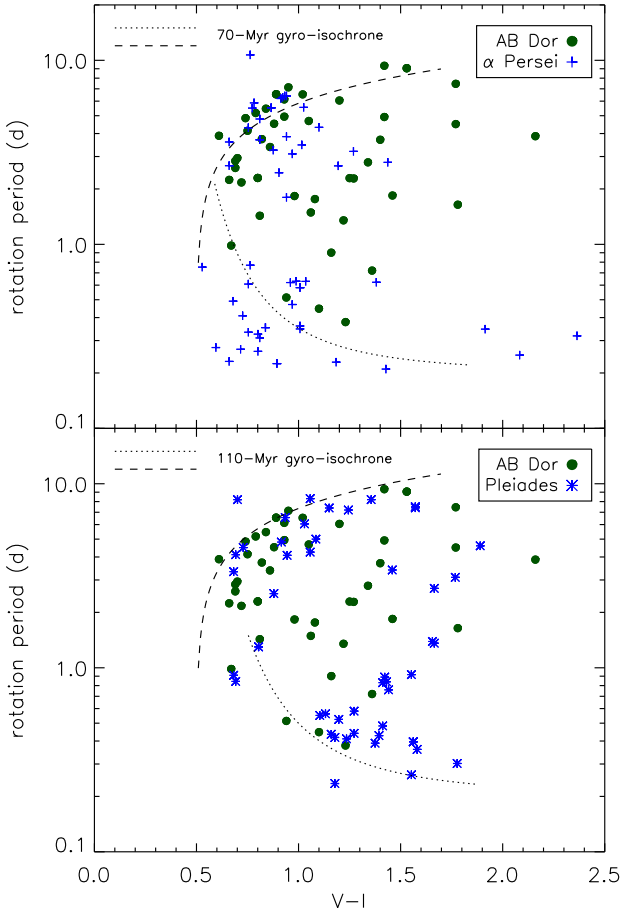


Fig. 9 Rotation period distribution of AB Dor members as compared to α Persei (top panel) and Pleiades members (bottom panel). Dashed and dotted lines represent the gyro-isochrones from Barnes (2003).

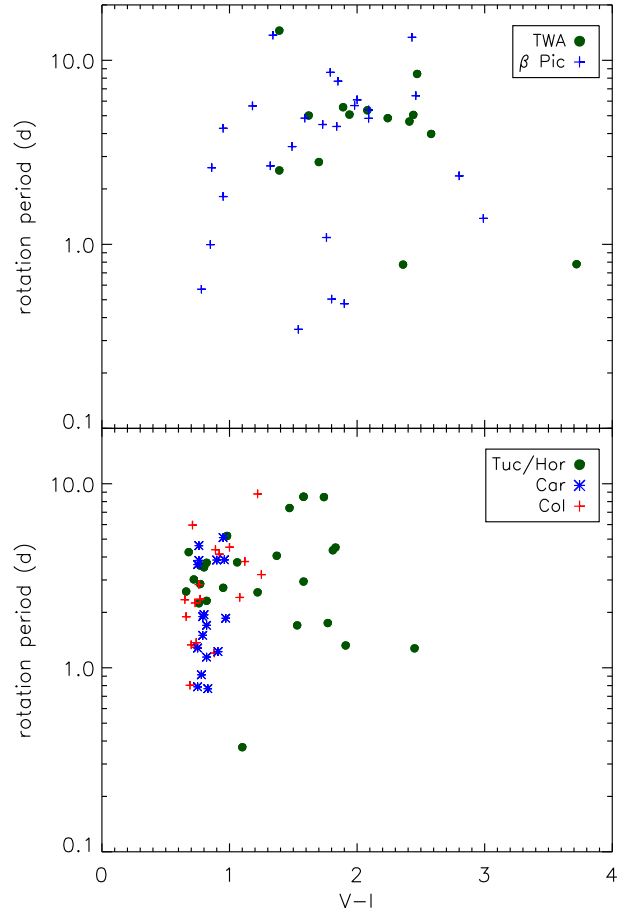


Fig. 10 Rotation period distribution of TWA and β Pic (top panel), and Tucana/Horologium, Columba and Carina (bottom panel)

- About 91% of our stars have mass in the $0.6 < M < 1.2 M_{\odot}$ range. We could determine in this mass range the rotation period distributions and derive their median and mean rotation period. Such values are the first available at ages of 8, 10, and 30 Myr in this mass range.
- In the $0.8 - 1.2 M_{\odot}$ range, we found the most significant variations of the rotation period distribution to be the spin-up between 9 and 30 Myr and the spin-down

between 70 and 110 Myr. Two sided KS tests confirm the significance of such variations. Between 1 and 9 Myr the moderate spin-up is poorly supported by the KS test. The KS test on the spin-up between 30 and 70 Myr does not allow us to draw definitive conclusions. Our analysis is therefore consistent with a considerable disk-locking before 9 Myr, followed by a moderate but unambiguous spin-up from 9 to 30 Myr, consistent with stellar contraction towards the ZAMS. Variations be-

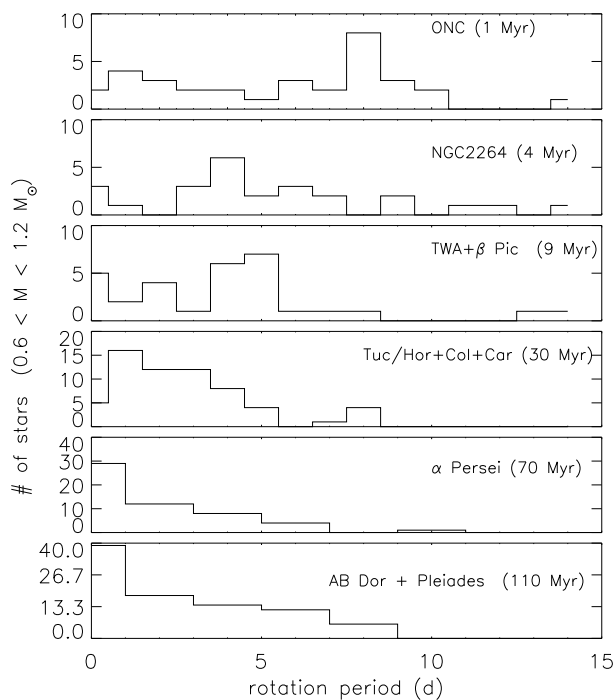


Fig. 11 Histograms of the rotation period distribution at the ages considered in the present study in the mass range $0.6 < M/M_{\odot} < 1.2$.

tween 30 and 70 Myr are rather doubtful, despite the median indicates a significant spin-up. The unambiguous spin-down from 70 to 110 Myr is consistent with the fact that, starting from the 70 Myr age bin, all stars in the $0.8 - 1.2 M_{\odot}$ mass range have entered the MS phase and therefore the angular momentum evolution is dominated by wind-braking.

The same considerations can be applied to the extended ($0.6 - 1.2$) M_{\odot} range, despite all KS-probabilities are lower than in the ($0.8 - 1.2$) M_{\odot} range. The moderate spin-up from 30 to 70 Myr is somewhat more significant, which is likely to be due to a higher number of stars ending their contraction towards the ZAMS at ages later than 30 Myr.

- We found that the photospheric magnetic activity, as described by the upper bound of the light curve amplitude distribution, correlates with the rotation period starting from an age of about 70 Myr. Moreover, stars of similar mass and rotation show evidence of an age dependence of the activity level. It is highest at ages younger than 10 Myr, where hot spots and accretion processes are dominant. Then, the light curve amplitude is observed to be at minimum level at an age of 30 Myr, when only dynamo-generated cool spots are expected to dominate the variability. Then the level of spot activity again increases reaching its maximum level at the age of Pleiades. This behaviour suggests the ex-

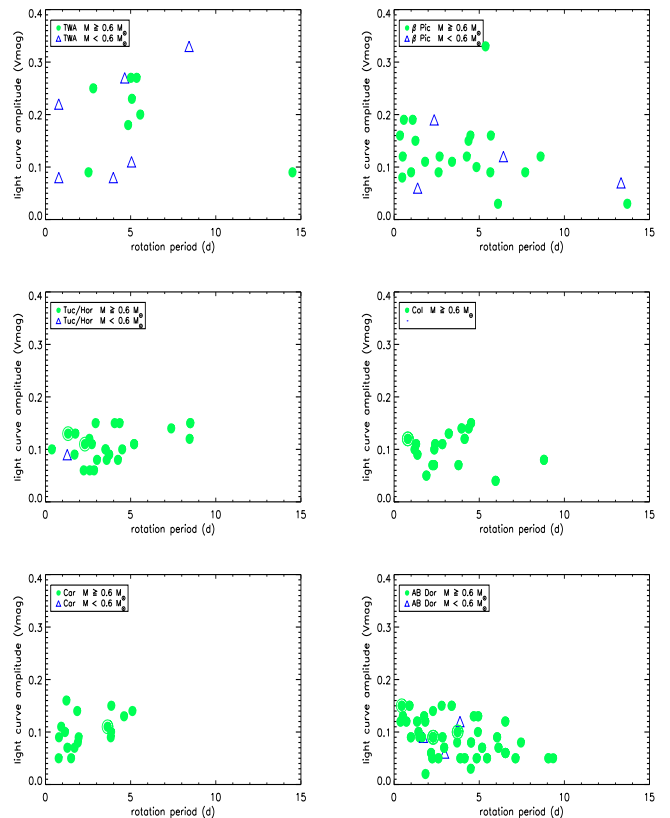


Fig. 13 V-band peak-to-peak light curve amplitude vs. rotation period. Circled symbols are stars whose $v \sin i$ is inconsistent with the equatorial velocity $v_{\text{eq}} = 2\pi R/P$.

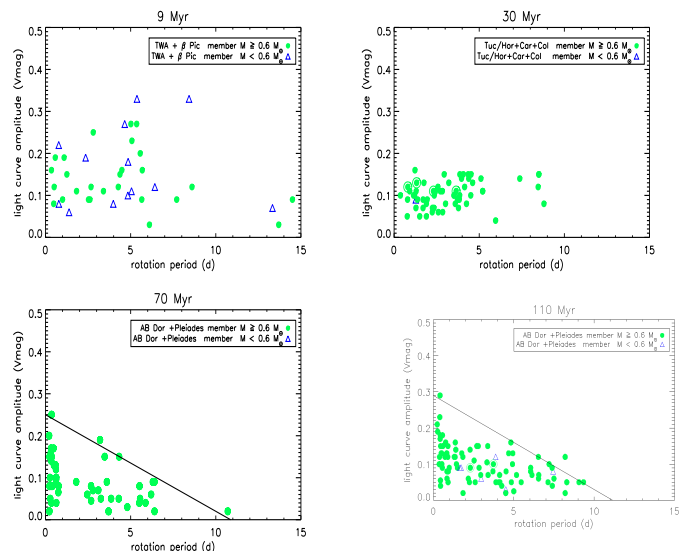


Fig. 14 Similar to Fig. 13 but with data of coeval stars plotted together. Solid lines mark the decreasing upper bound of the amplitude distribution.

istence of some age-dependent parameter which, apart from rotation and mass, also plays a role in driving the level of photospheric magnetic activity.

Appendix A: Individuals

A.1. TW Hydrae

TW Hya: the most recent and extensive study of the variability of TW Hya was carried out by Rucinsky et al. (2008). It is based on the MOST satellite high-precision photometry and the contemporaneous ASAS photometry. Their analysis reveals a number of periodicities probably arising from different mechanisms either operating in the photosphere (starspot activity) or related to accretion processes from its disk (veiling, accretion). The highest power peak detected in our periodograms is at $P=6.86\text{d}$ which is probably not related to rotation. For the aim of the present study, we adopt the ΔV light curve amplitude and the $P=2.80\text{d}$ period determined by Lawson & Crause (2005), which is in good agreement with earlier determinations by Koen & Eyer (2002) and by Alencar & Bathala (2002).

TWA 2: is a visual binary whose components are separated by 0.55 arcsec and differ by $\Delta V=1.0$ mag.

TWA 3AB: is a visual binary whose components are separated by 1.5 arcsec, differ by $\Delta V=0.9$ mag, and are not resolved by ASAS system. We could not determine the rotation period of neither the A nor the B component.

TWA 4: is a quadruple system formed by two pairs of SB at 0.8 arcsec and with $\Delta V=0.5$. TWA 4A is a SB1 with $P_{orb}=262\text{d}$ (Torres et al. 1995); TWA 4B is a SB2 with $P_{orb}=315\text{d}$ (Torres et al. 1995). Aa, Ba, and Bb have similar brightness. One of the components is a classical T Tauri star (CTTS). Our periodogram analysis found a high confidence level rotation period of $P=14.29\text{d}$ in 9 out of the 14 analysed time intervals in which we divided the complete magnitude series. This period is different from the rotation period $P=2.521\text{d}$ reported by Koen & Eyer (2002) and derived from the Hipparcos photometry. Since in both cases the system components are not resolved and have similar brightness, they may be both responsible for the observed photometric variability. Assuming that $P=2.521\text{d}$ is the correct period of TWA4A, which is consistent with the $v \sin i = 8.9 \text{ km s}^{-1}$ and the derived stellar radius, the $P=14.29\text{d}$ period may be attributed to TWA4B, which may have dominated the observed variability during the ASAS observations.

TWA 5: is a triple system consisting of a binary with period 5.94 yr (Konopacky 2007), $\Delta \text{mag} \sim 0.1$ (JHK) plus a brown dwarf at 2 arcsec (Lowrance et al. 1999). Our analysis shows the highest power peak at $P=0.776\text{d}$, which is in good agreement with the value of $P=0.77\text{d}$ reported in the ACVS.

TWA 6: we adopt the rotation period from the literature (Lawson & Crause 2005), since the available ASAS photometry did not provide any periodicity. TWA 6 was not included in the high-probability member list by Torres et al. (2008). The $v \sin i$ is from Skelly et al. (2008).

TWA 7: we found a rotation period in good agreement with the literature value (Lawson & Crause 2005).

TWA 8AB: is a visual binary whose components have a separation of 13.2 arcsec, a magnitude difference $\Delta V=3.2$, and are not resolved by ASAS system. Our rotation period agrees with that reported by Lawson & Crause (2005) for the brighter component TWA8A. For TWA 8B we adopt the rotation period of Lawson & Crause (2005).

TWA 9AB: is a visual binary whose components have a separation of 5.8 arcsec and $\Delta V=2.7$. For the brighter component TWA9A our period agrees with that reported

by Lawson & Crause (2005), whereas it disagrees with the $P=0.83\text{d}$ in the ACVS. The ASAS photometry could not resolve the fainter TWA9B whose rotation period is taken from Lawson & Crause (2005). The $v \sin i$ of both components are from Scholz et al. (2007).

TWA 10 and **TWA 12:** our rotation periods agree with those reported by Lawson & Crause (2005). TWA 12 was not included in the high-probability member list by Torres et al. (2008).

TWA 13AB: is visual binary whose components are separated by 5.1 arcsec and have $\Delta V=0.5$. The ASAS system does not resolve the components of the binary. However, the observed variability is likely due to both components. In fact, our analysis revealed two rotation periods: $P=5.56\text{d}$ which is in agreement with the determination by Lawson & Crause (2005), and $P=5.35\text{d}$ which is also in good agreement with the rotation period that Lawson & Crause (2005) report for TWA 13B.

TWA 14: our analysis did not reveal any significant periodicity. We adopt the rotation period determined by Lawson & Crause (2005). It was not included in the high-probability member list by Torres et al. (2008).

TWA 15AB: is visual binary rejected as member of the TW Hya group by Torres et al. (2008). Since our analysis did not reveal the rotation period, we adopt the rotation periods from Lawson & Crause (2005). The $v \sin i$ are from Scholz et al. (2007).

TWA 16: is a binary with components separated by 0.7 arcsec. Its membership to the TW Hya group must be confirmed yet according to Torres et al. (2008).

TWA 17: our analysis did not reveal any significant periodicity. We adopt the rotation period of Lawson & Crause (2005) and the $v \sin i$ of Reid (2003). It was not included in the high-probability member list by Torres et al. (2008).

TWA 18: our analysis did not reveal any significant periodicity. We adopt the $P=1.11\text{d}$ period and light curve amplitude of Lawson & Crause (2005). The $v \sin i$ is from Scholz et al. (2007). It was not included in the high-probability member list by Torres et al. (2008).

TWA 19AB: is a visual binary with a separation between the components of 37 arcsec and $\Delta V=2.8$. It was rejected as member by Torres et al. (2008). The ASAS photometry is probably contaminated by the light contribution by the fainter component. We could not determine any periodicity.

TWA 20: We could not determine any significant periodicity.

TWA 21 and **TWA 24:** were rejected as members by Torres et al. (2008).

TWA 23: were not included in the high-probability member list by Torres et al. (2008) due to lack of complete kinematic data.

A.2. β Pictoris

TYC 1186 706 1: this star was recently discovered to be a β Pic member by Lepine & Simon (2009). Our period is in good agreement with the literature value (Norton et al. 2007).

HIP 12545: is classified as SB1 by Torres et al. (2008). The period $P = 0.5569\text{d}$ reported in the ACVS is not confirmed by our period analysis (see the periodogram in Fig. ??). The $v \sin i = 9.5 \text{ km s}^{-1}$ is from Scholz et al. (2007).

GJ 3305: is a close binary (Kasper et al. 2007) and has a probable further wide companion (51 Eri=HIP 21547, F0V; Feigelson et al. 2006) at an angular distance of 66 arcsec. Our analysis did not reveal any significant periodicity. In the following analysis we adopt the period $P=6.1$ d of Feigelson et al. (2006). The $v \sin i$ is from Scholz et al. (2007).

HIP 23200: our period is in good agreement with both the literature (Alekseev 1996) and the ACVS values. The $v \sin i$ is from Favata et al. (1995).

HIP 23418: is a triple system consisting of a SB2 binary (the primary is a M3V) with orbital period $P_{orb}=11.96$ d and eccentricity $e=0.323$, and of a visual companion with $\Delta V \sim 1$ at an angular distance of 0.7-1.0 arcsec (Delfosse et al. 1999). The $v \sin i$ is from Scholz et al. (2007).

BD-21 1074: is a triple system consisting of a M2V ($V=10.29$) star and a binary companion at separation of 23 arcsec (M3, $V=11.61$). We detected a periodicity of $P=13.3$ d in 4 out of 14 time intervals as well as when the whole time series was analysed. Unfortunately, no $v \sin i$ value is at present available to check the consistency between $v \sin i$ and equatorial velocity.

HIP 76629: is a triple system consisting of a binary system (the primary is a K0V) and of a fainter visual component (at a separation of 10.0 arcsec and $\Delta V=6.8$). The RV trend by Gunther & Esposito (2007a) and the Hipparcos acceleration imply the presence of an additional closer companion with period of several years. Our rotation period agrees with the period found by Cutispoto (1998a).

TWA 22: it was an unconfirmed member of TWA according to Torres et al. (2008) because of incomplete kinematic information. The revised kinematic data by Teixeira et al. (2009) indicate its membership to β Pic moving group, that we adopt here.

HIP 84586: is an SB2 system (G5 IV + K0 IV) with an additional visual companion HD 155555C, 5.6 mag fainter in V at 33 arcsec. Our rotation period is in agreement with the literature values, e.g. by Cutispoto (1998b), Pasquini et al. (1991), Strassmeier & Rice (2000) and with the orbital period. The system is tidally-locked.

TYC 8742 2065 1: is classified as SB2 (the primary is a K0IV) by Torres et al. (2006). It has a very close optical companion (Torres et al. 2008) of similar brightness ($\Delta V=0.2$). We detected two periodicities of $P=2.61$ d and $P=1.61$ d of comparable power in almost each of about half of the selected time intervals. Probably, they represent the rotation period of either the SB2 or the optical companion, respectively. We are not in the position to assign to the SB2 system the corresponding rotation period. However, due the relative small difference, an incorrect assignment it would not imply significant difference in the results of the rotation period distribution analysis.

HIP88399: has a brighter F6V companion at a distance of 6.5 arcsec, which falls within the aperture radius used to extract the ASAS photometry.

V4046 Sgr: is an SB2 (the primary is a K5) tidally-locked binary accreting object (CTTS). Our rotation period agrees with the $P=2.42$ d found by Quast et al. (2000). The $v \sin i$ is from Quast et al. (2000).

UCAC2 18035440: GSC7396-0759 is a probable co-moving system at 169 arcsec (Torres et al. 2008). We note in its periodogram numerous peaks at confidence level higher than 99%. However, we could not identify which peak is related to stellar rotation.

TYC 9077 2489 1: is a triple system consisting of a binary (the primary is a K5Ve) with a separation of 0.18 arcsec ($= 5.2$ AU) and $\Delta K=2.3$ (Chauvin et al. 2009), and a wide companion (HIP 92024, A7V) at a 70 arcsec distance. This distance is sufficiently large to allow the ASAS system to observe the only close visual binary system.

HIP 92680: our rotation period agrees with the period reported by Innis et al. (2007).

TYC 6878 0195 1: is reported by Torres et al. (2006) as visual binary system (the brighter component is a K4Ve) whose components have a separation of 1.10 arcsec and $\Delta V=3.50$.

HIP 102141: is a binary system formed by two very similar M dwarfs ($\Delta V < 0.05$) at a separation of about 3 arcsec. Our analysis did not reveal the rotation period.

HIP 102409: our rotation period is in good agreement with literature values of, e.g., Hebb et al. (2007), Rodonò et al. (1986).

TYC 6349 0200 1: is reported by Neuhauser et al. (2003) as a visual binary (the brighter star is a K6Ve) with a separation of 2.2 arcsec and $\Delta K=1.6$.

TYC 2211 1309 1: this star was recently discovered to be a β Pic member by Lepine & Simon (2009). Our period is in good agreement with the literature value (Norton et al. 2007).

HIP 112312: its companion TX PsA is sufficiently distant (36 arcsec) to not contribute to the observed variability.

HIP 11437: is at declination +30 and no ASAS photometry exists. The rotation period is taken from Norton et al. (2007). It has a companion at an angular distance of 22 arcsec and $\Delta V=2.4$. The $v \sin i$ is from Cutispoto et al. (2000)

HIP10679: has a nearby F5V companion (HIP 10680) at a distance of 13.8 arcsec.

A.3. Tucana/Horologium

HIP 490: the $v \sin i$ is from Cutispoto et al. (2002).

HIP 1910: is a binary system, its components having a separation of 0.7 arcsec and $\Delta V=2.4$.

HIP 2729: our analysis did not find any significant periodicity. We adopt the $P=0.37$ d rotation period found by Koen & Eyer (2002) using the Hipparcos photometry.

TYC 8852 0264 1: our analysis revealed a rotation period $P=4.8$ d that we detected with high confidence level in 8 out of 11 time intervals and which is about half the value reported in the ACVS. The latter has no power peak in our periodogram. Nonetheless, the 4.8d period, together with computed stellar radius, give an equatorial velocity inconsistent with the three independent measurements of $v \sin i$ which agree within errors (30.22 ± 1.09 km s⁻¹ Scholz et al. 2007; 32.7 ± 1.8 km s⁻¹, Torres et al. 2006; 32 km s⁻¹ De La Reza & Pinzon 2004). In any case it is not included when determining the rotation period distribution because it was rejected as member of Tuc/Hor by Torres et al. (2008).

HIP 6485: our rotation period agrees with the period found by Koen & Eyer (2002) using the Hipparcos photometry.

HIP 9141: is a binary system, its components having a separation of 0.15 arcsec, and $\Delta H=0.1$ (Biller et al. 2007). The $v \sin i$ is from Nordstrom et al. (2004).

HIP 9892: is a SB1 system with long period but no other orbital elements determined (Gunther & Esposito

2007a). Our rotation period is about half the period from the literature $P=4.3215$ d (Koen & Eyer 2002). As shown in the online Fig. ??, the latter period is not present at all in our periodogram.

TYC 8489 1155 1: is the wide companion of the F7V star HIP 9902. The components are sufficiently separated to be resolved by the ASAS photometry. However, we could not determine the rotation period.

TYC 8497 0995 1: our analysis revealed a rotation period of $P=7.38$ d which is about half the period reported in the ACVS. The latter is not present in our periodogram as shown in the online Fig. ??

AF Hor and **TYC 8491 0656 1** are an M2V and K6V stars, respectively, separated by about 22 arcsec. They are too close to be separated by the ASAS photometry. Our analysis revealed a period of $P=1.275$ d which likely represents the rotation period of the brighter star (TYC 8491 0656 1) dominating the observed variability.

TYC 7026 0325 1: in the ACVS is reported with a rotation period of $P=2.2613$ d. However, our analysis revealed the $P=8.48$ d to be the only significant periodicity.

TYC 8060 1673 1: the $v \sin i$ is from Viana Almeida et al. (2009).

HIP 16853: is a binary system with astrometric orbit ($P=200$ d).

HIP 21632: we adopt the rotation period from Koen & Eyer (2002), since the analysis of ASAS photometry did not reveal any significant periodicity.

TYC 5907 1244 1: it is classified as SB2 by Torres et al. (2008). However, neither its orbital elements nor the spectral type are known. In the ACVS this star is reported with a rotation period of $P=1.10473$ d, whereas our analysis gives the $P=5.21$ d as the most significant periodicity.

TYC 7600 0516 1: it is rejected as member of Tuc/Hor association by Torres et al. (2008). Our period is in good agreement with the $P=2.47$ d reported by Cutispoto et al. (1999).

TYC 7065 0879 1: it is a close visual binary with very similar components according to Torres et al. (2006). It is rejected as member of Tuc/Hor association by Torres et al. (2008)

HIP 105404: is the only eclipsing binary star in our sample. It is a triple system composed by a very short-period eclipsing binary and a long-period SB ($P=3$ y, Guenther et al. 2007a). Since the Lomb-Scargle periodogram is best suited to search for single sinusoidal flux variations, it fails to detect the right orbital period. However, using as first guess the rotation period available from the literature and the phase dispersion minimization the ASAS extended time series has allowed us to improve the estimation of the orbital period. It is rejected as member of Tuc/Hor association by Torres et al. (2008)

TYC 9344 0293 1: is binary system whose components have a separation of 0.2 arcsec (Torres et al. 2008). The rotation period, that we detected with high confidence level in 8 out of 12 time intervals, when combined with the stellar radius, gives an equatorial velocity inconsistent with the only available measurements of $v \sin i=61$ km s⁻¹ (Torres et al. 2006). We can guess that the vsini value was overestimated due to line blending, since the binary components have a very small separation.

TYC 9529 0340 1: we have information neither on spectral type nor on binarity. The $P=2.31$ d rotation period, that we detected with high confidence level in 11 out of 13

time intervals, in combination with the computed stellar radius provides an equatorial velocity inconsistent with the only available measurement of $v \sin i=73.90$ km s⁻¹ (Torres et al. 2006).

HIP 116748AB: is a binary system whose components have a separation of 5.3 arcsec and $\Delta V=1.3$.

A.4. Columba

TYC 8047 0232 1: has a brown dwarf companion at 3.2 arcsec (Chauvin et al. 2003).

HIP 16413: is a binary system whose components have a separation of 0.90 arcsec and $\Delta V=1.90$.

TYC 5882 1169 1: although previously classified as member of the Tuc/Hor association, it is proposed by Torres et al. (2008) as high-probability member of Columba association. The $v \sin i$ is from Scholz et al. (2007).

TYC 6457 2731 1: the $v \sin i$ is from Viana Almeida et al. (2009).

TYC 7584 1630 1: the rotation period we found is half the value reported in the ACVS, which is absent in our periodogram (see online Fig. ??).

TYC 8077 0657 1: is a binary system whose components have a separation of 21.3 arcsec and $\Delta V=3.20$ (Torres et al. 2006). The ASAS photometry does not resolve this star from UCAC2 11686780.

HIP 25709: is classified as SB2 by Torres et al. (2008), but no orbital elements were derived.

TYC 7617 0549 1: in the ACVS is reported with a rotation period of $P=1.3038$ d. However, in the periodogram no significant power peak is evident other than that at $P=4.1395$ d.

TYC 7100 2112 1: the rotation period, that we detected with high confidence level in 11 out of 15 time intervals, when combined with the stellar radius, gives an equatorial velocity inconsistent with the only available measurements of $v \sin i=170$ km s⁻¹ (Torres et al. 2006).

AG Lep: the rotation period is retrieved from the literature (Messina et al. 2001), no ASAS photometry being available. The $v \sin i$ is from Cutispoto et al. (1999).

A.5. Carina

HIP 30034: is a member of Tuc/Hor according to Zuckerman & Song (2004). In the present study is considered as member of Carina according to Torres et al. (2008). It has a brown dwarf companion at wide separation (Chauvin et al. 2005).

HIP 32235 and **HIP 33737:** are member of Tuc/Hor according to Zuckerman & Song (2004). In the present study are considered as member of Carina according to Torres et al. (2008).

TYC 8559 1016 1: is a visual binary whose components have a separation of 5.8 arcsec and $\Delta V=3.0$ (Torres et al. 2006).

TYC 8929 0927 1: we find two peaks of comparable power and very high confidence level. However, only the $P=0.73$ d period combined the computed stellar radius gives an equatorial velocity consistent with the measured $v \sin i$.

TYC 8569 3597 1: is a SB2, with orbital period $P_{orb}=24.06$ d (Torres et al. 2008).

TYC 8160 0958 1: the rotation period we found is half the period reported in the ACVS, which is absent in our periodogram.

TYC 8586 2431 1: the rotation period, that we detected with high confidence level in 9 out of 14 time intervals, when combined with the stellar radius computed from PMS tracks, gives an equatorial velocity inconsistent with the only available measurements of $v \sin i = 128 \text{ km s}^{-1}$ (Torres et al. 2006). The luminosity class IV assigned to this star may indicate that the star has already left the MS and its radius has already started increasing. However, a stellar radius larger than about $6R_{\odot}$ would reconcile $v \sin i$ and v_{eq} .

A.6. AB Doradus

HIP 5191: is a visual binary whose components are separated by 23 arcsec.

TYC 8042 1050 1: is a visual binary whose components are separated by 21.7 arcsec.

HIP 10272: is a binary whose components are separated by 1.8 arcsec and have $\Delta V = 1.6$.

HIP 13027: is a binary whose components are separated by 3.6 arcsec and with $\Delta V = 0.8$.

HIP 14809: together with HIP 14807 represent a binary whose components are separated by 33.2 arcsec and with $\Delta V = 2.0$.

HIP 22738AB: is a binary whose components are separated by 7.8 arcsec and have $\Delta V = 0.9$. The ASAS system could not resolve the components.

HIP 25647: is a quadruple system (very low mass star at about 1 AU + close pair of M dwarfs at 9 arcsec). Our rotation period agrees with periods from the literature, e.g., Cutispoto & Rodonò (1988). The $v \sin i$ is from Wichmann et al. (2003).

TYC 7059 1111 1: our period is in good agreement with the literature value (Cutispoto et al. 2003). However, the derived $v_{eq} = 2\pi R/P$ is inconsistent with two independent measurements of $v \sin i$ which agree within errors ($41.5 \pm 3.5 \text{ km s}^{-1}$, Torres et al. 2006; 40 km s^{-1} , Tagliaferri et al. 1994).

HIP 26373 - HIP 26369 is a binary system whose components are separated by 18.3 arcsec and with $\Delta V = 1.9$. Our rotation period agrees with that from Cutispoto et al. (1999). The ASAS photometry does not resolve the component of this K0+K6 system.

HIP 27727: is a possible binary system, but to be confirmed yet. Our rotation period agrees with the period from the literature (Strassmeier et al. 1997).

TYC 7598 1488 1: our period is in good agreement with the literature value reported by Cutispoto et al. (2001). However, when it is combined with the stellar radius, the derived equatorial velocity is inconsistent with two independent measurements (Torres et al. 2006; Tagliaferri et al. 1994) which give the same value of $v \sin i$ (55 km s^{-1}). A larger stellar radius of about 3-4 R_{\odot} , as reported by Cutispoto (1998b) and based on a photometric distance $d > 86 \text{ pc}$, would partly solve the disagreement of v_{eq} with $v \sin i$.

HIP 30314: is a binary whose components are separated by 16.2 arcsec.

HIP 31711: is a binary whose components are separated by 0.8 arcsec and with $\Delta V = 2.3$. Since our periodogram shows several peaks of similar power, we adopt

the period from Cutispoto et al. (1999) which gives a reasonably smooth light curve.

TYC 1355 214 1: our rotation period agrees with that determined by Norton et al. (2007).

HIP 36108: is a binary whose components are separated by 1.20 arcsec and with $\Delta V = 1.2$

HIP 36349: is a binary whose components are separated by 0.3 arcsec and with $\Delta V = 1.9$. Our period agrees with the period $P = 1.642 \text{ d}$ of Koen & Eyer (2002) derived from the Hipparcos photometry.

HIP 76768: is a binary whose components are separated by 0.9 arcsec and with $\Delta V = 1.3$. Our period $P = 3.70 \text{ d}$ differs from the period $P = 0.336 \text{ d}$ reported in the ACVS, which is absent in our periodogram. The latter period, if correct, together with the $v \sin i = 8.0 \text{ km s}^{-1}$ would imply a pole-on orientation of the rotation axis.

BD-13 4687: the $v \sin i = 140.0 \text{ km s}^{-1}$ is from da Silva et al. (2009).

HIP 93375: is a binary whose components are separated by 11.2 arcsec (Torres et al. 2008). The $v \sin i$ is from Nordstrom et al. (2004).

HIP 94235: the $v \sin i$ is from Nordstrom et al. (2004).

TYC 1090-0543: our analysis gives a rotation period in agreement with the period $P = 2.2374 \text{ d}$ found by Norton et al. (2007).

HIP 106231: our period analysis revealed the most significant periodicity to be $P = 0.42312$, which is in agreement with the known LO Peg rotation period from either ACVS and literature (e.g., Jeffries et al. 1994). The $v \sin i$ is from Barnes et al. (2005).

HIP 113597: is a binary whose components are separated by 1.8 arcsec and with $\Delta V = 0.6$.

HIP 114530: is a binary whose components are separated by 19.6 arcsec and with $\Delta V = 4.2$.

PW And: the rotation period is taken from the literature (Strassmeier & Rice 2006), no ASAS photometry being available. The $v \sin i$ is from Strassmeier & Rice (2006).

HIP 26401: is a binary whose components are separated by 3.9 arcsec and with $\Delta V = 1.1$

HIP 63742: is an astrometric (Hipparcos) and spectroscopic (Gunther & Esposito 2007a) binary. We adopt the rotation period from Gaidos et al. (2000), no ASAS photometry being available. The $v \sin i$ is from Zuckerman et al. (2004).

HIP 86346: is a triple system whose brightest component has a close companion at 0.2 arcsec (Hortmuth et al. 2007) and a companion at 19.1 arcsec. We adopt the rotation period from Henry et al. (1995), no ASAS photometry being available. Both B-V and V-I colors are taken from Weis (1993). The $v \sin i$ is from Zuckerman et al. (2004).

HIP 114066: we adopt the rotation period of Koen & Eyer (2002), no ASAS photometry being available. The $v \sin i$ is from Zuckerman et al. (2004).

HIP 16563: is a binary whose components are separated by 9.5 arcsec and with $\Delta V = 2.9$. We adopt the rotation period of Messina (1998), no ASAS photometry being available.

HIP 12635-12638: is a binary whose components are separated by 14.6 arcsec and with $\Delta V = 1.5$.

HIP 110526AB: is a binary whose components are separated by 1.8 arcsec and with $\Delta V = 0.1$.

Acknowledgements

This work was supported by the Italian Ministero dell'Università, dell'Istruzione e della Ricerca (MIUR) and the Istituto Nazionale di Astrofisica (INAF). The extensive use of the SIMBAD and ADS databases operated by the CDS center, Strasbourg, France, is gratefully acknowledged. The Authors would like to thank Dr. G. Pojmański for the extensive use we made of the ASAS database. The Authors would like to thank the Referee for helpful comments.

References

- Alekseev, I.Y. 1996, *Astron. Rep.*, 40, 74
- Alencar, S.H.P., & Bathala, C. 2002, *ApJ*, 571, 378
- Allain, S. 1998, *A&A*, 333, 629
- Baraffe, I., Chabrier, G., Allard, F., & Hauschildt, P. 1998, *A&A*, 337,403
- Barnes, S., 2003, *ApJ*, 586, 464
- Barnes, J.R.; Collier Cameron, A., Lister, T.A., Pointer, G.R., Still, M.D. 2005, *MNRAS*, 356, 1501
- Bessel, M.S., 1979, *PASP*, 91, 589
- Beuzit, J.-L., Feldt, M., Dohlen, K., et al. 2008, *Ground-based and Airborne Instrumentation for Astronomy II*. Ed. McLean, I. S., & Casali, M. M. *Proceedings of the SPIE*, Volume 7014, 701418
- Billar, B.A., Close, L.M., Masciadri, E., et al. 2007, *ApJS*, 173, 143
- Bouvier, J. 2008, *A&A*,489, 53
- Burrows, A., Marley, M., Hubbard, W. B et al. 1997, *ApJ*, 491, 856
- Chauvin, G., Thomson, M., Dumas, C., et al. 2003, *A&A*, 404, 157
- Chauvin G., Lagrange A.-M., Zuckerman B., et al. 2005, *A&A*, 438, 29C
- Chauvin, G., Lagrange, A. -M., Bonavita, M., et al. 2009., *A&A*, 2010, 509, 52
- Collier Cameron, A., Davidson, V.A., Hebb, L., et al. 2009, *MNRAS*, Cutispoto, G., & Rodonó, M. 1988, *IBVS*, 3232
- Cutispoto, G. 1998a, *A&AS* 127, 207
- Cutispoto, G. 1998b, *A&AS* 131, 321
- Cutispoto, G.; Pastori, L.; Tagliaferri, G.; Messina, S.; Pallavicini, R. 1999, *A&AS*, 138, 87
- Cutispoto, G., Pastori, L., Guerrero, A. et al. 2000 *A&A*, 364, 205
- Cutispoto, G., Messina, S., & Rodonó, M. 2001, *A&A*, 367, 910
- Cutispoto, G., Pastori, L., Pasquini, L. et al. 2002 *A&A*, 384, 491
- Cutispoto, G., Messina, S., Rodonó, M. 2003, *A&A*, 400, 659
- da Silva, L., Torres, C.A.O., de la Reza, R. et al. 2009, *A&A*, 508, 833
- De La Reza, R. & Pinzon, G. 2004, *AJ*, 128, 1812
- Delfosse, X., Forveille, T., Beuzit, J.-L., et al. 1999, *A&A*, 344, 897
- Favata, F., Barbera, M., Micela, G., Sciortino, S. 1995 *A&A* 295, 147
- Feigelson E.D., Lawson W.A., Stark M., Townsley L. & Garmire G.P. 2006, *AJ*, 131, 1730
- Gaidos, E. J.; Henry, G. W.; Henry, S. M., 2000, *AJ*, 120, 1006
- Guenther, E. W., Esposito, M., Mundt, R., et al. 2007, *A&A*, 467,1147
- Guenther, E. W. & Esposito, M. arXiv:0701293
- Jeffries, R. D., Byrne, P. B., Doyle, J. G., et al. 1994, *MNRAS*, 270, 153
- Hartman, J. D., Gaudi, B. S., Pinsonneault, M. H., et al. 2009, *ApJ*, 691,342
- Hebb, L., Petro, L., Ford, H.C., et al. 2007, *MNRAS*, 379, 63
- Henry, Gregory W.; Fekel, Francis C.; Hall, Douglas S., 1995, *AJ*, 110, 2926
- Herbst, W., & Wittenmyer, R. 1996, *BAAS*, 28, 1338
- Herbst, W., Bailer-Jones, C. A. L., Mundt, R., Meisenheimer, K., & Wackermann, R. 2002, *A&A*, 396, 513
- Herbst, W., & Mundt, R. 2005, *ApJ*, 633, 967
- Herbst, W., Eislöffel, J., Mundt, R., & Scholz, A. 2007, *Protostars and Planets V*, B. Reipurth, D. Jewitt, and K. Keil (eds.), University of Arizona Press, Tucson, 951 pp., 2007., p.297-311
- Hodgkin, S.T., Irwin, J.M., Aigrain, S., et al. 2006, *AN*, 327, 9
- Hormuth, F., Brandner, W., Hippler, S., Janson, M., & Henning, T., 2007, *A&A*, 463, 707
- Horne, J.H., & Baliunas, S.L. 1986, *ApJ*, 302, 757
- Kasper, M., Apai, D., Janson, M., Brandner, W. 2007 *A&A*, 472, 321
- Kawaler, S.D., 1988, *ApJ*, 333,236
- Keppens, R., MacGregor, K. B., & Charbonneau, P. 1995, *A&A*, 294, 469
- Koen, C., Eyer, L, 2002, *MNRAS*, 331,45
- Konopacky, Q. M., Ghez, A. M., Duchne, G., McCabe, C., Macintosh, B. A. 2007, *AJ*, 133, 2008
- Kovacs, G. 1981, *Ap&SS*, 78, 175
- Krishnamurthi, A., Pinsonneault, M.H., Barnes, S. & Sofia, S. 1997, *ApJ*, 480, 303
- Innis, J.; Coates, D. W.; Kaye, T. G.; Borisova, A.; Tsvetkov, M. , 2007, *Peremennye Zvezdy*, vol.27, no. 4.
- Irwin, J., Aigrain, S., Bouvier, J., et al. 2009, *MNRAS*, 392, 1456
- Lamm, M. H., Bailer-Jones, C. A. L., Mundt, R., Herbst, W., & Scholz, A. 2004, *A&A*, 417, 557
- Lanza, A.F., Bonomo, A.S., Moutou, C., et al. 2010, *A&A*, submitted
- Lanza, A.F. 2010, *A&A*, in press, 2009arXiv0912.4585L
- Lawson, W. A., & Crause, L.A., 2005, *MNRAS*, 357,1399
- Lepine, S., & Simon, M., 2009, *AJ*,137, 3632
- Lowrance, P. J., McCarthy, C., Becklin, E. E., 1999, *ApJ*, 512, 69
- Luhman, K.L., Stauffer, J.R., & Mamajek, E.E., 2005, *ApJ*, 628, L69
- MacGregor, K.B., & Brenner, M. 1991, *ApJ*, 376, 204
- Marois, C., Macintosh, B., Barman, T. et al. 2008, *Sci* 322, 1348
- Messina, S., 1998, PhD Thesis, University of Catania
- Messina, S., Rodonó, M., & Guinan, E. F. 2001, *A&A*, 366,215
- Messina, S., Pizzolato, N., Guinan, E. F., & Rodonó, M 2003, *A&A*, 410,671
- Messina, S., Rodonó, M., & Cutispoto, G. 2004, *AN*, 325, 660
- Messina, S., 2007, *Memorie Società Astron. It.*, 78, 628
- Messina, S., Distefano, E., Parihar, P., et al. 2008, *A&A*, 483, 253
- Messina, S., Parihar, P., Koo, J.-R. et al. 2009, *A&A*, in press
- Neuhuser, R., Guenther, E. W., Alves, J., et al. 2003, *AN*, 324, 535
- Nielsen, E.L. & Close, L.M. 2009, arXiv:0909.4531
- Nordstrom, B., Mayor, M., Andersen, J. et al. 2004, *A&A* 418, 989
- Norton, A. J.; Wheatley, P. J.; West, R. G., et al. 2007, *A&A*, 467, 785
- O'Dell, M. A., Hendry, M. A., & Collier Cameron, A. 1994, *MNRAS*, 268, 181
- Ortega, V.G., Jilinski, E., de la Reza, R., & Bazzanella, B. 2007, *MNRAS*, 377, 441
- Parihar, P., Messina, S., Distefano, E., Shantikumar N., S., & Medhi, B. J. , 2009, *MNRAS*, 400, 603
- Pasquini, L., Cutispoto, G., Gratton, R., Mayor M. 1991, *A&A* 248, 72, 80
- Perryman, M. A. C., Lindegren, L., Kovalevsky, J., et al. 1997, *A&A*, 323, 49
- Pojmanski G., 1997, *Acta Astronomica*, 47, 467
- Pojmanski G., 1998, *Acta Astronomica*, 48, 35
- Pojmanski G., 2002, *Acta Astronomica*, 52, 397
- Pojmanski G., 2003, *Acta Astronomica*, 53, 341
- Pont, F. 2009, *MNRAS*, 396, 1789
- Press, W.H., Teukolsky, S.A., Vetterling, W.T., & Flannery, B.P., 1992, *Numerical Recipes*, Cambridge University
- Prosser, C.F., Stauffer, J., & Kraft R.P. 1991. *AJ*, 101, 1361
- Quast, G. R., Torres, C.A. O., de La Reza, R. et al. 2000, *IAU Symp.* 200 'The Formation of Binary Stars' Ed. Bo Reipurth and Hans Zinnecker, 28.
- Radick, R.R., Thompson, D.T., Lockwood, G.W., Duncan, D.K., & Bagget, W.E., 1987, *ApJ*, 321, 459
- Rebull, L.M., Madikon, R.B., Strom, S.E., et al. 2002, *AJ*, 123, 1528
- Rebull, L.M., Wolff, S.C., & Strom, S.E. 2004, *AJ*, 127, 1029
- Reid, N. 2003 *MNRAS* 342, 837
- Rhode, K.L., Herbst, W., & Mathieu, R.D., 2001, *AJ*, 122, 3258
- Rodonó, M., Cutispoto, G., Pazzani, V., et al. 1986, *A&A*, 165, 135
- Rucinski, S. M., & Krautter, J., 1983, *A&A*, 121, 217
- Rucinski, S. M., Slavek, M., Matthews, J.M., et al. 2008, *MNRAS*, 391, 1913
- Scargle, J.D., 1982, *ApJ*, 263, 835
- Schwarnberg-Czerny, A. 1989, *MNRAS*, 241, 153
- Scholz, A., Coffey, J., Brandeker, A., & Jayawardhana, R. 2007, *ApJ*, 662,1254
- Scholz, A., Eisloffel, J., & Mundt, R., 2009, *MNRAS*.tmp 1474
- Setiawan, J., Weise, P., Henning, Th., et al. 2008, in *Precision Spectroscopy in Astrophysics*, Edited by N.C. Santos, L. Pasquini, A.C.M. Correia, and M. Romaniello, p. 201 (arxiv 0704.2145)
- Skelly M.B., Unruh, Y.C., Collier Cameron, A. et al. 2008, *MNRAS* 385, 708
- Stassun, K.G., Mathieu, R.D., Mazeh, T., & Vrba, F. 1999, *AJ*, 117, 2941
- Stauffer, J.R. 1982a, *AJ* 87, 899
- Stauffer, J.R. 1982b *AJ* 87, 1507

- Stauffer, J.R. 1984, ApJ, 280, 189 Optical and infrared photometry of late type stars in the Pleiades 1984ApJ...280..189S
- Stauffer, J.R., Hartmann, L.W., Burnham, J.N., & Jones B.F. 1985, ApJ, 289, 247
- Stauffer, J.R., Hartmann, L.W., & Jones B.F. 1989, ApJ, 346, 160
- Strassmeier K.G., Bartus J., Cutispoto G. & Rodonò M., 1997, A&AS, 125, 11
- Strassmeier, K.G. & Rice J.B 2000 A&A 360, 1019
- Strassmeier, K. G.; Rice, J. B., 2006, A&A, 460, 715
- Tagliaferri, G., Cutispoto, G., Pallavicini, R., Randich, S., Pasquini, L. 1994, A&A 285, 272
- Teixeira, R., Ducourant, C., Chauvin, G. et al. 2009, A&A 503, 281
- Torres, G., Stefanik, R. P., Latham, D.W., & Mazeh, T. 1995, ApJ, 452, 870
- Torres, C.A.O., Quast, G.R., da Silva, L. et al. 2006, A&A, 460, 695
- Torres, C.A.O., Quast, G.R., Melo, C.H.F., Sterzik, M.F. 2008, Handbook of Star Forming Regions, Volume II: The Southern Sky ASP Monograph Publications, Vol. 5. Edited by Bo Reipurth, p.757 (arXiv:0808.3362)
- Urban, S. E., Corbin, T. E., & Wycoff, G. L. 1998, AJ, 115, 2161
- Viana Almeida, P., Santos, N.C., Melo, C. et al. 2009, A&A, 501, 965
- von Braun, Lee, B.L., Seager, S., et al. 2005, PASP, 117, 141
- Weis, E.W. 1993, AJ, 195, 1962
- Wichmann, R., Schmitt, J.H.M.M., Hubrig, S. 2003, A&A 399, 983
- Zuckerman, B. & Song, I. 2004, Ann. Rev. Astron. Astr. 42, 685
- Zuckerman, B., Song, I., Bessell, M.S 2004, ApJ 613, L65
- Zuckerman, B., Bessell, M.S., Song, I., Kim, S. 2006, ApJ 649, L11

Online Material

Table A.1 TW Hydrae association. Summary data from the literature and mass derived from evolutionary tracks. Note n1=1 indicates that V–I is derived from B–V; note n2=m indicates a confirmed member.

name	RA (2000.0)	DEC (2000.0)	V (mag)	B–V (mag)	V–I (mag)	M _V (mag)	d (pc)	$v \sin i$ (km s ⁻¹)	Mass (M _⊙)	Radius (R _⊙)	Sp.T	mgr	n1	n2	
TWHya	HIP53911	11 1 51.90	-34 42 17.0	10.50	0.97	1.70	6.88	53.00	6.00	1.0	1.4	K6Ve	TWA	–	m
TWA2	CD-298887	11 9 13.80	-30 1 40.0	11.07	1.48	2.24	8.01	41.00	12.60	0.6	1.5	M2Ve	TWA	–	m
TWA4	HIP55505	11 22 5.30	-24 46 40.0	9.42	1.17	1.39	6.20	44.00	8.90	1.0	1.2	K5V	TWA	–	m
TWA5A	CD-337795	11 31 55.30	-34 36 27.0	12.12	1.47	2.36	8.85	45.00	53.50	0.4	1.1	M2Ve	TWA	–	m
TWA7	GSC7190-2111	10 42 30.10	-33 40 17.0	11.65	1.46	2.44	9.41	28.00	4.40	0.3	1.0	M2Ve	TWA	–	m
TWA8A	CD-268623A	11 32 41.20	-26 51 56.0	12.23	1.46	2.41	9.27	39.00	6.60	0.4	1.0	M3Ve	TWA	–	m
TWA8B	xxxxx	11 32 41.16	-26 52 9.00	15.20	1.50	3.72	12.19	40.00	11.00	0.2	0.6	M6	TWA	–	m
TWA9A	HIP57589	11 48 24.30	-37 28 49.0	11.26	1.26	1.62	7.10	68.00	11.26	0.9	1.1	K5V	TWA	–	m
TWA9B	CD-387429B	11 48 24.30	-37 28 49.0	14.00	1.43	2.58	9.84	68.00	8.39	0.3	0.9	M1V	TWA	–	m
TWA10	GSC7766-0743	12 35 4.20	-41 36 39.0	12.96	1.43	2.47	9.38	52.00	3.00	0.3	1.0	M2Ve	TWA	–	m
TWA13A	CD-347390A	11 21 17.20	-34 46 46.0	11.46	1.42	1.89	7.76	55.00	12.30	0.8	1.1	M1Ve	TWA	–	m
TWA13B	CD-347390B	11 21 17.40	-34 46 50.0	11.96	1.47	2.08	8.26	55.00	12.00	0.7	1.0	M5	TWA	–	m
TWA20	xxx	12 31 38.10	-45 58 59.0	13.00	1.10	2.30	8.68	73.00	30.00	0.5	1.0	M2	TWA	–	m
TWA25	CD-397538	12 15 30.70	-39 48 43.0	11.44	1.41	1.94	7.90	51.00	12.90	0.8	1.1	M1Ve	TWA	–	m

Table A.2 β Pictoris association. Summary data from the literature and mass derived from evolutionary tracks. Note n1=1 indicates that V–I is derived from B–V; note n2=m indicates a confirmed member.

name	RA (2000.0)	DEC (2000.0)	V (mag)	B–V (mag)	V–I (mag)	M _V (mag)	d (pc)	$v \sin i$ (km s ⁻¹)	Mass (M _⊙)	Radius (R _⊙)	Sp.T	mgr	n1	n2	
HIP12545	BD+05378	2 41 25.90	5 59 18.0	10.37	1.21	1.59	7.41	39.00	40.00	0.8	0.9	K6Ve	BPIC	–	m
HIP23200	V1005Ori	4 59 34.83	1 47 0.68	10.05	1.39	1.84	8.15	24.00	14.00	0.7	0.8	M0.5Ve	BPIC	–	m
HIP23309	CD-571054	5 0 47.10	-57 15 25.0	10.00	1.40	1.79	7.91	26.20	5.80	0.8	1.0	M0Ve	BPIC	–	m
HIP23418	GJ3322	5 1 58.80	9 59 0.00	11.45	1.54	2.46	8.79	34.00	7.67	0.4	1.2	M3V	BPIC	–	m
HIP29964	HD45081	6 18 28.20	-72 2 41.0	9.80	1.13	1.32	6.87	38.60	16.40	0.8	0.8	K4Ve	BPIC	–	m
HIP76629	HD139084A	15 38 57.50	-57 42 27.0	7.97	0.81	0.95	4.98	39.70	16.60	1.0	1.2	K0V	BPIC	–	m
HIP84586	HD155555AB	17 17 25.50	-66 57 4.00	7.23	0.76	0.84	4.75	31.40	31.00	1.0	1.2	G5IV	BPIC	–	m
TYC872822621	CD-547336	17 29 55.10	-54 15 49.0	9.55	0.85	0.95	5.45	66.00	35.30	1.0	1.0	K1V	BPIC	–	m
TYC874220651	HD161460	17 48 33.70	-53 6 43.0	9.61	0.83	0.86	5.26	74.00	10.00	1.0	1.0	K0IV	BPIC	–	m
V4046Sgr	HD319139	18 14 10.50	-32 47 33.0	10.44	0.95	1.33	6.15	72.00	14.2	1.0	1.2	K5	BPIC	–	m
HIP89829	HD168210	18 19 52.20	-29 16 33.0	8.89	0.69	0.78	4.51	75.20	114.70	1.0	1.3	G1V	BPIC	–	m
TYC907307621	AC4357199	18 46 52.60	-62 10 36.0	12.08	1.46	2.09	8.46	53.00	9.90	0.6	1.1	M1Ve	BPIC	–	m
TYC740800541	CD-3116041	18 50 44.50	-31 47 47.0	11.20	1.35	1.76	7.71	50.00	49.70	0.8	0.9	K8Ve	BPIC	–	m
HIP92680	HD174429	18 53 5.90	-50 10 50.0	8.29	0.77	0.85	4.80	49.80	69.00	1.0	1.2	K8Ve	BPIC	–	m
TYC687210111	AC3111475	18 58 4.20	-29 53 5.00	11.78	1.30	1.80	7.32	78.00	33.80	0.9	1.2	M0Ve	BPIC	–	m
TYC687801951	CD-2613904	19 11 44.70	-26 4 9.00	10.27	1.05	1.18	5.78	79.00	9.80	1.0	1.0	K4V(e)	BPIC	–	m
HIP102141A	HD196982	20 41 51.20	-32 26 7.00	10.99	1.54	2.99	11.10	9.50	10.10	0.2	0.8	M4+M4	BPIC	–	m
HIP102409	HD197481	20 45 9.50	-31 20 27.0	8.73	1.49	2.09	8.75	9.90	9.30	0.6	0.8	M1Ve	BPIC	–	m
TYC634902001	HD358623	20 56 2.70	-17 10 54.0	10.62	1.22	1.49	7.31	46.00	15.60	0.8	0.9	K6Ve+M	BPIC	–	m
TYC934004371	CP-722713	22 42 48.90	-71 42 21.0	10.60	1.35	1.73	7.82	36.00	7.50	0.8	1.0	K7Ve+K	BPIC	–	m
HIP112312	GJ871.1A	22 44 58.00	-33 15 2.00	11.70	1.48	2.80	10.19	20.00	12.10	0.2	1.0	M4IVe	BPIC	–	m
TYC583206661	BD-136424	23 32 30.90	-12 15 52.0	10.54	1.43	1.98	8.30	28.00	8.80	0.7	M0Ve	0.9	BPIC	–	m
HIP11437	BD+30397A	2 27 29.25	30 58 24.6	10.12	1.21	1.34	6.95	43.00	5.00	0.8	K8	0.8	BPIC	–	m
GJ3305	RBS561	4 37 37.30	-2 29 28.0	10.59	1.45	2.00	8.22	29.80	5.30	0.7	1.0	M0.5	BPIC	–	m
BD-211074A	GJ3331A	5 6 49.90	-21 35 9.00	10.29	1.52	2.43	9.01	18.00	999.00	0.4	1.2	M2	BPIC	1	m

Table A.3 Tucana/Horologium association. Summary data from the literature and mass derived from evolutionary tracks. Note n1=1 indicates that V–I is derived from B–V; note n2=m indicates a confirmed member; n2=n indicates a rejected member.

name	RA (2000.0)	DEC (2000.0)	V (mag)	B–V (mag)	V–I (mag)	M _V (mag)	d (pc)	$v \sin i$ (km s ⁻¹)	Mass (M _⊙)	Radius (R _⊙)	Sp.T	mgr	n1	n2	
HIP1113	HD987	0 13 53.00	-74 41 18.0	8.78	0.74	0.82	5.57	43.90	7.30	1.0	1.0	G8V	TUC	–	m
HIP1910	GSC8841-0065	0 24 9.00	-62 11 4.00	11.55	1.40	1.77	8.33	44.00	20.90	0.7	0.8	M0Ve	TUC	–	m
HIP1993	GSC8841-1145	0 25 14.70	-61 30 48.0	11.47	1.35	1.81	8.30	43.00	7.30	0.7	0.8	M0Ve	TUC	–	m
HIP2729	HD3221	0 34 51.20	-61 54 58.0	9.61	1.05	1.10	6.30	45.90	122.80	0.9	0.8	K4Ve	TUC	–	m
TYC935111101	CD-7824	0 42 20.30	-77 47 40.0	10.21	1.06	1.22	6.72	50.00	19.50	0.8	0.8	K3Ve	TUC	–	m
HIP6485	HD8558	1 23 21.30	-57 28 51.0	8.51	0.68	0.77	5.05	49.30	13.80	1.0	1.1	G7V	TUC	–	m
HIP9141	HD12039	1 57 49.00	-21 54 5.00	8.00	0.65	0.72	4.86	42.40	15.00	1.0	1.2	G4V	TUC	–	m
HIP9892	HD13183	2 7 18.10	-53 11 56.0	8.63	0.65	0.76	5.12	50.30	24.00	1.0	1.1	G7V	TUC	–	m
TYC849709951	CD-58553	2 42 33.00	-57 39 37.0	10.98	1.23	1.47	7.49	50.00	5.60	0.7	0.7	K5Ve	TUC	–	m
TYC702603251	CD-351167	3 19 8.70	-35 7 0.00	11.12	1.30	1.58	7.90	44.00	6.10	0.7	0.7	K7Ve	TUC	1	m
TYC806016731	CD-461064	3 30 49.10	-45 55 57.0	9.63	0.95	1.06	6.41	44.00	10.0	0.9	0.9	K3V	TUC	1	m
TYC757408031	CD-441173	3 31 55.70	-43 59 14.0	10.90	1.30	1.58	7.78	42.00	10.70	0.7	0.8	K6Ve	TUC	–	m
TYC5907-1244-1	BD-20951	4 52 49.50	-19 55 2.00	10.12	0.87	0.98	5.83	72.00	999.00	0.9	0.9	XX	TUC	1	m
TYC5908-230-1	BD-191062	4 59 32.00	-19 17 42.0	10.60	1.20	1.37	6.44	68.00	999.00	1.0	1.2	XX	TUC	1	m
BD-091108	xxxxx	5 15 36.50	-9 30 51.0	9.79	0.67	0.95	5.33	78.00	999.00	1.0	1.1	G5	TUC	–	m
TYC704814531	CD-302310	5 18 29.00	-30 1 32.0	11.66	1.27	1.53	7.56	66.00	7.10	0.8	0.7	K4Ve	TUC	–	m
HIP105388	HD202917	21 20 50.00	-53 2 3.00	8.69	0.72	0.80	5.38	45.90	15.40	1.0	1.0	G7V	TUC	–	m
HIP107345	GSC9116-1363	21 44 30.10	-60 58 39.0	11.61	1.41	1.83	8.25	47.00	8.20	0.7	0.8	M0Ve	TUC	–	m
TYC934402931	AC4600438	23 26 10.70	-73 23 50.0	11.82	1.39	1.91	8.51	46.00	61.00	0.7	0.8	XX	TUC	–	m
HIP116748A	HD222259A	23 39 39.50	-69 11 45.0	8.49	0.70	0.77	5.16	46.30	18.30	1.0	1.1	G6V+K3	TUC	–	m
RBS332	GSC8056-0482	2 36 51.70	-52 3 4.00	12.11	1.48	2.33	9.38	35.10	36.00	0.4	0.9	M2V	TUC	–	n
TYC760005161	CD-392075	5 37 5.30	-39 32 26.0	9.52	0.80	0.97	5.87	53.80	20.40	0.9	0.9	K1V(e)	TUC	–	n
TYC706508791	CD-342406	5 42 34.30	-34 15 42.0	11.35	0.82	0.93	6.04	115.10	14.20	0.9	0.9	K0V	TUC	–	n
HIP105404	HD202947	21 20 59.80	-52 28 40.0	9.82	0.88	1.04	6.50	46.10	12.80	0.8	0.8	G9V	TUC	–	n
HIP16853	HD22705	3 36 53.40	-49 57 28.9	7.62	0.59	0.66	4.52	41.70	19.00	1.0	1.3	G2V	TUC	–	m
HIP21632	HD29615	4 38 43.90	-27 2 2.00	8.47	0.61	0.68	4.78	54.60	17.53	1.0	1.2	G3V	TUC	–	m

Table A.4 Columba association. Summary data from the literature and mass derived from evolutionary tracks. Note n1=1 indicates that V–I is derived from B–V; note n2=m indicates a confirmed member.

name	RA (2000.0)	DEC (2000.0)	V (mag)	B–V (mag)	V–I (mag)	M_V (mag)	d (pc)	$v \sin i$ (km s ⁻¹)	Mass (M_\odot)	Radius (R_\odot)	Sp.T	mgr	n1	n2	
TYC804702321	CD-52381	1 52 14.60	-52 19 33.0	10.89	0.95	1.08	6.07	92.00	19.80	0.9	0.9	K2V(e)	COL	–	m
BD-16351	xxx	2 1 35.60	-16 10 0.00	10.40	1.10	1.25	5.94	78.00	999.00	1.0	1.2	K5	COL	1	m
TYC755806551	CD-44753	2 30 32.40	-43 42 23.0	10.42	1.07	1.22	6.84	52.00	7.00	0.8	0.8	K5V(e)	COL	1	m
HIP16413	HD21955	3 31 20.80	-30 30 59.0	9.93	0.64	0.73	4.50	122.00	22.30	1.0	1.3	G7IV	COL	–	m
HIP19775	HD26980	4 14 22.60	-38 19 2.00	9.08	0.58	0.65	4.50	82.60	13.90	1.0	1.3	G3V	COL	–	m
TYC645727311	HD27679	4 21 10.30	-24 32 21.0	9.43	0.62	0.69	5.05	75.00	11.00	1.0	1.3	G2V	COL	1	m
TYC758416301	CD-431395	4 21 48.70	-43 17 33.0	10.18	0.69	0.77	4.40	143.00	25.70	1.0	1.3	G7V	COL	–	m
TYC704405351	CD-361785	4 34 50.80	-35 47 21.0	10.84	0.84	0.99	6.41	77.00	9.10	0.9	0.9	K1Ve	COL	–	m
TYC807706571	HD31242	4 51 53.50	-46 47 13.0	9.85	0.69	0.76	5.56	72.00	999.00	1.0	1.0	G5V	COL	–	m
TYC808012061	HD272836	4 53 5.20	-48 44 39.0	10.78	0.87	1.00	6.38	76.00	999.90	0.9	0.9	K2V(e)	COL	1	m
HIP25709	HD36329	5 29 24.10	-34 30 56.0	9.18	0.65	0.71	4.82	74.60	8.30	1.0	1.2	G3V	COL	–	m
TYC650211881	CD-292531	5 50 21.40	-29 15 21.0	11.31	0.66	0.74	5.44	149.00	999.00	1.0	1.0	K0V(e)	COL	1	m
TYC761705491	CD-402458	6 26 6.90	-41 2 54.0	10.00	0.80	0.92	5.20	91.00	11.60	1.0	1.0	K0V	COL	1	m
TYC710021121	CD-363202	6 52 46.70	-36 36 17.0	11.22	0.62	0.69	5.57	135.00	170.00	1.0	1.0	K2V(e)	COL	1	m
TYC811808711	HD51797	6 56 23.50	-46 46 55.0	9.84	0.78	0.89	5.46	75.00	15.60	1.0	1.0	K0V(e)	COL	1	m
TYC762928241	CD-393026	7 1 51.80	-39 22 4.00	11.05	0.63	0.70	4.67	189.00	999.00	1.0	1.2	G9V(e)	COL	1	m
AGLep	BD-191194	5 30 19.00	-19 16 3.00	9.62	0.60	0.66	4.39	111.00	20.00	1.0	1.3	G5V	COL	1	m
TYC588211691	BD-15705	4 2 16.50	-15 21 30.0	10.17	1.01	1.12	6.72	49.00	6.80	0.8	0.8	K3/4!	COL	1	m

Table A.5 Carina association. Summary data from the literature and mass derived from evolutionary tracks. Note n1=1 indicates that V–I is derived from B–V; note n2=m indicates a confirmed member.

name	RA (2000.0)	DEC (2000.0)	V (mag)	B–V (mag)	V–I (mag)	M_V (mag)	d (pc)	$v \sin i$ (km s ⁻¹)	Mass (M_\odot)	Radius (R_\odot)	Sp.T	mgr	n1	n2	
TYC939003221	HD42270	5 53 29.30	-81 56 53.0	9.14	0.79	0.97	5.29	59.00	30.30	1.0	1.2	K0V+VI	CAR	–	m
TYC855910161	CD-571709	7 21 23.70	-57 20 37.0	10.72	0.64	0.76	5.72	100.00	11.70	0.9	1.0	K0V+D	CAR	1	m
TYC892909271	CD-63408	8 24 6.00	-63 34 3.00	9.87	0.63	0.75	4.78	104.00	73.00	1.0	1.2	G5V	CAR	–	m
TYC856917611	CP-531875	8 45 52.70	-53 27 28.0	10.29	0.63	0.75	4.48	145.00	45.00	1.0	1.0	G2V	CAR	1	m
TYC939521391	CD-75392	8 50 5.40	-75 54 38.0	10.59	0.76	0.82	5.57	101.00	43.80	1.0	1.0	G9V	CAR	–	m
TYC856935971	CD-532515	8 51 56.40	-53 55 57.0	11.06	0.69	0.79	5.31	141.00	29.00	1.0	1.0	G9V	CAR	–	m
TYC816009581	CD-494008	8 57 52.20	-49 41 51.0	10.51	0.73	0.80	5.28	111.00	33.20	1.0	1.0	G9V	CAR	–	m
TYC858605181	CP-551885	9 0 3.40	-55 38 24.0	10.83	0.68	0.78	5.40	122.00	44.00	1.0	1.0	G5V	CAR	–	m
TYC858711261	CD-552543	9 9 29.40	-55 38 27.0	10.20	0.73	0.83	4.58	133.00	14.60	1.0	1.3	G8V	CAR	1	m
TYC858722901	CD-542644	9 13 16.90	-55 29 3.00	11.36	0.66	0.79	5.76	132.00	39.50	0.9	1.0	G5V(e)	CAR	–	m
HIP46063	HD81544	9 23 35.00	-61 11 36.0	10.86	0.86	0.96	6.22	84.70	14.70	0.9	0.9	K1V(e)	CAR	–	m
TYC894612251	CP-621293	9 43 8.80	-63 13 4.00	10.44	0.68	0.82	6.01	77.00	35.30	0.9	0.9	G6V	CAR	–	m
HIP30034	HD44627	6 19 12.90	-58 3 16.0	9.13	0.86	0.90	5.84	45.50	11.50	0.9	0.9	K1V(e)	CAR	–	m
HIP32235	HD49855	6 43 46.20	-71 58 35.0	8.94	0.70	0.76	5.18	56.50	12.40	1.0	1.1	G6V ^a	CAR	–	m
HIP33737	HD55279	7 0 30.50	-79 41 46.0	10.11	0.91	0.95	6.08	64.10	9.30	0.9	0.9	K2V ^a	CAR	–	m

Table A.6 AB Doradus association. Summary data from the literature and mass derived from evolutionary tracks. Note n1=1 indicates that V–I is derived from B–V; note n2=m indicates a confirmed member.

name		RA	DEC	V	B–V	V–I	M _V	d	$v \sin i$	Mass	Radius	Sp.T	mgr	n1	n2
		(2000.0)	(2000.0)	(mag)	(mag)	(mag)	(mag)	(pc)	(km s ⁻¹)	(M _⊙)	(R _⊙)				
HIP5191	HD6569	1 6 26.15	-14 17 47.1	9.50	0.91	0.95	6.01	50.00	10.00	0.9	0.9	K1V	ABDOR	-	m
TYC804210501	CD-46644	2 10 55.40	-46 3 59.0	11.24	0.91	1.16	6.53	87.40	36.00	0.9	0.8	K3IVe	ABDOR	-	m
HIP10272	HD13482	2 12 15.41	23 57 29.5	7.94	1.13	0.93	5.39	32.30	6.00	1.0	1.1	K1	ABDOR	-	m
HIP14684	ISEri	3 9 42.30	-9 34 47.0	8.48	0.81	0.84	5.46	40.20	7.00	1.0	1.0	G0	ABDOR	-	m
HIP17695	EUVEJ0347-01.9	3 47 23.34	-1 58 19.9	11.59	1.51	2.16	10.53	16.30	18.00	0.4	0.4	M3	ABDOR	-	m
HIP22738AB	CD-561032B	4 53 30.50	-55 51 32.0	11.16	1.56	2.56	10.91	11.20	999.00	0.2	0.6	M3Ve	ABDOR	-	m
TYC758709251	CD-401701	5 2 30.40	-39 59 13.0	10.57	0.88	1.02	6.24	73.60	6.80	0.9	0.9	K4V	ABDOR	1	m
HIP25283	HD35650	5 24 30.17	-38 58 10.7	9.08	1.25	1.42	7.84	17.70	4.00	0.7	0.7	K6V	ABDOR	1	m
HIP25647	HD36705A	5 28 44.83	-65 26 54.8	6.74	0.83	0.94	5.87	14.90	53.00	0.9	0.9	K0V	ABDOR	-	m
TYC705911111	UXCol	5 28 56.50	-33 28 16.0	10.46	1.06	1.25	6.90	51.50	41.50	0.8	0.8	K3Ve	ABDOR	-	m
HIP26373	HD37572	5 36 56.85	-47 57 52.8	7.86	0.85	0.88	5.93	24.30	17.70	0.9	0.9	K0V	ABDOR	-	m
CP-19878	xxxx	5 39 23.20	-19 33 29.0	10.71	0.91	1.06	6.45	71.00	32.00	0.9	0.9	K1V	ABDOR	-	m
HIP27727	HD39576	5 52 16.00	-28 39 25.0	9.04	0.63	0.69	4.33	87.70	20.90	1.0	1.3	G3V	ABDOR	-	m
TYC759814881	TYCol	5 57 50.80	-38 4 3.00	9.56	0.69	0.82	5.26	72.50	55.00	1.0	1.0	G6V(e)	ABDOR	-	m
TYC707900681	CD-342676	6 8 33.90	-34 2 55.0	10.17	0.79	0.86	5.55	83.80	4.70	1.0	1.0	G9Ve	ABDOR	1	m
TYC708407941	CD-352722	6 9 19.20	-35 49 31.0	10.98	1.69	2.56	12.40	5.20	13.00	0.2	0.3	M1Ve	ABDOR	1	m
HIP31878	CD-611439	6 39 50.02	-61 28 41.5	9.71	1.26	1.53	8.01	21.90	12.00	0.7	0.7	K7V(e)	ABDOR	-	m
UCAC206727592	GSC8544-1037	6 47 53.40	-57 13 32.0	11.50	0.90	1.20	6.49	100.30	7.00	0.9	0.8	K4V	ABDOR	-	m
TYC855811481	CD-571654	7 10 50.60	-57 36 46.0	10.44	0.68	0.70	4.80	134.50	29.20	1.0	1.2	G2V	ABDOR	1	m
TYC1355-214-1	BD+201790	7 10 50.60	-57 36 46.0	9.93	1.15	1.34	7.84	26.20	0.00	0.7	0.7	K3	ABDOR	1	m
HIP36108	HD59169	7 26 17.70	-49 40 51.0	10.22	0.43	0.61	4.87	117.60	11.00	1.0	1.2	G7V	ABDOR	1	m
HIP36349	V372Pup	7 28 51.37	-30 14 48.5	9.96	1.44	1.78	8.99	15.60	20.50	0.6	0.6	M1Ve	ABDOR	-	m
TYC949308381	CD-8480	7 30 59.50	-84 19 28.0	9.96	0.83	0.93	5.73	70.20	3.00	1.0	1.0	G9V	ABDOR	1	m
HIP76768	HD139751	15 40 28.39	-18 41 46.1	10.44	1.24	1.40	7.56	37.60	8.00	0.7	0.7	K3/K4V	ABDOR	-	m
HIP81084	LP745-70	16 33 41.61	-9 33 11.9	11.30	1.44	1.77	8.78	31.90	7.00	0.6	0.6	M0.5	ABDOR	-	m
TYC737902791	HD317617	17 28 55.60	-32 43 57.0	10.45	0.93	1.10	6.71	56.00	4.00	0.8		XX	ABDOR	1	m
BD-134687	HD159911	17 37 46.47	-13 14 46.6	10.17	0.93	1.10	6.31	59.10	140.00	0.9	0.9	K3/K4I	ABDOR	1	m
HIP93375	HD176367	19 1 6.00	-28 42 50.0	8.48	0.56	0.62	4.49	62.90	17.00	1.0	1.3	G1V	ABDOR	-	m
HIP94235	HD178085	19 10 57.90	-60 16 20.0	8.34	0.59	0.66	4.56	57.10	24.00	1.0	1.3	G1V	ABDOR	-	m
TYC0486-4943	xxx	19 33 3.80	3 45 40.0	11.29	0.95	1.22	7.03	71.00	11.00	0.8	0.8	K3V	ABDOR	-	m
HD189285	BD-044987	19 59 24.10	-4 32 6.00	9.46	0.71	0.74	4.99	78.20	9.00	1.0	1.1	G5	ABDOR	1	m
TYC5164-567-1	BD-034778	20 4 49.40	-2 39 20.0	10.17	0.90	1.05	6.27	60.30	8.00	0.9	0.9	XX	ABDOR	1	m
TYC1090-0543	xxxx	20 54 28.00	9 6 7.00	11.73	1.07	1.27	7.35	75.00	18.00	0.7	0.7	XX	ABDOR	1	m
TYC635102861	HD201919	21 13 5.30	-17 29 13.0	10.64	1.21	1.42	7.56	41.30	7.90	0.7	0.7	K6Ve	ABDOR	-	m
HIP106231	LOPeg	21 31 1.71	23 20 7.37	9.19	1.05	1.23	7.19	25.10	65.85	0.8	0.7	K8	ABDOR	-	m
HIP107684	HD207278	21 48 48.50	-39 29 9.00	9.66	0.69	0.75	5.04	84.00	10.40	1.0	1.1	G7V	ABDOR	-	m
HIP114530	HD218860A	23 11 52.05	-45 8 10.6	8.75	0.80	0.79	5.23	50.60	6.60	1.0	1.0	G8V	ABDOR	-	m
HIP116910	HD222575	23 41 54.30	-35 58 40.0	9.39	0.71	0.80	5.41	62.50	31.10	1.0	1.0	G8V	ABDOR	-	m
PWAnd	HD1405	0 18 20.89	30 57 22.2	8.86	0.92	1.08	6.31	32.40	23.90	0.9	K2V	0.9	ABDOR	1	m
HIP31711	HD48189	6 38 0.36	-61 32 0.19	6.15	0.62	0.69	4.47	21.70	17.60	1.0	1.3	G2V	ABDOR	-	m
HIP63742	HD113449	13 3 49.65	-5 9 42.5	7.69	0.85	0.89	5.97	22.10	5.20	0.9	0.9	G5V	ABDOR	-	m
HIP86346	HD160934	17 38 39.63	61 14 16.1	10.45	1.23	1.46	7.86	33.00	17.00	0.7	0.7	M0	ABDOR	-	m
HIP114066	GJ9809	23 6 4.84	63 55 34.3	10.87	1.44	1.77	8.89	24.90	8.00	0.6	0.6	M0	ABDOR	-	m
HIP16563	HD21845	3 33 13.49	46 15 26.5	8.15	0.80	0.81	5.51	33.80	7.00	1.0	1.0	G5+M0	ABDOR	-	m
HD32981	BD-161042	5 6 27.70	-15 49 30.0	9.13	0.58	0.67	4.39	88.60	6.00	1.0	1.3	F8V	ABDOR	1	m
TYC649412281	CD-262415	5 44 13.40	-26 6 15.0	10.88	0.86	0.98	6.10	90.20	999.90	0.9	0.9	K2Ve	ABDOR	1	m
HIP30314	HD45270	6 22 30.94	-60 13 7.15	6.53	0.61	0.66	4.67	23.50	17.60	1.0	1.2	G1V	ABDOR	-	m
HIP113579	HD217343	23 0 19.29	-26 9 13.5	7.47	0.65	0.72	4.94	32.00	12.40	1.0	1.2	G5V	ABDOR	-	m
HIP113597	HD217379	23 0 27.95	-26 18 42.8	10.45	1.34	1.59	8.06	30.00	6.40	0.7	0.7	K7V	ABDOR	-	m

Table A.7. Summary of period search.

Target	ASAS number	JD initial	JD final	Period (d)	ΔP (d)	Normalized power	Power at 99% confidence level
TW Hydrae							
TWA2	110914-3001.7	1869.8491	1971.7092	4.845	0.107	13.06	6.07
TWA2	110914-3001.7	1971.7092	2080.4703	4.860	0.072	5.49	5.00
TWA2	110914-3001.7	2577.8675	2683.7281	4.932	0.148	6.57	5.14
TWA2	110914-3001.7	2683.7281	2784.5825	4.845	0.107	12.63	7.49
TWA2	110914-3001.7	2971.8337	3072.8017	4.833	0.106	7.04	5.41
TWA2	110914-3001.7	3702.8454	3804.7395	4.833	0.106	10.39	5.73
TWA2	110914-3001.7	3804.7395	3906.6103	4.863	0.072	13.31	6.04
TWA2	110914-3001.7	4192.7428	4294.5382	4.827	0.071	9.23	3.86
TWA2	110914-3001.7	4530.6658	4631.5631	4.845	0.071	5.54	4.22
TWA4	112205-2446.7	1869.8517	1971.7029	14.306	0.621	2.59	2.56
TWA4	112205-2446.7	1971.7029	2080.4765	14.823	0.667	10.29	5.33
TWA4	112205-2446.7	2577.8698	2678.7525	13.773	1.152	8.95	4.25
TWA4	112205-2446.7	2678.7525	2783.5668	14.350	0.625	18.49	5.72
TWA4	112205-2446.7	2957.8519	3061.6796	13.435	0.820	5.69	4.20
TWA4	112205-2446.7	3061.6796	3162.6211	14.900	0.674	6.74	4.96
TWA4	112205-2446.7	3356.8211	3458.7097	14.066	0.904	8.33	6.18
TWA4	112205-2446.7	4089.8363	4192.6453	14.413	0.943	12.62	4.90
TWA4	112205-2446.7	4429.8464	4531.7230	14.712	0.983	9.06	6.92
TWA5A	113155-3436.5	2971.8337	3073.7926	0.770	0.003	5.50	3.59
TWA5A	113155-3436.5	4530.6658	4631.5631	0.776	0.002	8.04	7.08
TWA7	104230-3340.3	2678.7318	2782.6014	5.120	0.119	6.07	5.19
TWA8A	113241-2651.9	3704.8468	3805.7131	4.612	0.097	7.74	5.35
TWA8A	113241-2651.9	3805.7131	3907.5635	4.669	0.066	8.53	5.25
TWA8A	113241-2651.9	4089.8363	4193.6730	4.681	0.100	8.54	5.41
TWA8A	113241-2651.9	4431.8477	4535.6905	4.642	0.098	5.96	3.59
TWA9A	114824-3728.8	1870.8445	1971.7291	5.021	0.115	15.86	5.90
TWA9A	114824-3728.8	1971.7291	2078.4546	4.962	0.075	8.28	4.77
TWA9A	114824-3728.8	2222.8428	2266.8058	4.944	0.261	6.29	3.47
TWA9A	114824-3728.8	2622.8176	2722.8229	5.010	0.114	6.87	4.75
TWA9A	114824-3728.8	2722.8229	2827.4612	4.956	0.075	7.48	5.18
TWA9A	114824-3728.8	2973.8497	3075.7272	5.001	0.114	8.95	6.76
TWA9A	114824-3728.8	3075.7272	3177.5869	4.965	0.075	12.57	7.01
TWA9A	114824-3728.8	3459.6810	3560.5429	5.024	0.077	7.21	6.13
TWA9A	114824-3728.8	3701.8557	3802.6876	5.034	0.115	8.26	5.61
TWA9A	114824-3728.8	3802.6876	3904.5237	5.021	0.077	9.99	6.94
TWA9A	114824-3728.8	4205.7224	4311.5306	5.019	0.076	9.59	5.33
TWA9A	114824-3728.8	4435.8292	4536.7339	5.024	0.115	8.82	4.36
TWA9A	114824-3728.8	4536.7339	4639.5002	5.016	0.076	13.46	5.36
TWA10	123504-4136.6	1870.8577	1971.7490	8.385	0.319	5.60	4.86
TWA10	123504-4136.6	3456.7380	3559.5201	8.394	0.214	8.91	4.06
TWA12	112105-3845.3	1869.8421	1971.7064	3.302	0.050	21.94	6.01
TWA12	112105-3845.3	1971.7064	2080.4637	3.305	0.033	8.56	5.58
TWA12	112105-3845.3	2622.7856	2723.8191	3.296	0.049	14.28	6.88
TWA12	112105-3845.3	2723.8191	2826.4769	3.323	0.034	6.02	4.16
TWA12	112105-3845.3	3699.8381	3801.7085	1.431	0.009	11.62	4.38
TWA12	112105-3845.3	4091.7926	4194.7590	3.311	0.050	7.09	6.69
TWA12	112105-3845.3	4194.7590	4296.5018	3.314	0.033	5.73	4.73
TWA12	112105-3845.3	4532.6565	4639.4970	3.302	0.033	15.11	7.27
TWA13A	112117-3446.8	1869.8491	1971.7092	5.485	0.137	21.44	5.58

Table A.7 (cont'd)

Target	ASAS number	JD initial	JD final	Period (d)	ΔP (d)	Normalized power	Power at 99% confidence level
TWA13A	112117-3446.8	1971.7092	2080.4703	5.676	0.098	6.76	5.69
TWA13A	112117-3446.8	2679.7256	2782.6166	5.377	0.131	11.02	5.82
TWA13A	112117-3446.8	2782.6166	2868.4663	5.485	0.091	7.10	4.47
TWA13A	112117-3446.8	2971.8337	3073.7926	5.470	0.136	6.19	5.76
TWA13A	112117-3446.8	3357.8303	3458.7145	5.335	0.130	9.88	4.28
TWA13A	112117-3446.8	3458.7145	3561.5009	5.458	0.090	9.19	4.74
TWA13A	112117-3446.8	3702.8454	3804.7395	5.306	0.128	9.29	5.46
TWA13A	112117-3446.8	3804.7395	3906.6103	5.449	0.090	15.12	5.92
TWA13A	112117-3446.8	4192.7428	4294.5382	5.494	0.092	8.47	3.67
TWA13A	112117-3446.8	4429.8408	4530.6658	5.515	0.138	8.07	4.58
TWA13A	112117-3446.8	4530.6658	4631.5631	5.228	0.083	6.28	3.89
TWA21	101315-5230.9	2117.4793	2217.8209	4.441	0.243	7.01	4.48
TWA21	101315-5230.9	2680.7207	2782.5468	4.367	0.058	10.36	2.27
TWA21	101315-5230.9	2782.5468	2908.8949	4.433	0.149	8.59	6.03
TWA21	101315-5230.9	2908.8949	3010.7677	4.436	0.089	8.99	4.81
TWA21	101315-5230.9	3010.7677	3111.7718	4.456	0.090	5.52	4.31
TWA21	101315-5230.9	4192.7016	4293.4843	4.334	0.057	6.53	4.46
TWA21	101315-5230.9	4524.6437	4626.5014	4.385	0.058	6.97	5.47
TWA24	120942-5854.8	2622.7870	2723.8621	0.647	0.001	7.04	5.28
TWA24	120942-5854.8	2978.8378	3085.7643	0.686	0.002	5.25	2.94
TWA24	120942-5854.8	3458.7211	3562.5278	0.686	0.001	6.40	4.61
TWA24	120942-5854.8	4103.8367	4204.6921	0.686	0.002	6.36	3.76
TWA24	120942-5854.8	4438.8378	4540.6524	0.686	0.002	8.83	4.98
TWA25	121531-3948.7	1870.8445	1971.7291	5.057	0.116	17.88	5.90
TWA25	121531-3948.7	1971.7291	2078.4546	5.075	0.078	12.37	5.33
TWA25	121531-3948.7	2622.8176	2722.8229	5.066	0.117	12.94	6.07
TWA25	121531-3948.7	2722.8229	2827.4612	5.072	0.078	11.89	6.00
TWA25	121531-3948.7	2973.8497	3075.7272	5.051	0.116	10.28	4.17
TWA25	121531-3948.7	3075.7272	3177.5869	5.066	0.078	11.50	4.95
TWA25	121531-3948.7	3457.6827	3558.5267	5.030	0.077	9.29	5.29
TWA25	121531-3948.7	3701.8557	3802.6876	5.063	0.116	6.81	5.62
TWA25	121531-3948.7	3802.6876	3904.5237	2.525	0.019	10.00	5.50
TWA25	121531-3948.7	4089.8199	4190.7446	5.057	0.116	9.90	4.68
TWA25	121531-3948.7	4190.7446	4291.5889	5.096	0.079	8.67	6.28
TWA25	121531-3948.7	4435.8292	4536.7053	5.069	0.117	17.23	6.44
TWA25	121531-3948.7	4536.7053	4639.5002	5.096	0.079	19.77	5.31

 β Pictoris members

TYC1186-706-1	002335+2014.5	2869.9122	2932.9122	7.710	0.361	5.81	4.54
HIP12545	024126+0559.3	2812.9288	2915.7638	4.85	0.10	6.39	2.24
HIP12545	024126+0559.3	2915.7638	3018.5612	4.82	0.10	12.35	4.80
HIP12545	024126+0559.3	3562.9116	3663.7348	4.84	0.07	7.40	5.92
HIP12545	024126+0559.3	4284.9221	4386.7595	4.82	0.07	7.29	5.01
HIP23200	045935+0147.0	2621.6619	2723.5293	4.420	0.089	9.94	5.29
HIP23200	045935+0147.0	2943.7331	3044.5393	4.352	0.058	6.65	4.82
HIP23200	045935+0147.0	3044.5393	3110.4715	4.391	0.088	6.82	5.31
HIP23200	045935+0147.0	4090.6508	4192.5137	4.376	0.087	8.94	3.60
HIP23200	045935+0147.0	4302.9399	4406.7829	4.453	0.090	7.02	4.97
HIP23200	045935+0147.0	4406.7829	4509.5594	4.441	0.060	9.78	4.50
HIP23200	045935+0147.0	4509.5594	4576.4667	4.415	0.089	6.61	5.73
HIP23200	045935+0147.0	4684.9082	4786.7110	4.394	0.059	14.24	5.33

Table A.7 (cont'd)

Target	ASAS number	JD initial	JD final	Period (d)	ΔP (d)	Normalized power	Power at 99% confidence level
HIP23200	045935+0147.0	4786.7110	4888.5813	4.391	0.087	17.95	6.14
HIP23309	050047-5715.4	1868.6855	1978.5925	8.867	0.357	8.36	4.42
HIP23309	050047-5715.4	2104.9392	2206.7750	8.705	0.344	14.10	6.70
HIP23309	050047-5715.4	2206.7750	2262.6303	8.660	0.571	11.81	5.53
HIP23309	050047-5715.4	2574.7130	2675.5558	8.669	0.459	8.29	4.43
HIP23309	050047-5715.4	2675.5558	2776.4572	8.663	0.341	3.68	3.40
HIP23309	050047-5715.4	2877.8545	2979.6915	8.645	0.339	10.17	4.44
HIP23309	050047-5715.4	2979.6915	3080.5359	8.648	0.340	9.11	5.68
HIP23309	050047-5715.4	3355.6052	3460.5059	8.891	0.359	12.35	4.59
HIP23309	050047-5715.4	3618.8440	3720.7068	8.654	0.227	7.20	4.22
HIP23309	050047-5715.4	3720.7068	3821.5471	8.744	0.347	11.25	3.98
HIP23309	050047-5715.4	4333.8507	4435.6749	8.720	0.231	17.61	6.99
HIP23309	050047-5715.4	4435.6749	4538.5658	8.630	0.338	9.02	4.47
HIP23418	050159+0959.0	2562.7588	2664.5912	6.331	0.305	4.59	3.64
HIP23418	050159+0959.0	3400.5408	3468.4777	6.280	0.180	5.10	4.76
HIP23418	050159+0959.0	4091.6549	4196.5100	6.499	0.128	5.79	5.48
HIP23418	050159+0959.0	4332.8993	4437.6879	3.102	0.029	5.54	5.04
BD-211074A	050650-2135.1	1868.7126	1978.5976	14.129	0.906	7.35	6.42
BD-211074A	050650-2135.1	2206.7909	2264.6563	16.327	2.030	5.67	4.25
BD-211074A	050650-2135.1	3618.9036	3720.8036	13.615	0.563	6.17	3.21
BD-211074A	050650-2135.1	4440.6650	4541.5737	13.358	0.542	7.04	3.38
BD-211074A	050650-2135.1	4802.6655	4905.5599	14.063	0.898	5.38	5.36
HIP29964	061828-7202.7	2621.7497	2722.6239	2.668	0.032	16.83	6.44
HIP29964	061828-7202.7	2722.6239	2841.9405	2.683	0.022	4.18	3.61
HIP29964	061828-7202.7	2841.9405	2943.7870	2.647	0.032	5.56	4.72
HIP29964	061828-7202.7	2943.7870	3044.6415	2.662	0.032	11.26	5.01
HIP29964	061828-7202.7	3044.6415	3146.5163	2.662	0.021	17.06	4.72
HIP29964	061828-7202.7	3355.6876	3457.5443	2.659	0.032	8.46	5.05
HIP29964	061828-7202.7	3457.5443	3578.9303	2.656	0.022	5.91	3.96
HIP29964	061828-7202.7	3578.9303	3680.8310	2.710	0.033	4.01	3.33
HIP29964	061828-7202.7	3680.8310	3787.7105	2.680	0.033	7.76	3.47
HIP29964	061828-7202.7	3787.7105	3890.4766	2.668	0.022	21.23	8.07
HIP29964	061828-7202.7	4305.9301	4408.7451	2.651	0.021	5.18	4.54
HIP29964	061828-7202.7	4508.7861	4610.4743	2.647	0.021	6.44	3.33
HIP76629	153857-5742.5	1919.8473	2025.6697	4.322	0.113	5.74	5.50
HIP76629	153857-5742.5	2775.6861	2877.6380	4.334	0.057	12.35	4.17
HIP76629	153857-5742.5	3131.7534	3190.6892	4.304	0.141	8.33	5.52
HIP76629	153857-5742.5	3490.7282	3592.5170	4.328	0.057	15.25	5.55
HIP76629	153857-5742.5	3592.5170	3663.4951	4.271	0.111	7.82	4.38
HIP76629	153857-5742.5	3764.8304	3865.7344	4.352	0.086	6.10	3.77
HIP76629	153857-5742.5	4329.5272	4389.4948	4.406	0.118	5.55	5.01
HIP84586	171726-6657.1	2678.8486	2782.7538	1.667	0.013	12.00	2.15
HIP84586	171726-6657.1	3390.8716	3492.7999	1.676	0.013	8.03	5.55
HIP84586	171726-6657.1	3492.7999	3597.6768	1.685	0.009	12.73	8.19
HIP84586	171726-6657.1	4129.8669	4231.7809	1.685	0.013	5.59	3.29
HIP84586	171726-6657.1	4231.7809	4332.5306	1.688	0.009	9.64	3.83
HIP84586	171726-6657.1	4332.5306	4411.5321	1.673	0.017	12.50	3.05
HIP84586	171726-6657.1	4517.8652	4618.7335	1.646	0.012	7.08	5.34
HIP84586	171726-6657.1	4618.7335	4720.6061	1.682	0.013	12.57	4.25
TYC872822621	172955-5415.8	1939.8804	2040.7846	1.810	0.015	7.72	5.35
TYC872822621	172955-5415.8	2441.6492	2543.6223	1.825	0.015	14.99	2.18
TYC872822621	172955-5415.8	2782.7686	2883.5521	1.831	0.015	9.88	5.45

Table A.7 (cont'd)

Target	ASAS number	JD initial	JD final	Period (d)	ΔP (d)	Normalized power	Power at 99% confidence level
TYC872822621	172955-5415.8	3057.8933	3159.7084	1.822	0.015	9.13	4.88
TYC872822621	172955-5415.8	3404.8696	3508.8079	1.825	0.015	6.01	2.72
TYC872822621	172955-5415.8	4133.8735	4234.8409	1.828	0.015	7.59	5.27
TYC872822621	172955-5415.8	4517.8930	4623.7322	1.807	0.015	5.79	3.26
TYC872822621	172955-5415.8	4623.7322	4725.6221	1.828	0.010	11.59	4.71
TYC874220651	174834-5306.7	1939.8804	2052.7022	2.618	0.021	8.22	4.70
TYC874220651	174834-5306.7	2052.7022	2156.4923	2.615	0.021	10.53	5.39
TYC874220651	174834-5306.7	2441.6492	2543.6223	2.630	0.031	7.64	5.67
TYC874220651	174834-5306.7	2678.8716	2782.7686	2.585	0.030	2.81	2.54
TYC874220651	174834-5306.7	2883.5521	2954.5032	2.594	0.031	5.96	3.98
TYC874220651	174834-5306.7	3057.8933	3159.7084	2.618	0.031	6.83	4.84
TYC874220651	174834-5306.7	3508.8079	3616.5523	2.606	0.021	6.86	5.00
TYC874220651	174834-5306.7	4517.8930	4622.8466	2.618	0.031	7.44	4.89
V4046Sgr	181411-3247.5	2083.6515	2184.5314	2.420	0.018	5.75	5.42
V4046Sgr	181411-3247.5	2442.6656	2544.5826	2.417	0.026	7.55	5.56
V4046Sgr	181411-3247.5	2683.8689	2784.7339	2.408	0.026	5.38	4.91
V4046Sgr	181411-3247.5	3055.8855	3156.7094	2.414	0.026	7.55	6.85
V4046Sgr	181411-3247.5	3411.8850	3517.7802	2.420	0.027	7.69	2.55
V4046Sgr	181411-3247.5	3786.8135	3887.7507	2.408	0.026	12.22	4.20
V4046Sgr	181411-3247.5	4622.7401	4725.6340	2.414	0.018	9.56	3.44
V4046Sgr	181411-3247.5	4725.6340	4775.5246	2.396	0.035	7.92	3.27
HIP89829	181952-2916.5	2786.7180	2888.5939	0.572	0.001	7.51	4.73
HIP89829	181952-2916.5	2888.5939	2959.5088	0.569	0.002	20.31	5.86
HIP89829	181952-2916.5	3059.8771	3162.7454	0.569	0.002	13.00	6.22
HIP89829	181952-2916.5	3162.7454	3191.8820	0.569	0.004	13.78	4.40
HIP89829	181952-2916.5	3792.8775	3893.7454	0.572	0.002	4.68	2.92
HIP89829	181952-2916.5	4256.7767	4359.4978	0.569	0.001	13.85	7.21
HIP89829	181952-2916.5	4622.8527	4728.5967	0.569	0.001	13.77	4.59
TYC907724891	184537-6451.8	2683.8879	2784.7688	0.354	0.001	5.13	3.44
TYC907724891	184537-6451.8	2886.5303	2969.5206	0.354	0.001	6.26	4.85
TYC907724891	184537-6451.8	3538.7476	3643.5140	0.354	0.000	8.50	4.93
TYC907724891	184537-6451.8	4254.6904	4356.6371	0.354	0.000	10.14	5.12
TYC907724891	184537-6451.8	4531.8626	4633.7455	0.354	0.001	7.13	6.42
TYC907307621	184653-6210.6	1954.8712	2055.7403	5.407	0.089	7.55	5.37
TYC907307621	184653-6210.6	2055.7403	2164.4855	5.315	0.086	6.59	4.28
TYC907307621	184653-6210.6	2164.4855	2234.5129	5.419	0.178	8.21	6.78
TYC907307621	184653-6210.6	2442.6901	2544.6317	2.674	0.033	7.03	5.26
TYC907307621	184653-6210.6	2683.8879	2784.7688	2.680	0.033	6.78	4.63
TYC907307621	184653-6210.6	2784.7688	2886.5303	5.362	0.087	8.88	4.67
TYC907307621	184653-6210.6	2886.5303	2969.5206	5.374	0.131	10.04	4.74
TYC907307621	184653-6210.6	3072.8783	3176.6964	5.341	0.130	9.33	6.92
TYC907307621	184653-6210.6	3426.8762	3538.7476	5.359	0.130	13.55	5.47
TYC907307621	184653-6210.6	3538.7476	3643.5140	5.359	0.087	11.91	6.10
TYC907307621	184653-6210.6	3803.8883	3905.7481	5.404	0.133	9.65	5.92
TYC907307621	184653-6210.6	4633.7455	4736.6036	5.309	0.086	8.19	4.24
TYC740800541	185044-3147.8	2442.6802	2544.5857	1.042	0.005	7.55	4.25
TYC740800541	185044-3147.8	2684.8814	2786.7180	1.090	0.005	7.38	5.80
TYC740800541	185044-3147.8	2786.7180	2892.5890	1.090	0.005	60.73	5.20
TYC740800541	185044-3147.8	3059.8895	3162.7709	1.087	0.005	6.58	4.56
TYC740800541	185044-3147.8	3517.7967	3621.6109	1.042	0.003	4.69	3.69
TYC740800541	185044-3147.8	3792.8796	3893.7552	1.042	0.005	14.72	3.40
TYC740800541	185044-3147.8	4160.8893	4269.7754	1.042	0.005	7.33	3.84

Table A.7 (cont'd)

Target	ASAS number	JD initial	JD final	Period (d)	ΔP (d)	Normalized power	Power at 99% confidence level
TYC740800541	185044-3147.8	4269.7754	4371.5816	1.042	0.003	11.55	6.28
TYC740800541	185044-3147.8	4631.7562	4733.6386	1.042	0.003	9.17	4.13
TYC740800541	185044-3147.8	4733.6386	4793.5118	1.042	0.007	5.47	3.46
HIP92680	185306-5010.8	2440.6899	2544.6414	0.940	0.004	10.86	7.00
HIP92680	185306-5010.8	2683.8827	2786.7313	0.943	0.004	12.77	5.81
HIP92680	185306-5010.8	2786.7313	2888.7253	0.940	0.003	6.58	6.45
HIP92680	185306-5010.8	2888.7253	2964.5136	0.940	0.005	5.50	5.09
HIP92680	185306-5010.8	3064.8814	3170.7550	0.946	0.004	8.32	5.09
HIP92680	185306-5010.8	3418.8868	3523.8097	0.946	0.004	6.99	6.00
HIP92680	185306-5010.8	3796.8804	3900.7680	0.949	0.004	6.32	4.07
HIP92680	185306-5010.8	4519.8811	4623.7031	0.943	0.004	4.76	4.19
TYC687210111	185804-2953.1	2694.8885	2795.7456	0.498	0.008	57.21	4.73
TYC687210111	185804-2953.1	2795.7456	2897.6609	0.548	0.002	32.30	2.68
TYC687801951	191145-2604.2	2065.7160	2167.5015	5.772	0.152	9.98	7.15
TYC687801951	191145-2604.2	2442.7047	2546.5665	5.596	0.142	6.25	4.34
TYC687801951	191145-2604.2	2699.8909	2808.8642	5.802	0.153	10.47	5.98
TYC687801951	191145-2604.2	2808.8642	2909.5902	5.733	0.100	6.24	5.72
TYC687801951	191145-2604.2	3550.7505	3655.5094	5.611	0.096	6.08	4.10
TYC687801951	191145-2604.2	3798.8878	3901.7812	5.700	0.147	8.38	6.99
TYC687801951	191145-2604.2	4639.7619	4742.5516	5.605	0.095	6.56	4.88
HIP102409	204510-3120.4	1982.8977	2085.7160	4.824	0.071	6.56	4.78
HIP102409	204510-3120.4	2085.7160	2187.5341	4.824	0.071	7.26	6.14
HIP102409	204510-3120.4	2439.7776	2545.6510	4.893	0.073	11.33	5.60
HIP102409	204510-3120.4	3098.9117	3191.7908	4.848	0.107	8.07	5.62
HIP102409	204510-3120.4	3560.7740	3661.5945	4.851	0.071	10.02	4.05
HIP102409	204510-3120.4	3821.9007	3907.8846	4.971	0.112	6.96	3.55
TYC634902001	205603-1710.9	2086.6786	2189.5217	3.398	0.035	8.77	3.72
TYC634902001	205603-1710.9	2443.7596	2545.6374	3.413	0.053	14.23	5.60
TYC634902001	205603-1710.9	2714.9075	2816.8622	3.413	0.053	6.05	5.23
TYC634902001	205603-1710.9	3446.9053	3547.8077	3.392	0.052	5.73	5.26
TYC634902001	205603-1710.9	3811.9060	3913.8320	3.404	0.053	9.53	3.07
TYC634902001	205603-1710.9	4278.7821	4381.6692	3.395	0.035	10.40	4.83
TYC634902001	205603-1710.9	4547.9087	4648.7876	3.407	0.053	5.86	3.14
TYC2211-1309-1	220042+2715.2	2886.9104	2946.9104	0.477	0.001	6.02	5.56
TYC934004371	224249-7142.3	2443.8408	2544.7693	4.456	0.090	13.30	3.78
TYC934004371	224249-7142.3	2544.7693	2645.5351	4.480	0.061	8.43	5.67
TYC934004371	224249-7142.3	2866.7478	2968.5674	4.486	0.061	7.53	3.62
TYC934004371	224249-7142.3	3497.8854	3602.7470	4.486	0.061	5.76	4.42
TYC934004371	224249-7142.3	4329.7434	4431.5524	4.385	0.058	6.65	3.97
TYC934004371	224249-7142.3	4585.8958	4691.6991	4.453	0.060	8.19	4.38
HIP112312	224458-3315.1	2011.9152	2113.8034	2.366	0.025	7.61	6.41
HIP112312	224458-3315.1	4329.7515	4432.5878	2.345	0.025	5.93	4.77
TYC583206661	233231-1215.9	2130.7996	2232.5430	5.772	0.152	7.80	7.08
TYC583206661	233231-1215.9	2444.8179	2545.7861	5.754	0.150	7.26	5.04
TYC583206661	233231-1215.9	2859.7308	2961.5931	5.688	0.098	13.22	4.79
TYC583206661	233231-1215.9	3511.8937	3619.6926	5.700	0.148	6.69	6.51
TYC583206661	233231-1215.9	3619.6926	3722.5561	5.644	0.097	11.07	3.68
TYC583206661	233231-1215.9	4691.7744	4792.5695	5.682	0.002	6.30	5.84

Tucana/Horologium members

HIP1113	001353-7441.3	1873.5807	1949.5159	3.709	0.084	9.43	4.44
---------	---------------	-----------	-----------	-------	-------	------	------

Table A.7 (cont'd)

Target	ASAS number	JD initial	JD final	Period (d)	ΔP (d)	Normalized power	Power at 99% confidence level
HIP1113	001353-7441.3	2015.9238	2094.9238	7.431	0.335	3.75	3.17
HIP1113	001353-7441.3	2094.9238	2173.9238	3.721	0.063	12.85	4.77
HIP1113	001353-7441.3	2173.9238	2252.9238	3.727	0.084	19.36	14.42
HIP1113	001353-7441.3	2446.8718	2525.8718	3.736	0.064	11.73	5.13
HIP1113	001353-7441.3	2604.8718	2683.8718	3.721	0.084	15.31	3.85
HIP1113	001353-7441.3	2871.8490	2958.8490	3.691	0.062	17.14	6.16
HIP1113	001353-7441.3	2958.8490	3045.8490	3.703	0.062	20.40	5.44
HIP1113	001353-7441.3	3512.9315	3600.9315	3.727	2.022	9.30	7.67
HIP1113	001353-7441.3	3688.9315	3776.9315	3.745	0.064	9.18	4.76
HIP1113	001353-7441.3	3861.9271	3911.9184	3.676	0.103	12.91	4.57
HIP1113	001353-7441.3	4322.9159	4415.9159	3.598	0.059	38.60	4.48
HIP1113	001353-7441.3	4415.9159	4508.9159	3.583	0.039	15.30	5.39
HIP1910	002409-6211.1	1872.6035	1948.5159	1.744	0.018	18.63	6.05
HIP1910	002409-6211.1	2186.8901	2262.8901	1.715	0.018	11.31	4.40
HIP1910	002409-6211.1	2598.8992	2677.8992	1.754	0.019	17.32	4.45
HIP1910	002409-6211.1	2849.9221	2942.9221	1.744	0.009	12.27	5.39
HIP1910	002409-6211.1	3357.5784	3414.5152	1.748	0.019	8.58	4.24
HIP1910	002409-6211.1	3599.9243	3686.9243	1.750	0.014	15.29	5.29
HIP1910	002409-6211.1	3686.9243	3773.9243	1.756	0.014	12.83	4.56
HIP1910	002409-6211.1	3850.9230	3912.9226	1.742	0.018	4.86	3.88
HIP1910	002409-6211.1	4397.9306	4565.9306	1.744	0.014	27.38	6.71
HIP1910	002409-6211.1	4565.9306	4733.9306	1.748	0.009	11.43	7.32
HIP1993	002515-6130.8	2034.8901	2110.8901	4.352	0.115	11.26	4.89
HIP1993	002515-6130.8	2110.8901	2186.8901	4.325	0.086	31.50	5.23
HIP1993	002515-6130.8	2186.8901	2262.8901	4.358	0.115	37.35	4.18
HIP1993	002515-6130.8	2849.9221	2942.9221	4.319	0.057	10.30	6.39
HIP1993	002515-6130.8	2942.9221	3035.9221	4.373	0.058	14.45	6.51
HIP1993	002515-6130.8	3126.9283	3210.9164	4.376	0.116	11.59	5.68
HIP1993	002515-6130.8	3512.9013	3599.9013	4.364	0.116	12.56	5.16
HIP1993	002515-6130.8	3599.9013	3686.9013	4.289	0.084	10.76	5.89
HIP1993	002515-6130.8	3850.9230	3912.9226	4.397	0.117	11.24	3.67
HIP1993	002515-6130.8	4398.9083	4566.9083	4.391	0.059	13.32	4.91
TYC935111101	004220-7747.7	2098.9028	2179.9028	2.558	0.030	19.18	4.43
TYC935111101	004220-7747.7	2179.9028	2260.9028	2.561	0.030	8.03	5.36
TYC935111101	004220-7747.7	2440.8720	2641.8720	2.576	0.020	26.32	5.71
TYC935111101	004220-7747.7	2842.8720	3043.8720	2.582	0.020	10.98	8.79
TYC935111101	004220-7747.7	3503.9326	3593.9326	2.426	0.027	5.34	4.26
TYC935111101	004220-7747.7	4229.9222	4321.9222	2.555	0.040	7.55	7.39
TYC935111101	004220-7747.7	4321.9222	4413.9222	2.579	0.020	14.59	5.19
TYC935111101	004220-7747.7	4674.9125	4771.9125	2.564	0.020	9.53	4.80
TYC885202641	011315-6411.6	2053.9349	2121.9349	4.857	0.143	9.15	5.86
TYC885202641	011315-6411.6	2121.9349	2189.9349	4.740	0.103	11.40	4.92
TYC885202641	011315-6411.6	2189.9349	2257.9349	4.797	0.140	21.17	4.29
TYC885202641	011315-6411.6	2445.8437	2529.8437	4.770	0.138	4.86	3.99
TYC885202641	011315-6411.6	2613.8437	2697.8437	4.839	0.142	5.97	3.89
TYC885202641	011315-6411.6	3606.9243	3700.9243	4.782	0.104	9.73	5.28
TYC885202641	011315-6411.6	3700.9243	3794.9243	4.767	0.069	11.34	5.97
TYC885202641	011315-6411.6	4426.9293	4524.9293	4.794	0.070	9.88	4.78
HIP6485	012321-5728.9	2446.8471	2534.8471	3.473	0.073	6.13	4.96
HIP6485	012321-5728.9	2534.8471	2622.8471	3.509	0.131	7.81	3.15
HIP6485	012321-5728.9	2622.8471	2710.8471	3.389	0.052	7.49	5.39
HIP6485	012321-5728.9	2975.9163	3069.9163	3.535	0.038	6.11	5.84

Table A.7 (cont'd)

Target	ASAS number	JD initial	JD final	Period (d)	ΔP (d)	Normalized power	Power at 99% confidence level
HIP6485	012321-5728.9	3610.9188	3707.9188	3.628	0.060	4.99	3.94
HIP9141	015749-2154.1	2446.8910	2531.8910	3.006	0.055	6.42	5.44
HIP9141	015749-2154.1	2616.8910	2701.8910	3.033	0.042	11.18	4.63
HIP9141	015749-2154.1	2892.9073	2978.9073	3.024	0.042	9.45	3.28
HIP9892	020718-5311.9	2124.9349	2192.9349	2.525	0.029	5.70	5.17
HIP9892	020718-5311.9	2447.8841	2540.8841	2.366	0.034	6.80	4.84
HIP9892	020718-5311.9	2904.9084	2998.9084	2.232	0.023	10.22	2.92
HIP9892	020718-5311.9	2998.9084	3092.9084	2.393	0.026	10.13	6.07
HIP9892	020718-5311.9	3625.9216	3723.9216	2.268	0.023	7.62	4.62
HIP9892	020718-5311.9	4349.9253	4450.9253	2.292	0.024	3.03	2.62
HIP9892	020718-5311.9	4450.9253	4551.9253	2.229	0.015	7.36	4.08
RBS332	023652-5203.1	2124.9349	2192.9349	1.538	0.011	7.56	7.17
RBS332	023652-5203.1	2633.8841	2726.8841	1.541	0.011	7.27	5.01
RBS332	023652-5203.1	2810.9084	2904.9084	1.529	0.007	5.18	4.94
RBS332	023652-5203.1	2904.9084	2998.9084	1.538	0.011	8.38	3.99
RBS332	023652-5203.1	3382.7614	3470.7614	1.538	0.011	7.44	6.83
RBS332	023652-5203.1	3731.9216	3833.9216	1.526	0.007	8.37	6.25
TYC849106561	024147-5259.9	1872.6255	1917.6255	1.275	0.012	6.54	5.05
TYC849106561	024147-5259.9	2124.9349	2192.9349	1.272	0.007	7.37	3.64
TYC849106561	024147-5259.9	2192.9349	2260.9349	1.278	0.007	7.54	4.65
TYC849106561	024147-5259.9	4370.9442	4461.9442	1.272	0.007	8.70	4.48
TYC849709951	024233-5739.6	1871.6346	1932.6346	7.428	0.335	22.39	3.25
TYC849709951	024233-5739.6	2124.9349	2192.9349	7.273	0.242	9.67	5.65
TYC849709951	024233-5739.6	2192.9349	2260.9349	7.396	0.250	18.60	5.53
TYC849709951	024233-5739.6	2446.9107	2540.9107	7.449	0.337	12.98	5.36
TYC849709951	024233-5739.6	2634.9107	2728.9107	7.201	0.235	18.57	7.28
TYC849709951	024233-5739.6	2806.9349	2902.9349	7.324	0.244	13.31	3.53
TYC849709951	024233-5739.6	2902.9349	2998.9349	7.417	0.250	26.45	6.37
TYC849709951	024233-5739.6	2998.9349	3094.9349	7.348	0.164	11.23	5.97
TYC849709951	024233-5739.6	4416.9394	4573.9394	7.336	0.082	9.83	2.87
TYC849709951	024233-5739.6	4573.9394	4730.9394	7.428	0.251	6.02	4.48
TYC702603251	031909-3507.0	1871.6343	1933.6343	8.493	0.438	14.44	5.21
TYC702603251	031909-3507.0	2125.9395	2194.9395	8.502	0.330	17.62	4.88
TYC702603251	031909-3507.0	2194.9395	2263.9395	8.544	0.334	27.35	5.08
TYC702603251	031909-3507.0	2445.9253	2543.9253	8.702	0.230	6.37	5.00
TYC702603251	031909-3507.0	2641.9253	2739.9253	8.627	0.226	5.61	4.49
TYC702603251	031909-3507.0	2812.9380	2909.9380	8.376	0.319	7.85	3.82
TYC702603251	031909-3507.0	2909.9380	3006.9380	8.493	0.328	16.92	5.13
TYC702603251	031909-3507.0	3006.9380	3103.9380	8.478	0.218	10.37	6.49
TYC702603251	031909-3507.0	3641.9329	3737.9329	8.463	0.325	10.95	4.74
TYC702603251	031909-3507.0	4284.9312	4379.9312	8.562	0.223	7.06	4.87
TYC806016731	033049-4555.9	2911.9380	3011.9380	3.745	0.064	10.54	4.29
TYC806016731	033049-4555.9	3011.9380	3111.9380	3.909	0.046	7.71	2.33
TYC806016731	033049-4555.9	3407.8290	3480.8290	3.802	0.066	10.10	5.89
TYC806016731	033049-4555.9	3657.9219	3752.9219	3.775	0.065	6.44	4.82
TYC806016731	033049-4555.9	4373.9392	4472.9392	3.775	0.065	8.39	4.01
TYC806016731	033049-4555.9	4472.9392	4571.9392	3.733	0.042	5.78	2.99
TYC806016731	033049-4555.9	4629.9390	4724.9390	3.787	0.065	7.41	4.47
TYC757408031	033156-4359.2	1871.6523	1934.6523	2.953	0.053	9.78	6.07
TYC757408031	033156-4359.2	2133.9410	2195.9410	2.958	0.053	7.06	3.93
TYC757408031	033156-4359.2	2195.9410	2257.9410	2.943	0.040	10.56	4.30
TYC757408031	033156-4359.2	2558.8800	2655.8800	2.934	0.039	2.93	2.44

Table A.7 (cont'd)

Target	ASAS number	JD initial	JD final	Period (d)	ΔP (d)	Normalized power	Power at 99% confidence level
TYC757408031	033156-4359.2	3011.9380	3111.9380	2.934	0.026	4.70	4.56
TYC757408031	033156-4359.2	3398.8290	3462.8290	2.923	0.065	6.31	4.29
TYC757408031	033156-4359.2	3544.9406	3640.9406	2.941	0.026	5.29	4.70
TYC757408031	033156-4359.2	3640.9406	3736.9406	2.923	0.039	10.51	4.82
TYC757408031	033156-4359.2	3736.9406	3832.9406	2.926	0.026	10.59	6.10
TYC757408031	033156-4359.2	4274.9392	4370.9392	2.920	0.026	7.77	5.47
TYC757408031	033156-4359.2	4370.9392	4466.9392	2.938	0.039	11.32	4.10
TYC757408031	033156-4359.2	4629.9390	4725.9390	2.946	0.039	6.54	4.72
TYC808304551	044801-5041.4	2087.9266	2174.9266	8.388	0.320	5.99	3.13
TYC808304551	044801-5041.4	2174.9266	2261.9266	8.592	0.337	8.47	5.79
TYC808304551	044801-5041.4	3563.9255	3662.9255	8.511	0.220	8.85	4.38
TYC808304551	044801-5041.4	4498.9314	4711.9314	8.215	0.205	9.57	5.77
TYC5907-1244-1	045249-1955.0	1872.6985	1940.6985	5.231	0.125	17.39	5.22
TYC5907-1244-1	045249-1955.0	2089.9401	2178.9401	5.171	0.121	8.86	5.82
TYC5907-1244-1	045249-1955.0	2178.9401	2267.9401	5.177	0.122	23.33	5.33
TYC5907-1244-1	045249-1955.0	2466.9353	2564.9353	5.153	0.081	7.72	6.73
TYC5907-1244-1	045249-1955.0	2564.9353	2662.9353	5.228	0.083	4.33	3.56
TYC5907-1244-1	045249-1955.0	2662.9353	2760.9353	5.117	0.080	4.26	2.84
TYC5907-1244-1	045249-1955.0	2832.9296	2930.9296	5.111	0.119	6.89	4.99
TYC5907-1244-1	045249-1955.0	2930.9296	3028.9296	5.222	0.124	8.73	5.55
TYC5907-1244-1	045249-1955.0	3028.9296	3126.9296	5.192	0.082	8.28	5.41
TYC5907-1244-1	045249-1955.0	3416.6812	3475.6812	5.213	0.166	6.60	5.65
TYC5907-1244-1	045249-1955.0	3666.9245	3758.9245	5.317	0.128	10.74	4.49
TYC5907-1244-1	045249-1955.0	4748.9310	4830.9310	5.273	0.126	8.14	4.44
TYC5908-230-1	045932-1917.7	2096.9386	2176.9386	4.053	0.100	7.09	4.53
TYC5908-230-1	045932-1917.7	2945.8955	3035.8955	3.960	0.048	7.03	4.79
TYC5908-230-1	045932-1917.7	3035.8955	3125.8955	4.119	0.077	10.03	5.41
TYC5908-230-1	045932-1917.7	3357.6812	3416.6812	4.044	0.100	6.97	5.70
TYC5908-230-1	045932-1917.7	3666.9245	3758.9245	4.026	0.074	7.05	5.16
TYC5908-230-1	045932-1917.7	3758.9245	3850.9245	4.065	0.075	7.98	5.82
TYC5908-230-1	045932-1917.7	4390.9278	4481.9278	4.035	0.099	6.62	5.12
TYC5908-230-1	045932-1917.7	4481.9278	4572.9278	4.083	0.051	14.27	4.43
TYC5908-230-1	045932-1917.7	4749.9310	4832.9310	4.235	0.081	4.76	3.85
TYC5908-230-1	045932-1917.7	4832.9310	4915.9310	4.029	0.014	6.14	4.71
BD-091108	051537-0930.8	2183.9378	2261.9378	2.755	0.035	8.82	2.57
BD-091108	051537-0930.8	2582.8871	2671.8871	2.725	0.045	7.32	6.36
BD-091108	051537-0930.8	2671.8871	2760.8871	2.719	0.034	9.40	5.15
BD-091108	051537-0930.8	3029.9378	3123.9378	2.728	0.034	7.77	1.82
BD-091108	051537-0930.8	4492.9364	4582.9364	2.740	0.140	5.90	5.44
TYC704814531	051829-3001.5	2664.9322	2762.9322	1.694	0.009	5.68	3.25
TYC704814531	051829-3001.5	2936.9408	3038.9408	1.697	0.013	9.33	5.15
TYC760005161	053705-3932.4	1872.7106	1951.7106	2.465	0.037	11.65	6.01
TYC760005161	053705-3932.4	3428.6342	3500.6342	2.462	0.028	5.37	3.48
TYC760005161	053705-3932.4	3562.9387	3664.9387	2.450	0.018	10.46	6.00
TYC760005161	053705-3932.4	3766.9387	3868.9387	2.459	0.018	10.53	4.93
TYC760005161	053705-3932.4	4090.7715	4162.7715	2.420	0.027	6.80	5.42
TYC760005161	053705-3932.4	4162.7715	4234.7715	2.474	0.028	7.81	4.23
TYC760005161	053705-3932.4	4442.9398	4586.9398	2.453	0.018	20.66	5.11
TYC706508791	054234-3415.7	1871.7231	1950.7231	3.897	0.069	26.03	5.65
TYC706508791	054234-3415.7	1950.7231	2029.7231	3.882	0.115	6.98	4.66
TYC706508791	054234-3415.7	2105.9249	2183.9249	3.855	0.090	6.57	4.99
TYC706508791	054234-3415.7	2183.9249	2261.9249	3.820	0.067	15.82	5.37

Table A.7 (cont'd)

Target	ASAS number	JD initial	JD final	Period (d)	ΔP (d)	Normalized power	Power at 99% confidence level
TYC706508791	054234-3415.7	2468.9322	2692.9322	3.811	0.044	9.55	8.57
TYC706508791	054234-3415.7	2692.9322	2916.9322	3.948	0.047	5.59	5.03
TYC706508791	054234-3415.7	2916.9322	3140.9322	3.879	0.023	19.91	4.76
TYC706508791	054234-3415.7	4504.9385	4605.9385	3.890	0.000	6.80	2.97
HIP105388	212050-5302.0	2081.9042	2167.9042	3.497	0.056	7.91	3.55
HIP105388	212050-5302.0	2440.7815	2506.7815	3.535	0.076	9.44	4.50
HIP105388	212050-5302.0	2506.7815	2572.7815	3.601	0.079	7.84	2.55
HIP105388	212050-5302.0	3638.8837	3730.8837	3.359	0.034	6.14	2.02
HIP105388	212050-5302.0	4279.8981	4367.8981	3.365	0.052	7.53	4.92
HIP105388	212050-5302.0	4367.8981	4455.8981	3.398	0.070	5.37	1.72
HIP105388	212050-5302.0	4548.8991	4609.8991	3.410	0.088	7.88	3.73
HIP105404	212100-5228.7	1995.9042	2081.9042	3.829	0.044	4.71	4.59
HIP105404	212100-5228.7	2715.9063	2809.9063	0.408	0.001	5.36	4.99
HIP107345	214430-6058.6	2084.8985	2168.8985	4.567	0.095	6.43	4.77
HIP107345	214430-6058.6	2168.8985	2252.8985	4.540	0.094	7.61	5.31
HIP107345	214430-6058.6	4284.9087	4374.9087	4.516	0.093	10.18	5.45
HIP107345	214430-6058.6	4374.9087	4464.9087	4.519	0.093	5.20	4.51
HIP107345	214430-6058.6	4642.9073	4731.9073	4.480	0.061	7.69	5.90
TYC934402931	232611-7323.8	1873.5505	2002.5505	1.329	0.011	4.08	3.76
TYC934402931	232611-7323.8	2131.5505	2260.5505	1.335	0.008	7.90	6.74
TYC934402931	232611-7323.8	2444.8408	2699.8408	1.326	0.005	17.68	5.97
TYC934402931	232611-7323.8	2699.8408	2954.8408	1.326	0.005	8.58	5.02
TYC934402931	232611-7323.8	2954.8408	3209.8408	1.323	0.008	10.89	5.45
TYC934402931	232611-7323.8	4609.5559	4871.5559	1.326	0.005	13.97	6.39
TYC952903401	232749-8613.3	1871.6867	1998.6867	2.304	0.024	10.36	6.83
TYC952903401	232749-8613.3	1998.6867	2125.6867	2.325	0.016	9.93	8.93
TYC952903401	232749-8613.3	2125.6867	2252.6867	2.307	0.016	14.38	13.28
TYC952903401	232749-8613.3	2440.8676	2673.8676	2.316	0.016	16.83	7.15
TYC952903401	232749-8613.3	2906.8676	3139.8676	2.357	0.017	11.52	7.64
TYC952903401	232749-8613.3	3356.6151	3541.6151	2.298	0.008	8.74	8.38
TYC952903401	232749-8613.3	3541.6151	3726.6151	2.307	0.016	12.49	6.34
TYC952903401	232749-8613.3	3726.6151	3911.6151	2.340	0.008	11.34	5.18
TYC952903401	232749-8613.3	4218.5287	4351.5287	2.345	0.017	7.99	5.10
TYC952903401	232749-8613.3	4351.5287	4484.5287	2.360	0.017	4.84	4.61
TYC952903401	232749-8613.3	4674.8070	4806.8070	2.366	0.025	12.30	6.55
HIP116748A	233939-6911.8	2179.9238	2261.9238	2.860	0.050	11.44	4.73
HIP116748A	233939-6911.8	2604.8718	2683.8718	2.938	0.052	5.76	5.17
HIP116748A	233939-6911.8	3671.9162	3774.9162	2.851	0.037	5.26	3.90
HIP116748A	233939-6911.8	3850.9230	3911.9184	2.839	0.049	7.94	3.72
HIP116748A	233939-6911.8	4561.8751	4727.8751	2.851	0.025	10.24	3.46
Columba members							
TYC804702321	015215-5219.6	2056.8962	2124.8962	2.396	0.035	4.26	3.76
TYC804702321	015215-5219.6	2975.9163	3069.9163	2.402	0.018	6.21	3.28
TYC804702321	015215-5219.6	3513.9289	3643.9289	2.402	0.026	12.63	5.39
TYC804702321	015215-5219.6	3643.9289	3773.9289	2.426	0.018	4.78	4.61
TYC804702321	015215-5219.6	4466.9094	4685.9094	2.384	0.017	8.98	4.76
BD-16351	020136-1610.0	1872.6217	1948.5239	3.195	0.062	6.02	4.26
BD-16351	020136-1610.0	2125.9315	2193.9315	3.222	0.047	4.43	4.22
BD-16351	020136-1610.0	2193.9315	2261.9315	3.213	0.047	7.37	7.10
BD-16351	020136-1610.0	2612.9066	2695.9066	3.201	0.047	3.86	3.82

Table A.7 (cont'd)

Target	ASAS number	JD initial	JD final	Period (d)	ΔP (d)	Normalized power	Power at 99% confidence level
BD-16351	020136-1610.0	2890.9140	2974.9140	3.177	0.031	10.52	4.41
BD-16351	020136-1610.0	2974.9140	3058.9140	3.189	0.046	7.26	5.27
BD-16351	020136-1610.0	3364.6163	3433.5054	3.236	0.048	7.74	6.41
BD-16351	020136-1610.0	3710.9287	3793.9287	3.186	0.046	7.44	4.99
BD-16351	020136-1610.0	4443.9093	4523.9093	3.147	0.045	6.50	5.42
TYC755806551	023032-4342.4	1871.6245	1917.6245	8.995	0.616	5.75	4.87
TYC755806551	023032-4342.4	2123.9320	2190.9320	9.249	0.391	8.69	5.82
TYC755806551	023032-4342.4	2190.9320	2257.9320	9.207	0.518	7.22	4.70
TYC755806551	023032-4342.4	2446.8960	2539.8960	9.019	0.372	11.90	4.76
TYC755806551	023032-4342.4	2632.8960	2725.8960	9.895	0.447	6.03	2.92
TYC755806551	023032-4342.4	2884.9272	2981.9272	10.248	0.319	5.94	5.35
TYC755806551	023032-4342.4	2981.9272	3078.9272	10.215	0.317	5.93	2.29
HIP16413	033121-3031.0	1872.6550	1933.6550	2.271	0.031	5.96	3.59
HIP16413	033121-3031.0	2543.9253	2641.9253	2.109	0.020	5.37	5.20
HIP16413	033121-3031.0	2910.9380	3008.9380	2.256	0.023	6.41	5.85
HIP16413	033121-3031.0	4284.9312	4379.9312	2.157	0.014	6.26	2.58
HIP16413	033121-3031.0	4474.9312	4569.9312	2.205	0.001	6.21	5.24
TYC588211691	040217-1521.5	1872.6855	1925.6855	3.805	0.088	2.38	2.17
TYC588211691	040217-1521.5	2174.9385	2261.9385	3.793	0.066	8.72	4.13
TYC588211691	040217-1521.5	2644.9310	2739.9310	3.787	0.043	8.50	3.32
TYC588211691	040217-1521.5	2924.9155	3016.9155	3.834	0.067	8.80	3.37
TYC588211691	040217-1521.5	3414.6681	3471.6681	3.867	0.091	5.73	5.58
TYC588211691	040217-1521.5	4298.9239	4389.9239	3.763	0.043	5.63	4.43
TYC588211691	040217-1521.5	4480.9239	4571.9239	3.805	0.066	3.62	2.69
HIP19775	041423-3819.0	1872.6680	1933.6680	2.459	0.037	5.54	5.29
HIP19775	041423-3819.0	3545.9422	3664.9422	2.337	0.017	9.36	3.29
HIP19775	041423-3819.0	3664.9422	3783.9422	2.337	0.025	7.60	6.00
TYC758416301	042149-4317.5	2081.9435	2142.9435	2.342	0.042	4.07	3.67
TYC758416301	042149-4317.5	2142.9435	2203.9435	2.372	0.043	19.84	7.05
TYC758416301	042149-4317.5	2203.9435	2264.9435	2.369	0.034	18.81	4.59
TYC758416301	042149-4317.5	2941.9302	3189.9302	2.366	0.009	21.13	8.70
TYC758416301	042149-4317.5	3789.9433	3906.9433	2.372	0.017	5.44	4.72
TYC807706571	045153-4647.2	1871.6793	1951.6793	2.824	0.048	24.89	4.59
TYC807706571	045153-4647.2	2174.9266	2261.9266	2.857	0.037	15.30	5.23
TYC807706571	045153-4647.2	2466.9322	2565.9322	2.411	0.026	4.89	4.82
TYC807706571	045153-4647.2	2664.9322	2763.9322	2.943	0.026	10.16	7.13
TYC807706571	045153-4647.2	2831.9237	2931.9237	2.854	0.025	7.72	4.26
TYC807706571	045153-4647.2	3031.9237	3131.9237	2.836	0.024	6.89	3.95
TYC807706571	045153-4647.2	3424.8336	3497.8336	2.872	0.050	6.36	5.17
TYC807706571	045153-4647.2	3563.9255	3664.9255	2.827	0.024	11.82	4.46
TYC807706571	045153-4647.2	3664.9255	3765.9255	2.857	0.037	9.46	5.42
TYC807706571	045153-4647.2	4091.8181	4161.8181	2.734	0.057	6.32	4.73
TYC807706571	045153-4647.2	4498.9278	4598.9278	2.839	0.025	12.30	6.55
TYC807706571	045153-4647.2	4752.9355	4839.9355	2.884	0.038	6.00	5.44
TYC807706571	045153-4647.2	4839.9355	4926.9355	2.842	0.037	6.95	4.74
TYC808012061	045305-4844.6	1871.6793	1951.6793	4.573	0.127	28.52	5.77
TYC808012061	045305-4844.6	1951.6793	2031.6793	4.573	0.159	8.51	5.59
TYC808012061	045305-4844.6	2087.9266	2174.9266	4.612	0.097	15.85	5.91
TYC808012061	045305-4844.6	2174.9266	2261.9266	4.507	0.093	16.49	5.62
TYC808012061	045305-4844.6	2664.9322	2763.9322	4.612	0.065	12.98	5.87
TYC808012061	045305-4844.6	2931.9237	3031.9237	4.612	0.097	18.24	5.38
TYC808012061	045305-4844.6	3474.8336	3670.8336	4.627	0.065	11.22	6.05

Table A.7 (cont'd)

Target	ASAS number	JD initial	JD final	Period (d)	ΔP (d)	Normalized power	Power at 99% confidence level
TYC808012061	045305-4844.6	4091.8181	4161.8181	4.468	0.152	5.46	5.30
TYC808012061	045305-4844.6	4498.9278	4598.9278	4.606	0.064	9.44	6.26
TYC808609541	052855-4535.0	1872.7055	1951.7055	4.471	0.121	5.45	4.59
TYC808609541	052855-4535.0	2666.9111	2763.9111	4.737	0.068	6.86	2.49
TYC808609541	052855-4535.0	3432.8336	3509.8336	4.462	0.091	6.98	5.54
TYC808609541	052855-4535.0	4706.9411	4917.9411	4.717	0.067	5.98	5.91
HIP25709	052924-3430.9	2178.9416	2261.9416	6.095	0.170	6.75	6.02
HIP25709	052924-3430.9	2936.9408	3038.9408	5.614	0.143	6.17	4.00
HIP25709	052924-3430.9	4833.9369	4916.9369	5.608	0.001	5.63	5.35
TYC650211881	055021-2915.3	2181.9412	2257.9412	1.371	0.009	13.86	5.75
TYC650211881	055021-2915.3	3777.9306	3876.9306	1.407	0.006	8.64	6.34
TYC650211881	055021-2915.3	4308.9280	4407.9280	1.395	0.009	6.08	4.98
TYC852000321	055101-5238.2	1872.7159	1951.7159	1.200	0.007	6.22	4.08
TYC852000321	055101-5238.2	2177.9479	2257.9479	1.203	0.007	16.69	7.19
TYC852000321	055101-5238.2	2498.8650	2729.8650	1.206	0.004	12.74	7.16
TYC852000321	055101-5238.2	2729.8650	2960.8650	1.197	0.004	10.62	6.77
TYC852000321	055101-5238.2	3356.6414	3434.6414	1.206	0.007	10.37	3.87
TYC852000321	055101-5238.2	3680.9338	3784.9338	1.200	0.006	13.46	4.34
TYC852000321	055101-5238.2	3784.9338	3888.9338	1.197	0.004	12.09	6.17
TYC852000321	055101-5238.2	4504.9365	4605.9365	1.212	0.004	6.38	3.98
TYC761705491	062607-4102.9	1872.7794	1933.7794	4.232	0.082	13.49	8.04
TYC761705491	062607-4102.9	1933.7794	1994.7794	4.247	0.082	7.17	4.62
TYC761705491	062607-4102.9	2716.9017	2935.9017	4.250	0.055	8.22	4.60
TYC761705491	062607-4102.9	2935.9017	3154.9017	4.128	0.026	18.35	5.52
TYC761705491	062607-4102.9	3442.6705	3526.6705	4.187	0.080	8.61	2.37
TYC761705491	062607-4102.9	3684.9365	3788.9365	4.116	0.077	10.92	4.86
TYC761705491	062607-4102.9	3788.9365	3892.9365	4.139	0.052	10.54	6.33
TYC761705491	062607-4102.9	4315.9349	4516.9349	4.175	0.053	7.30	3.60
TYC761705491	062607-4102.9	4717.9349	4918.9349	4.152	0.001	4.85	4.41
TYC810715911	062806-4826.9	1932.7833	1992.7833	1.293	0.013	6.17	2.70
TYC810715911	062806-4826.9	2590.9327	2691.9327	1.299	0.010	5.87	3.13
TYC810715911	062806-4826.9	2691.9327	2792.9327	1.287	0.005	10.64	4.15
TYC810715911	062806-4826.9	2962.8999	3063.8999	1.287	0.007	9.18	6.30
TYC810715911	062806-4826.9	3063.8999	3164.8999	1.293	0.008	12.72	5.34
TYC810715911	062806-4826.9	3695.9264	3797.9264	1.284	0.007	5.22	4.60
TYC810715911	062806-4826.9	4092.6751	4173.6751	1.296	0.008	6.07	4.18
TYC810715911	062806-4826.9	4521.9320	4627.9320	1.290	0.005	9.55	4.50
TYC710021121	065247-3636.3	1872.7794	1933.7794	0.806	0.004	5.95	5.31
TYC710021121	065247-3636.3	2116.9301	2189.9301	0.842	0.004	4.27	4.10
TYC710021121	065247-3636.3	2189.9301	2262.9301	0.803	0.003	5.85	4.92
TYC710021121	065247-3636.3	2497.9017	2716.9017	0.803	0.002	10.15	6.43
TYC710021121	065247-3636.3	2716.9017	2935.9017	0.806	0.002	12.48	6.38
TYC710021121	065247-3636.3	3357.7025	3442.7025	0.710	0.002	4.30	3.49
TYC710021121	065247-3636.3	3797.9196	3899.9196	0.806	0.002	6.44	5.08
TYC710021121	065247-3636.3	4091.6931	4271.6931	0.803	0.002	16.28	5.06
TYC710021121	065247-3636.3	4271.6931	4451.6931	0.803	0.003	6.70	4.61
TYC710021121	065247-3636.3	4764.9332	4843.9332	0.806	0.003	6.56	4.23
TYC811808711	065623-4646.9	1872.7833	1932.7833	4.570	0.128	6.69	4.77
TYC811808711	065623-4646.9	1932.7833	1992.7833	4.468	0.152	7.92	4.25
TYC811808711	065623-4646.9	2132.9039	2195.9039	4.310	0.085	5.03	3.84
TYC811808711	065623-4646.9	2195.9039	2258.9039	4.337	0.086	12.82	5.40
TYC811808711	065623-4646.9	2590.9327	2691.9327	4.334	0.114	9.37	4.81

Table A.7 (cont'd)

Target	ASAS number	JD initial	JD final	Period (d)	ΔP (d)	Normalized power	Power at 99% confidence level
TYC811808711	065623-4646.9	2691.9327	2792.9327	4.420	0.059	12.24	6.29
TYC811808711	065623-4646.9	2962.8999	3063.8999	4.382	0.087	7.04	4.73
TYC811808711	065623-4646.9	3063.8999	3164.8999	4.516	0.093	9.69	5.13
TYC811808711	065623-4646.9	3695.9264	3797.9264	4.352	0.086	5.08	3.83
TYC811808711	065623-4646.9	3797.9264	3899.9264	4.504	0.062	12.58	4.95
TYC811808711	065623-4646.9	4092.6751	4173.6751	4.439	0.090	8.43	5.02
TYC811808711	065623-4646.9	4521.9320	4627.9320	4.403	0.059	10.31	4.03
TYC762928241	070152-3922.1	1871.8279	1933.8279	1.344	0.011	11.65	4.08
TYC762928241	070152-3922.1	2191.9308	2253.9308	1.314	0.008	9.21	4.48
TYC762928241	070152-3922.1	2497.9017	2716.9017	1.338	0.005	14.80	5.75
TYC762928241	070152-3922.1	2716.9017	2935.9017	1.332	0.005	8.78	8.41
TYC762928241	070152-3922.1	2935.9017	3154.9017	1.335	0.003	23.08	6.94
TYC762928241	070152-3922.1	3359.7081	3540.7081	1.323	0.003	13.06	4.97
TYC762928241	070152-3922.1	3721.7081	3902.7081	1.332	0.003	16.65	4.99
TYC762928241	070152-3922.1	4091.7082	4173.7082	1.332	0.011	5.68	5.26
TYC762928241	070152-3922.1	4529.9261	4628.9261	1.332	0.005	12.76	4.90
Carina members							
TYC939003221	055329-8156.9	1871.7145	2001.7145	1.855	0.010	20.74	5.46
TYC939003221	055329-8156.9	2131.7145	2261.7145	1.885	0.016	32.05	2.14
TYC939003221	055329-8156.9	2442.4686	2681.4686	1.858	0.010	12.58	7.38
TYC939003221	055329-8156.9	2681.4686	2920.4686	1.888	0.011	20.07	5.32
TYC939003221	055329-8156.9	2920.4686	3159.4686	1.867	0.011	12.64	10.34
TYC939003221	055329-8156.9	3356.7548	3539.7548	1.858	0.005	21.44	4.34
TYC939003221	055329-8156.9	3539.7548	3722.7548	1.858	0.005	5.51	5.17
TYC939003221	055329-8156.9	3722.7548	3905.7548	1.858	0.010	10.71	3.03
TYC939003221	055329-8156.9	4090.6982	4367.6982	1.888	0.005	14.10	6.25
TYC939003221	055329-8156.9	4367.6982	4644.6982	1.855	0.010	37.50	9.59
TYC939003221	055329-8156.9	4644.6982	4921.6982	1.864	0.011	9.10	5.66
HIP30034	061913-5803.3	1872.7600	1950.7600	3.855	0.068	10.61	6.86
HIP30034	061913-5803.3	2719.8995	2940.8995	3.858	0.045	13.15	8.64
HIP30034	061913-5803.3	2940.8995	3161.8995	3.876	0.045	10.25	5.96
HIP30034	061913-5803.3	3356.6656	3536.6656	3.864	0.023	17.28	5.88
HIP30034	061913-5803.3	4303.6852	4515.6852	3.841	0.044	7.50	3.75
HIP30034	061913-5803.3	4515.6852	4727.6852	3.888	0.046	11.59	6.10
HIP32235	064346-7158.6	1933.7747	1994.7747	3.781	0.087	7.48	5.57
HIP32235	064346-7158.6	2192.9178	2255.9178	3.939	0.095	6.82	5.44
HIP32235	064346-7158.6	2489.9234	2715.9234	3.858	0.045	12.88	8.42
HIP32235	064346-7158.6	2715.9234	2941.9234	3.927	0.047	3.43	3.14
HIP32235	064346-7158.6	2941.9234	3167.9234	3.834	0.044	15.41	4.79
HIP32235	064346-7158.6	3538.6876	3720.6876	3.834	0.044	9.40	4.56
HIP32235	064346-7158.6	3720.6876	3902.6876	3.846	0.022	16.92	4.59
HIP32235	064346-7158.6	4271.6662	4450.6662	3.888	0.069	6.88	5.24
HIP33737	070030-7941.8	1872.7181	2002.7181	5.129	0.080	46.88	8.47
HIP33737	070030-7941.8	2002.7181	2132.7181	5.108	0.198	8.68	5.08
HIP33737	070030-7941.8	2132.7181	2262.7181	5.060	0.116	9.96	5.62
HIP33737	070030-7941.8	2442.4686	2690.4686	5.054	0.077	19.30	6.72
HIP33737	070030-7941.8	2690.4686	2938.4686	5.102	0.118	26.75	8.08
HIP33737	070030-7941.8	2938.4686	3186.4686	5.102	0.079	24.04	4.61
HIP33737	070030-7941.8	3357.7072	3539.7072	5.108	0.040	10.87	5.05
HIP33737	070030-7941.8	3539.7072	3721.7072	5.099	0.118	12.38	7.08

Table A.7 (cont'd)

Target	ASAS number	JD initial	JD final	Period (d)	ΔP (d)	Normalized power	Power at 99% confidence level
HIP33737	070030-7941.8	3721.7072	3903.7072	5.120	0.079	12.01	4.26
HIP33737	070030-7941.8	4091.6662	4302.6662	5.099	0.079	31.23	9.11
HIP33737	070030-7941.8	4302.6662	4513.6662	5.108	0.079	19.77	5.65
TYC855910161	072124-5720.6	1871.7711	1936.7711	4.878	0.109	7.15	6.77
TYC855910161	072124-5720.6	2192.9344	2255.9344	4.681	0.133	9.43	4.62
TYC855910161	072124-5720.6	2499.9145	2725.9145	4.576	0.063	15.04	4.47
TYC855910161	072124-5720.6	2725.9145	2951.9145	4.618	0.065	17.80	7.09
TYC855910161	072124-5720.6	2951.9145	3177.9145	4.603	0.064	21.78	7.17
TYC855910161	072124-5720.6	3714.7778	3904.7778	4.591	0.032	10.76	4.61
TYC855910161	072124-5720.6	4513.9391	4715.9391	4.723	0.068	8.07	2.57
TYC892909271	082406-6334.1	2195.9273	2249.9273	0.794	0.004	5.55	5.49
TYC892909271	082406-6334.1	2546.8234	2758.8234	0.788	0.014	*****	3.03
TYC892909271	082406-6334.1	2758.8234	2970.8234	0.788	0.002	13.20	5.45
TYC892909271	082406-6334.1	3622.9003	3716.9003	0.788	0.003	5.83	4.09
TYC892909271	082406-6334.1	4090.7246	4368.7246	0.797	0.001	12.01	5.38
TYC892909271	082406-6334.1	4368.7246	4646.7246	0.788	0.002	5.18	2.92
TYC892909271	082406-6334.1	4646.7246	4924.7246	0.797	0.002	9.89	2.58
TYC893006011	084200-6218.4	1872.8598	1942.8598	1.221	0.007	8.50	7.61
TYC893006011	084200-6218.4	2172.8936	2248.7278	1.224	0.007	8.13	7.30
TYC893006011	084200-6218.4	2546.8234	2642.8234	1.224	0.040	78.38	6.48
TYC893006011	084200-6218.4	2642.8234	2738.8234	1.227	0.007	14.36	4.78
TYC893006011	084200-6218.4	2738.8234	2834.8234	1.227	0.005	8.59	5.84
TYC893006011	084200-6218.4	2887.9059	2986.9059	1.224	0.007	8.50	5.15
TYC893006011	084200-6218.4	2986.9059	3085.9059	1.224	0.007	12.70	4.54
TYC893006011	084200-6218.4	3085.9059	3184.9059	1.227	0.005	12.46	4.44
TYC893006011	084200-6218.4	3723.8886	3814.8886	1.221	0.007	7.18	5.25
TYC893006011	084200-6218.4	4559.9091	4663.9091	1.224	0.005	5.76	3.54
TYC856917611	084553-5327.5	1872.7631	1941.7631	1.287	0.008	9.74	5.04
TYC856917611	084553-5327.5	2640.8299	2734.8299	1.260	0.007	7.49	5.57
TYC856917611	084553-5327.5	2734.8299	2828.8299	1.257	0.005	9.01	4.62
TYC856917611	084553-5327.5	2985.9180	3084.9180	1.287	0.007	7.84	2.33
TYC856917611	084553-5327.5	3084.9180	3183.9180	1.173	0.004	5.12	3.82
TYC856917611	084553-5327.5	3810.9120	3904.9120	1.260	0.005	9.74	2.90
TYC856917611	084553-5327.5	4090.7318	4279.7318	1.287	0.003	5.79	3.21
TYC856917611	084553-5327.5	4279.7318	4468.7318	1.293	0.005	6.08	5.91
TYC856917611	084553-5327.5	4468.7318	4657.7318	1.260	0.002	14.59	6.40
TYC856917611	084553-5327.5	4728.9038	4791.9038	1.290	0.015	4.99	4.94
TYC939521391	085005-7554.6	1871.7871	2000.7871	1.147	0.004	24.85	5.34
TYC939521391	085005-7554.6	2000.7871	2129.7871	1.149	0.006	4.69	4.47
TYC939521391	085005-7554.6	2129.7871	2258.7871	1.153	0.006	8.92	6.25
TYC939521391	085005-7554.6	2441.5036	2689.5036	1.143	0.002	7.28	5.38
TYC939521391	085005-7554.6	2689.5036	2937.5036	1.143	0.004	3.67	3.04
TYC939521391	085005-7554.6	2937.5036	3185.5036	1.159	0.004	2.81	2.45
TYC939521391	085005-7554.6	3424.7719	3492.7719	1.137	0.008	4.66	4.57
TYC939521391	085005-7554.6	3622.8983	3716.8983	1.159	0.006	5.80	3.78
TYC939521391	085005-7554.6	3716.8983	3810.8983	1.141	0.006	11.26	3.71
TYC939521391	085005-7554.6	3810.8983	3904.8983	1.149	0.004	12.37	4.19
TYC939521391	085005-7554.6	4368.7481	4646.7481	1.153	0.004	8.11	5.46
TYC856935971	085156-5355.9	1872.7631	1941.7631	2.053	0.019	9.92	5.97
TYC856935971	085156-5355.9	1941.7631	2010.7631	1.867	0.026	5.42	3.34
TYC856935971	085156-5355.9	2640.8499	2734.8499	1.942	0.017	11.38	4.87
TYC856935971	085156-5355.9	2985.9180	3084.9180	2.103	0.020	9.09	4.70

Table A.7 (cont'd)

Target	ASAS number	JD initial	JD final	Period (d)	ΔP (d)	Normalized power	Power at 99% confidence level
TYC856935971	085156-5355.9	2985.9180	3084.9180	1.903	0.016	8.12	3.32
TYC856935971	085156-5355.9	3084.9180	3183.9180	1.894	0.011	6.97	6.16
TYC856935971	085156-5355.9	3358.7697	3425.7697	2.046	0.032	5.66	5.18
TYC856935971	085156-5355.9	3425.7697	3492.7697	1.924	0.017	5.26	5.25
TYC856935971	085156-5355.9	3810.9120	3904.9120	1.906	0.011	5.68	4.01
TYC856935971	085156-5355.9	4091.7565	4367.7565	1.897	0.005	7.84	3.83
TYC856935971	085156-5355.9	4643.7565	4919.7565	1.942	0.006	9.14	5.26
TYC858230401	085746-5408.6	1918.7631	1964.7631	1.984	0.030	5.33	5.08
TYC858230401	085746-5408.6	2173.8772	2248.7399	1.990	0.024	6.38	5.13
TYC858230401	085746-5408.6	2640.8499	2734.8499	1.939	0.017	10.91	5.39
TYC858230401	085746-5408.6	2734.8499	2828.8499	1.700	0.009	6.24	4.85
TYC858230401	085746-5408.6	3716.9120	3810.9120	1.948	0.017	6.62	5.35
TYC858230401	085746-5408.6	3810.9120	3904.9120	2.005	0.012	6.86	3.82
TYC858230401	085746-5408.6	4367.7565	4643.7565	1.942	0.011	9.08	4.14
TYC858230401	085746-5408.6	4643.7565	4919.7565	2.055	0.006	9.12	4.20
TYC816009581	085752-4941.8	1872.8675	1942.8675	2.043	0.019	16.26	6.73
TYC816009581	085752-4941.8	1942.8675	2012.8675	1.978	0.030	9.28	4.75
TYC816009581	085752-4941.8	2638.8816	2735.8816	2.041	0.019	11.46	7.15
TYC816009581	085752-4941.8	2986.9163	3085.9163	1.975	0.018	5.57	4.17
TYC816009581	085752-4941.8	3085.9163	3184.9163	2.038	0.013	7.10	4.65
TYC816009581	085752-4941.8	3356.7807	3424.7807	2.043	0.025	7.50	3.88
TYC816009581	085752-4941.8	4455.9129	4559.9129	1.960	0.017	6.58	5.12
TYC858624311	085929-5446.8	1872.7631	1941.7631	3.667	0.061	8.01	4.51
TYC858624311	085929-5446.8	1941.7631	2010.7631	3.592	0.098	7.12	4.48
TYC858624311	085929-5446.8	2172.8936	2248.7399	3.607	0.059	13.38	5.44
TYC858624311	085929-5446.8	2886.9180	2985.9180	3.598	0.059	7.03	3.13
TYC858624311	085929-5446.8	3084.9180	3183.9180	3.583	0.039	6.55	5.81
TYC858624311	085929-5446.8	3425.7697	3492.7697	3.595	0.059	9.42	7.59
TYC858624311	085929-5446.8	3716.9120	3810.9120	3.655	0.061	6.54	4.58
TYC858624311	085929-5446.8	4367.7565	4643.7565	3.637	0.040	9.94	5.07
TYC858624311	085929-5446.8	4643.7565	4919.7565	3.568	0.019	9.66	6.28
TYC858605181	090003-5538.4	1872.7631	1941.7631	0.916	0.004	10.34	5.72
TYC858605181	090003-5538.4	2640.8499	2734.8499	0.919	0.004	14.74	5.21
TYC858605181	090003-5538.4	2734.8499	2828.8499	0.922	0.003	5.77	5.06
TYC858605181	090003-5538.4	2886.9180	2985.9180	0.566	0.002	6.15	3.61
TYC858605181	090003-5538.4	3716.9120	3810.9120	0.925	0.004	7.66	4.76
TYC858605181	090003-5538.4	4090.7912	4366.7912	0.919	0.001	12.14	4.84
TYC858605181	090003-5538.4	4366.7912	4642.7912	0.922	0.003	11.75	4.86
TYC858711261	090929-5538.4	1872.7631	1943.7631	0.776	0.003	17.96	5.82
TYC858711261	090929-5538.4	1943.7631	2014.7631	0.776	0.005	6.38	4.27
TYC858711261	090929-5538.4	2758.8499	2970.8499	0.773	0.002	5.94	4.37
TYC858722901	091317-5529.1	1872.7631	1943.7631	1.502	0.010	11.87	7.75
TYC858722901	091317-5529.1	2172.8936	2248.7550	1.511	0.014	6.03	5.42
TYC858722901	091317-5529.1	2759.8499	2972.8499	1.472	0.007	7.61	3.91
TYC858722901	091317-5529.1	3714.8327	3904.8327	1.472	0.006	8.57	3.85
HIP46063	092335-6111.6	1872.8598	1942.8598	3.891	0.069	13.92	4.11
HIP46063	092335-6111.6	2193.8505	2248.7550	3.885	0.092	9.84	3.64
HIP46063	092335-6111.6	2558.8324	2650.8324	3.844	0.067	6.12	4.81
HIP46063	092335-6111.6	2650.8324	2742.8324	3.841	0.067	3.95	3.49
HIP46063	092335-6111.6	2742.8324	2834.8324	4.002	0.049	6.75	3.83
HIP46063	092335-6111.6	2895.9043	2991.9043	3.882	0.068	8.58	6.69
HIP46063	092335-6111.6	3087.9043	3183.9043	3.864	0.045	9.20	3.23

Table A.7 (cont'd)

Target	ASAS number	JD initial	JD final	Period (d)	ΔP (d)	Normalized power	Power at 99% confidence level
HIP46063	092335-6111.6	3357.8059	3425.8059	3.891	0.092	6.25	4.73
HIP46063	092335-6111.6	3631.8996	3722.8996	3.900	0.069	5.95	4.47
HIP46063	092335-6111.6	3722.8996	3813.8996	3.781	0.065	5.70	3.90
HIP46063	092335-6111.6	4090.7246	4281.7246	3.918	0.023	15.21	4.74
HIP46063	092335-6111.6	4472.7246	4663.7246	3.853	0.045	14.06	5.72
HIP46063	092335-6111.6	4790.9017	4857.9017	3.853	0.090	8.41	4.28
HIP46063	092335-6111.6	4857.9017	4924.9017	3.909	0.093	6.58	6.28
TYC894612251	094309-6313.1	4471.8949	4568.8949	1.697	0.013	3.55	3.52
TYC894612251	094309-6313.1	4568.8949	4665.8949	1.697	0.009	10.17	6.80
TYC863413931	114552-5520.8	1881.8257	1964.8257	5.288	0.170	6.60	5.67
TYC863413931	114552-5520.8	2707.7870	2791.7870	5.356	0.087	7.95	6.34
TYC863413931	114552-5520.8	4611.8385	4701.8385	5.237	0.000	4.37	4.37

AB Doradus members

HIP5191	010626-1417.8	4333.9186	4419.9186	6.971	0.295	5.00	2.12
HIP5191	010626-1417.8	4419.9186	4505.9186	7.192	0.157	5.14	2.70
TYC804210501	021055-4604.0	2123.9320	2190.9320	1.045	0.005	5.11	4.68
TYC804210501	021055-4604.0	2190.9320	2257.9320	1.120	0.006	7.04	3.31
TYC804210501	021055-4604.0	2631.8814	2723.8814	1.117	0.006	8.58	7.06
TYC804210501	021055-4604.0	3623.9216	3719.9216	1.120	0.006	9.26	7.91
TYC804210501	021055-4604.0	4629.9149	4720.9149	1.117	0.008	5.67	3.46
TYC804210501	021055-4604.0	4720.9149	4811.9149	1.120	0.004	8.29	6.32
TYC804210501	021055-4604.0	4811.9149	4902.9149	1.120	0.006	6.82	6.16
HIP10272	021216+2357.5	2915.9213	2998.9213	6.349	0.184	5.45	4.13
HIP10272	021216+2357.5	3267.7378	3353.6747	6.197	0.410	7.28	5.44
HIP14684	030942-0934.8	2159.9383	2236.9383	5.578	0.142	8.03	4.03
HIP14684	030942-0934.8	2904.9340	2995.9340	5.440	0.090	11.67	2.28
HIP17695	034723-0158.3	2154.9427	2221.9427	3.861	0.091	8.33	4.32
HIP17695	034723-0158.3	3649.9320	3733.9320	3.903	0.069	7.26	5.52
HIP17695	034723-0158.3	3733.9320	3817.9320	3.867	0.068	6.35	3.92
HIP17695	034723-0158.3	4460.9336	4543.9336	3.853	0.068	6.81	4.95
HIP22738AB	045331-5551.5	1872.6868	1934.6868	1.502	0.010	6.46	5.12
HIP22738AB	045331-5551.5	2182.9392	2259.9392	1.487	0.010	7.41	6.36
HIP22738AB	045331-5551.5	2466.9125	2686.9125	1.526	0.004	6.65	6.19
TYC758709251	050230-3959.2	1872.7106	1951.7106	6.552	0.261	15.21	5.63
TYC758709251	050230-3959.2	2182.9443	2267.9443	6.409	0.188	7.34	5.87
TYC758709251	050230-3959.2	2689.9171	2910.9171	6.537	0.130	28.75	3.00
TYC758709251	050230-3959.2	2910.9171	3131.9171	6.535	0.129	24.33	6.07
TYC758709251	050230-3959.2	3356.6342	3428.6342	6.316	0.182	5.34	4.93
TYC758709251	050230-3959.2	3428.6342	3500.6342	6.388	0.249	5.14	4.77
TYC758709251	050230-3959.2	3664.9387	3766.9387	6.385	0.185	6.72	5.76
TYC758709251	050230-3959.2	3766.9387	3868.9387	6.585	0.132	8.39	6.06
TYC758709251	050230-3959.2	4090.7715	4367.7715	6.567	0.065	15.19	5.84
TYC758709251	050230-3959.2	4367.7715	4644.7715	6.576	0.066	10.76	4.83
TYC758709251	050230-3959.2	4644.7715	4921.7715	6.526	0.129	18.47	7.86
HD32981	050628-1549.5	2183.9313	2261.9313	0.985	0.004	8.53	4.69
HD32981	050628-1549.5	2672.8959	2759.8959	1.009	0.005	9.29	4.38
HD32981	050628-1549.5	2855.9090	2946.9090	0.988	0.004	7.17	2.46
HD32981	050628-1549.5	2946.9090	3037.9090	0.988	0.004	7.96	6.68
HIP25283	052430-3858.2	1872.7106	1951.7106	9.943	0.600	13.26	6.43
HIP25283	052430-3858.2	2097.9443	2182.9443	9.450	0.542	5.01	4.97

Table A.7 (cont'd)

Target	ASAS number	JD initial	JD final	Period (d)	ΔP (d)	Normalized power	Power at 99% confidence level
HIP25283	052430-3858.2	2182.9443	2267.9443	9.521	0.414	6.35	5.31
HIP25283	052430-3858.2	2472.9173	2691.9173	9.333	0.263	9.30	5.29
HIP25283	052430-3858.2	2910.9173	3129.9173	9.321	0.262	10.09	6.82
HIP25283	052430-3858.2	3766.9387	3868.9387	9.734	0.288	6.58	6.29
HIP25283	052430-3858.2	4522.7715	4738.7715	9.527	0.276	6.64	5.24
HIP25647	052845-6526.9	2502.8914	2721.8914	0.5874	0.0010	6.68	5.98
TYC705911111	052857-3328.3	1872.7203	1934.7203	2.298	0.024	10.73	8.74
TYC705911111	052857-3328.3	2178.9416	2261.9416	2.298	0.024	12.93	6.44
TYC705911111	052857-3328.3	2936.9408	3038.9408	2.289	0.024	8.90	4.71
TYC705911111	052857-3328.3	3038.9408	3140.9408	2.301	0.016	8.34	5.36
TYC705911111	052857-3328.3	3428.7683	3500.7683	2.301	0.032	7.20	6.12
TYC705911111	052857-3328.3	4833.9369	4916.9369	2.262	0.015	5.12	5.01
TYC706408391	053504-3417.9	2566.9322	2664.9322	7.608	0.263	6.78	4.31
HIP26373	053657-4757.9	3355.8336	3432.8336	4.899	0.146	10.76	6.48
HIP26373	053657-4757.9	3432.8336	3509.8336	4.433	0.090	7.34	3.67
HIP26373	053657-4757.9	3677.9228	3782.9228	4.914	0.110	10.14	4.89
HIP26373	053657-4757.9	3782.9228	3887.9228	4.917	0.073	7.97	2.22
HIP26373	053657-4757.9	4092.6573	4168.6573	4.579	0.096	8.27	4.92
HIP26373	053657-4757.9	4302.9365	4403.9365	4.543	0.002	6.40	4.73
CP-19878	053923-1933.5	2580.9266	2671.9266	1.523	0.018	7.60	2.88
CP-19878	053923-1933.5	2671.9266	2762.9266	1.493	0.010	10.10	5.46
CP-19878	053923-1933.5	2863.9101	2955.9101	1.496	0.014	11.58	4.59
CP-19878	053923-1933.5	2955.9101	3047.9101	1.493	0.010	9.48	4.69
CP-19878	053923-1933.5	3356.6632	3428.6632	1.323	0.011	6.49	5.17
CP-19878	053923-1933.5	3428.6632	3500.6632	1.499	0.010	6.84	4.53
CP-19878	053923-1933.5	4762.9202	4838.9202	1.520	0.011	6.14	3.57
TYC760514291	054114-4118.0	1871.7293	1951.7293	2.815	0.036	5.08	4.32
TYC760514291	054114-4118.0	2106.9241	2183.9241	2.761	0.035	5.98	4.24
TYC760514291	054114-4118.0	2183.9241	2260.9241	2.737	0.034	7.59	4.36
TYC649412281	054413-2606.3	3771.9326	3867.9326	1.843	0.010	7.51	6.92
TYC649412281	054413-2606.3	4405.9280	4502.9280	1.825	0.015	6.36	3.15
HIP27727	055216-2839.4	2181.9412	2257.9412	2.845	0.037	10.43	6.80
HIP27727	055216-2839.4	2587.9252	2685.9252	2.848	0.037	8.16	5.82
HIP27727	055216-2839.4	2685.9252	2783.9252	2.851	0.037	10.74	4.60
HIP27727	055216-2839.4	2940.9410	3039.9410	2.851	0.037	9.08	5.58
HIP27727	055216-2839.4	3039.9410	3138.9410	2.860	0.025	7.65	6.78
HIP27727	055216-2839.4	4308.9280	4405.9280	2.857	0.037	6.67	5.02
HIP27727	055216-2839.4	4845.9131	4925.9131	2.842	0.082	4.72	3.21
TYC759814881	055751-3804.1	2182.9376	2257.9376	3.634	0.060	12.26	6.06
TYC759814881	055751-3804.1	2498.8942	2716.8942	3.655	0.040	9.25	8.16
TYC759814881	055751-3804.1	2716.8942	2934.8942	3.787	0.043	13.56	5.64
TYC759814881	055751-3804.1	2934.8942	3152.8942	3.763	0.021	11.38	5.42
TYC759814881	055751-3804.1	3532.7210	3707.7210	3.589	0.039	8.81	6.47
TYC759814881	055751-3804.1	4435.6734	4607.6734	3.724	0.021	12.42	5.65
TYC707900681	060834-3402.9	1872.7432	1951.7432	3.383	0.052	14.97	6.11
TYC707900681	060834-3402.9	2181.9412	2257.9412	3.446	0.054	10.27	5.96
TYC707900681	060834-3402.9	2587.9252	2685.9252	3.374	0.052	8.96	3.66
TYC707900681	060834-3402.9	2685.9252	2783.9252	3.389	0.052	15.10	5.51
TYC707900681	060834-3402.9	2940.9410	3039.9410	3.410	0.053	10.02	6.48
TYC707900681	060834-3402.9	3039.9410	3138.9410	3.374	0.035	12.80	5.09
TYC707900681	060834-3402.9	3435.6648	3514.6648	3.413	0.053	4.50	3.59
TYC707900681	060834-3402.9	3777.9306	3876.9306	3.577	0.039	3.24	2.86

Table A.7 (cont'd)

Target	ASAS number	JD initial	JD final	Period (d)	ΔP (d)	Normalized power	Power at 99% confidence level
TYC707900681	060834-3402.9	4403.9385	4504.9385	3.416	0.053	6.54	4.17
TYC708407941	060919-3549.5	1872.7403	1951.7403	1.712	0.013	18.40	6.64
TYC708407941	060919-3549.5	2182.9376	2257.9376	1.718	0.013	10.61	4.15
TYC708407941	060919-3549.5	2489.9252	2710.9252	1.721	0.009	7.28	4.71
TYC708407941	060919-3549.5	2710.9252	2931.9252	1.715	0.009	9.34	5.53
TYC708407941	060919-3549.5	2931.9252	3152.9252	1.721	0.004	11.25	4.68
HIP31878	063950-6128.7	1871.7637	1951.7637	9.067	0.376	6.55	6.47
HIP31878	063950-6128.7	2863.9170	2966.9170	9.234	0.387	7.22	5.10
HIP31878	063950-6128.7	3358.6865	3540.6865	8.885	0.119	7.87	4.36
HIP31878	063950-6128.7	3540.6865	3722.6865	9.016	0.245	9.24	4.82
TYC762721901	064119-3820.6	2497.9017	2716.9017	2.716	0.022	6.83	4.04
TYC762721901	064119-3820.6	4366.6992	4641.6992	2.704	0.011	9.49	6.87
UCAC206727592	064753-5713.5	1871.7711	1999.7711	5.978	0.108	9.97	5.51
UCAC206727592	064753-5713.5	2127.7711	2255.7711	6.086	0.168	8.71	6.25
UCAC206727592	064753-5713.5	2950.8995	3176.8995	6.119	0.113	9.84	5.74
UCAC206727592	064753-5713.5	4368.6852	4645.6852	6.029	0.110	8.09	6.48
UCAC206727592	064753-5713.5	4645.6852	4922.6852	6.056	0.111	16.86	5.70
TYC855811481	071051-5736.8	1871.7711	1936.7711	2.932	0.039	14.50	4.80
TYC855811481	071051-5736.8	1936.7711	2001.7711	2.890	0.051	5.09	4.12
TYC855811481	071051-5736.8	2499.9145	2725.9145	2.953	0.026	10.54	5.30
TYC1355-214-1	072344+2025.0	2625.7468	2691.7468	2.794	0.048	15.67	4.74
TYC1355-214-1	072344+2025.0	2691.7468	2757.7468	2.767	0.035	9.18	6.46
TYC1355-214-1	072344+2025.0	2913.8868	2985.8868	2.797	0.048	7.57	3.47
TYC1355-214-1	072344+2025.0	2985.8868	3057.8868	2.806	0.036	18.01	5.92
TYC1355-214-1	072344+2025.0	3057.8868	3129.8868	2.815	0.036	9.67	4.35
TYC1355-214-1	072344+2025.0	3292.8812	3357.8812	2.806	0.085	38.86	12.46
HIP36108	072618-4940.8	2497.9271	2722.9271	3.822	0.044	8.62	5.82
HIP36349	072851-3014.8	1873.8217	1934.8217	1.643	0.017	29.76	4.38
HIP36349	072851-3014.8	1934.8217	1995.8217	1.640	0.021	12.81	4.93
HIP36349	072851-3014.8	2184.9192	2238.9192	1.652	0.021	6.31	4.63
HIP36349	072851-3014.8	2596.9238	2695.9238	1.649	0.012	10.28	5.46
HIP36349	072851-3014.8	2695.9238	2794.9238	1.643	0.012	14.32	4.58
HIP36349	072851-3014.8	2861.9222	2963.9222	1.643	0.012	11.95	6.61
HIP36349	072851-3014.8	2963.9222	3065.9222	1.640	0.012	13.74	4.81
HIP36349	072851-3014.8	3065.9222	3167.9222	1.646	0.008	9.11	5.91
HIP36349	072851-3014.8	3442.7025	3527.7025	1.643	0.016	15.16	4.82
HIP36349	072851-3014.8	3620.9050	3713.9050	1.640	0.012	10.93	4.92
HIP36349	072851-3014.8	3713.9050	3806.9050	1.640	0.012	7.47	4.91
HIP36349	072851-3014.8	3806.9050	3899.9050	1.646	0.008	6.33	4.20
HIP36349	072851-3014.8	4152.7220	4213.7220	1.640	0.016	7.91	6.58
HIP36349	072851-3014.8	4436.9238	4538.9238	1.643	0.012	8.92	6.17
HIP36349	072851-3014.8	4538.9238	4640.9238	1.643	0.012	5.26	3.70
TYC949308381	073100-8419.5	2442.4557	2670.4557	4.782	0.069	4.90	2.55
TYC949308381	073100-8419.5	3356.6151	3539.6151	4.983	0.038	8.67	3.05
TYC949308381	073100-8419.5	3539.6151	3722.6151	4.962	0.112	9.90	5.83
TYC949308381	073100-8419.5	4091.6662	4368.6662	4.815	0.035	9.87	4.63
TYC949308381	073100-8419.5	4368.6662	4645.6662	5.102	0.079	17.93	6.35
TYC949308381	073100-8419.5	4645.6662	4922.6662	5.114	0.079	12.72	3.84
HIP76768	154028-1841.8	1922.8648	2000.8648	3.583	0.058	7.83	5.35
HIP76768	154028-1841.8	2000.8648	2078.8648	3.706	0.063	6.13	4.71
HIP76768	154028-1841.8	2078.8648	2156.8648	3.601	0.079	7.84	3.69
HIP76768	154028-1841.8	2816.8696	2901.8696	3.574	0.039	7.92	4.22

Table A.7 (cont'd)

Target	ASAS number	JD initial	JD final	Period (d)	ΔP (d)	Normalized power	Power at 99% confidence level
HIP81084	163342-0933.2	4298.8789	4381.8789	7.443	0.253	5.48	4.16
HIP81084	163342-0933.2	4580.8779	4656.8779	7.423	0.252	5.99	4.66
BD-134687	173746-1314.8	2031.8767	2111.8767	0.447	0.001	5.56	5.23
BD-134687	173746-1314.8	2442.6568	2500.6568	0.447	0.001	10.53	5.87
BD-134687	173746-1314.8	2687.8671	2769.8671	0.447	0.001	11.30	4.78
BD-134687	173746-1314.8	2769.8671	2851.8671	0.447	0.001	6.69	5.04
BD-134687	173746-1314.8	2851.8671	2933.8671	0.447	0.001	10.31	5.96
BD-134687	173746-1314.8	3780.8387	3842.8387	0.447	0.001	12.47	2.80
BD-134687	173746-1314.8	4158.8722	4238.8722	0.447	0.001	7.34	5.47
BD-134687	173746-1314.8	4238.8722	4318.8722	0.447	0.001	6.01	3.24
BD-134687	173746-1314.8	4601.8772	4682.8772	0.447	0.001	9.30	4.58
BD-134687	173746-1314.8	4682.8772	4763.8772	0.447	0.001	6.05	5.45
HIP94235	191058-6016.3	1966.8737	2054.8737	2.076	0.013	4.41	3.55
HIP94235	191058-6016.3	2684.8879	2778.8879	2.223	0.022	4.38	2.64
TYC0486-4943	193304+0345.7	2793.9023	2874.9023	1.320	0.008	4.62	3.97
TYC0486-4943	193304+0345.7	3076.9058	3133.9058	1.356	0.014	7.82	5.04
TYC0486-4943	193304+0345.7	3602.9050	3676.9050	1.359	0.008	5.54	5.44
TYC0486-4943	193304+0345.7	4258.9028	4332.9028	1.362	0.011	5.28	4.97
TYC0486-4943	193304+0345.7	4332.9028	4406.9028	1.347	0.008	4.13	3.68
HD189285	195924-0432.1	2796.8976	2879.8976	4.749	0.103	5.51	4.36
HD189285	195924-0432.1	4714.9012	4791.9012	4.797	0.140	4.62	3.54
TYC5164-567-1	200449-0239.3	2882.8999	2962.8999	4.690	0.134	3.18	2.97
TYC5164-567-1	200449-0239.3	3528.9023	3601.9023	4.702	0.101	6.74	2.81
TYC5164-567-1	200449-0239.3	4348.8947	4426.8947	4.657	0.099	7.71	2.63
TYC5164-567-1	200449-0239.3	4633.9012	4706.9012	4.723	0.135	6.21	3.68
TYC5164-567-1	200449-0239.3	4706.9012	4779.9012	4.788	0.105	5.47	4.18
TYC1090-0543	205428+0906.1	4294.8995	4360.8995	2.268	0.024	6.25	4.51
TYC1090-0543	205428+0906.1	4708.9154	4782.9154	2.250	0.031	6.18	3.23
TYC635102861	211305-1729.2	2080.9030	2159.9030	4.884	0.109	10.97	6.88
TYC635102861	211305-1729.2	2159.9030	2238.9030	4.893	0.145	11.35	4.80
TYC635102861	211305-1729.2	2440.7907	2529.7907	4.860	0.108	10.97	6.29
TYC635102861	211305-1729.2	3540.9084	3626.9084	4.839	0.142	14.84	4.86
TYC635102861	211305-1729.2	3626.9084	3712.9084	4.761	0.138	4.77	4.70
TYC635102861	211305-1729.2	4722.9102	4810.9102	5.019	0.114	5.62	4.08
HIP106231	213102+2320.1	2820.9154	2880.9154	0.423	0.001	2.27	1.45
HIP106231	213102+2320.1	4666.9163	4741.9163	0.423	0.001	12.14	5.86
HIP107684	214849-3929.1	2173.9128	2261.9128	4.008	0.073	5.44	4.82
HIP107684	214849-3929.1	2446.7835	2509.7835	4.074	0.101	6.97	5.24
HIP107684	214849-3929.1	2509.7835	2572.7835	4.163	0.106	5.40	3.96
HIP107684	214849-3929.1	2903.9108	2993.9108	4.181	0.053	7.24	4.62
HIP107684	214849-3929.1	3548.9082	3640.9082	4.146	0.052	6.37	4.40
HIP113579	230019-2609.2	3568.9086	3653.9086	2.157	0.021	5.06	4.77
HIP114530	231154-4508.0	2445.8956	2517.8956	5.216	0.124	4.51	3.88
HIP114530	231154-4508.0	2924.9105	3017.9105	5.234	0.083	5.94	4.32
HIP114530	231154-4508.0	3480.9116	3573.9116	5.162	0.162	4.93	4.13
HIP114530	231154-4508.0	3573.9116	3666.9116	5.171	0.081	10.12	4.19
HIP116910	234154-3558.7	2178.9184	2258.9184	2.265	0.031	11.03	2.79
HIP116910	234154-3558.7	2445.8158	2520.8158	2.349	0.025	5.38	4.51
HIP116910	234154-3558.7	2955.7556	3017.7556	2.283	0.040	12.80	5.06
HIP116910	234154-3558.7	3511.8980	3595.8980	2.307	0.024	5.37	4.48
HIP116910	234154-3558.7	4406.9214	4494.9214	2.295	0.016	8.94	2.96
HIP116910	234154-3558.7	4674.9208	4760.9208	2.304	0.024	4.70	4.18

Table A.7 (cont'd)

Target	ASAS number	JD initial	JD final	Period (d)	ΔP (d)	Normalized power	Power at 99% confidence level
--------	----------------	---------------	-------------	---------------	-------------------	---------------------	----------------------------------